QUANTITATIVE ANALYSIS OF GOLD IN LOW-GRADE TAILINGS FROM DIFFERENT MATRICES, COUPLED WITH A STUDY INTO THE ASSOCIATED UNCERTAINTIES

Kedibone Nicholine Mashale

Supervisor: Prof Luke Chimuka

Co-supervisors: Dr James Tshilongo

: Dr James Sehata

A thesis submitted to the Faculty of Science, University of the Witwatersrand, in fulfilment of the requirements for the degree of Doctor of Philosophy.

November 2023

DECLARATION

I declare that this research is my own, unaided work. It is being submitted for the Degree of Doctor of Philosophy at the University of the Witwatersrand, Johannesburg. It has never been submitted before for any degree or examination at any other university. This research was conducted at Mintek, Analytical Chemistry Division.

---------- 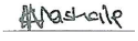 ----------

Kedibone Nicholine Mashale

This 23th day of November 2023 in Johannesburg

Supervisor Name: Prof Luke Chimuka

Co-supervisors: Dr. James Tshilongo and Dr. James Sehata

PUBLICATIONS AND CONFERENCES

1. Statistical evaluation of the uncertainties in the characterization of South African low-grade gold mine tailings

   Kedibone Mashale, Bambesiwe May, James Sehata, James Tshilongo and Luke Chimuka.

   Article published under the South African Journal of Chemistry (2023); 77(1), 42-47. https://doi.org/10.17159/0379-4350/2023/v77a07
2. Analysis of low-grade gold from mine tailings following gold deportment analysis, size fractionation, and acid digestion by ICP–MS and the associated uncertainties

   Kedibone Mashale, Napo Ntsasa, James Sehata, James Tshilongo and Luke Chimuka.

   (Manuscript)
3. The effectiveness of Fe and Sn in the gravimetric quantification of gold from low-grade tailings, supported by evaluation of measurement uncertainties

   Kedibone Mashale, Napo Ntsasa, James Sehata, James Tshilongo and Luke Chimuka.

   (Manuscript)

Other work

1. Detection and separation of silver ion from industrial wastewaters using fluorescent D-glucose carbon nanosheet and quaternary silver indium zinc sulphide quantum dots

   Bambesiwe M. May**,** Olayemi J. Fakayode, **Kedibone N. Mashale,** Mokae F. Bambo, Ajay K. Mishra, Edward N Nxumalo

   This article was published in the Journal of Water Processing Engineering (2022); 49, 102944 https://doi.org/10.1016/j.jwpe.2022.102944

Conferences

K.N. Mashale, J Sehata, J Tshilongo and L. Chimuka, Gravimetric quantification of gold in low-grade mine tailings, Test and Measurement, 24-26 October 2022, Persequor Park, Pretoria. (Oral). https://www.nla.org.za/?page_id=4191

K.N. Mashale, J Sehata, J Tshilongo and L Chimuka, Gravimetric quantification of gold in low-grade mine tailings, 44th SACI National Convention. 08-13 January 2023, Stellenbosch, South Africa. (Oral). https://www.saci.co.za/SACI2023

ABSTRACT

Gold is one of the precious group elements that is used for various purposes, such as jewellery, auto catalysts and as a form of investment. Various countries have gold reserves, with South Africa being the leading gold producer between 1980 and 2007. However, as of 2022, it is ranked as the eighth largest producer of gold, contributing 3% to the global contribution. The majority of gold is mainly mined from the Witwatersrand Basin in Johannesburg. It is well known that mining has been ongoing for decades, which means that a significant amount of land has been mined across the country. During gold mining, a large proportion of the ore material from which the gold is extracted is waste, together with the chemicals that were used, and this waste is termed mine tailings. This implies that based on the years that gold mining has occurred for and the depth of mining, a significant amount of the tailings have been deposited into free land around the mines, some of which are close to communities.

The tailings consist of traces of gold that were left due to inefficient extraction processes and other components, such as base metals. The disadvantage of this is that due to the other chemical composition of these tailings, they have the potential to be dangerous to the environment. Some tailings contain minerals such as jarosite ($KFe_2(SO_4)_2(OH)_6$) that cause acid mine drainage, while heavy metals such as lead, mercury, arsenic and chromium can leach into surface and ground waters, causing pollution. Furthermore, they pose a danger if the dams that they are stored in collapse, which was recently witnessed in South Africa. Because of these factors, there have been various advances made towards the beneficiation of tailings, such as utilizing them to make glass or bricks for construction. A major advancement was the reprocessing of these mine tailings to recover or extract the remaining gold, which benefits both the environment and the mining houses. Therefore, in a move to support this initiative, scientists have taken to the laboratory to develop new or optimize existing methods for the extraction and quantification of gold, which is expected to be of a low grade over time.

Various methods can be used for the quantification of gold, including the conventional fire assay, wet and dry chlorination and acid digestion. Most of these are suitable for medium- to high-grade gold ores but are known to experience challenges in regard to low-grade ores. The aim of this research was therefore to find the optimum method for the quantification of gold from mine tailings emanating from the Ventersdorp Contact Reef (VCR) and Barberton Greenstone Belt (GBS). Subsequent to chemical analysis, the samples were characterized for mineralogy using X-ray diffraction (XRD) and Brunauer–Emmett–Teller (BET) surface area

analysis. The mineralogical characterization of the material showed high quartz content (68-78%), muscovite (11.4-13.8%), chlorite (6.9-7.6%), pyrite, dolomite and calcite as minor minerals. The BET analysis reported a surface area of 2.3 $m^2.g^{-1}$ for the feed sample. The tailings were treated with acid digestion employing reverse aqua regia, which was both in the presence and absence of hydrofluoric acid (HF). This process was preceded by a gold deposition study to determine the association of gold with minerals such as quartz and pyrite. In the fire assay, the variables varied were sample mass (50, 100 and 120 g), the ratio of litharge to carbon (PbO:C, 8, 10 and 12) and the enhancement of the lead collection by adding tin (Sn) and iron (Fe). These methods were developed for the tailings sample (0.1 $g.t^{-1}$), which was a residue of a 0.32 $g.t^{-1}$ sample from a cyanide leaching process. Furthermore, it was investigated whether the lead started with at the beginning of the fusion was recovered, as its optimum recovery would indicate that the gold is being efficiently recovered. In an attempt to curb issues relating to sample homogeneity due to sample size, the use of commercial sodium hypochlorite (NaOCl) for the chlorination of gold in the ore sample (0.32 $g.t^{-1}$), in which the concentration of NaOCl, pH and leaching time were varied, was investigated. To assess the performance of the acid digestion and fire assay methods, measurement uncertainty was evaluated using the bottom-up approach, which focused on the major contributors.

The recoveries obtained from the methods were 50-79% for aqua regia, 81-83% for reverse aqua regia, 63-83% for aqua regia with HF and 81-111% for reverse aqua regia with HF, which fit the criteria set. Reverse aqua regia offered the highest recoveries, irrespective of the addition of HF, which implied that the process did not suffer from any gold encapsulation by minerals such as quartz. This is further supported by the gold depot test, in which 78% of the gold was free milled. This method yielded limits of detection (LOD) of 0.14-0.334 $\mu g.kg^{-1}$, which was impressive because there was no use of harsh acids and the sample mass of 1 g did not result in any homogeneity problems. In the assessment of the homogeneity, a homogeneity indicator of 8.9% was obtained, which indicated that the sample, at 1 g, was satisfactorily homogeneous. From the fire assay, a sample mass of 100 g, flux ratio of 10 and addition of 10 mg. L^{-1} Sn, obtained the highest recoveries greater than 80%. It was also proven that there is a correlation between the lead recovery after fusion and the recoveries of gold. Although a large mass of 300 g can be used for wet chlorination, this method encounters various issues. The results of these tests showed that at a pH of 4, 1.5 M NaOCl and 2 h extraction time, recoveries as high as 97% can be obtained. Furthermore, analysis of the initial sample and the residues indicated a change in the mineral composition, with minerals such as kaolinite appearing in the

diffractograms due to increased crystallization, while the surface area of the residues increased from 3.3 to 5.2 $m^2.g^{-1}$, showing that the oxidation process had occurred.

To statistically support the methods, evaluation of measurement uncertainty was carried out in which the bottom-up approach, which included quantifying the overall method uncertainty by assessing all the parameters involved, was used. The measurement uncertainty evaluations showed that the fire assay with a gravimetric finish is the best method, as it has values of ± 0.00432 $g.t^{-1}$, while that of acid digestion with inductively coupled plasma–mass spectrometry (ICP–MS) finish and fire assay with inductively coupled plasma optical emission spectroscopy (ICP–OES) finish had measurement uncertainties of 0.1 and 0.09 $g.t^{-1}$, respectively. This brings the expressions of the measurand as follows:

- Fire assay by gravimetry: 0.0904 ± 0.00432 $g.t^{-1}$
- Fire assay by ICP–OES: 0.26 ± 0.1 $g.t^{-1}$
- Acid digestion by ICP–MS: 0.258 ± 0.09 $g.t^{-1}$

This shows the importance of quantifying uncertainties in the methods for gold quantification, especially those that have major drawbacks. It was therefore concluded that although all three methods gave satisfactory results, a fire assay with the addition of Sn and a gravimetric finish would be best suited to quantify gold in these low-grade tailings.

The advantages of the methods presented in this study were the use of commercial bleach (NaOCl), the use of a small sample mass (1 g), the use of a simple acid combination of HCl and HNO_3 and the coupling of these to an uncertainty study. In terms of chlorination, most studies have used it on high-grade ores of at least 10 $g.t^{-1,}$ obtaining recoveries of less than 80%, while in this study, the feed sample was 0.32 $g.t^{-1}$ and offered as much recoveries. To curb the use of instrumental analysis, the gravimetric method using Sn and Fe showed good recoveries, which again, is an enormous achievement. In general, the superiority that these methods have over other studies is that they worked satisfactorily on low-grade samples, whereas in the literature, they were applied on high-grade ores.

DEDICATION

To my mother; Elizabeth Mbiza, late father; Ishmael Mashale and grandmother, Ellah Mbuyane.

To my daughter, Mokgethwa Duduzile.

ACKNOWLEDGEMENTS

I would like to acknowledge my supervisors, Prof Luke Chimuka, Dr James Sehata and Dr James Tshilongo, for their guidance in completing this Ph.D.

To Dr James Tshilongo, Ms. Nompumelelo Leshabane, and Mr. Napo Ntsasa, thank you for all the words of encouragement that came my way. Thank you for motivating me to be the best that I can and for always being available. Your efforts are very much appreciated.

Thank you to Ms. Hlengiwe Mnculwane, Dr. Odwa Mapazi, and Dr. Bambesiwe May for the ongoing support and for the outings that always relieved my stress.

A massive appreciation to my friends, Mr Basil Munjanja, Ms Portia Makhubela, Ms Amanda Mahlangu, Ms Leah Malapane, and Ms Patricia Mawela, for always encouraging me to push through.

NRF and Mintek are acknowledged for funding my doctoral studies.

Thank you to the ACD team at Mintek for assisting me when I needed help. Especially the fire assay team, thank you so much, and to everyone who helped in any way.

I would also like to acknowledge Dr Sabine Verryn of XRD Consulting, who gave me discounts on my XRD analysis.

Last, I offer massive appreciation to my family for their support, Elizabeth Mbiza, Diemetse Mashale, Clement Nake, Luyanda Mkhonto, Kamohelo Mashale, Accolade Sehlabela, and my precious daughter, Mokgethwa Duduzile.

CONTENTS

LIST OF FIGURES

LIST OF TABLES

LIST OF SYMBOLS

$mg.L^{-1}$	Milligram per litre
$ng.L^{-1}$	Nanogram per litre
$\mu g.L^{-1}$	Microgram per litre
kg	Kilogram
$g.L^{-1}$	Gram per litre
$kg.t^{-1}$	Kilogram per litre
$g.t^{-1}$	Gram per tonne
cm	Centimetre
km	Kilometre
g	Gram
mg	Milligram
°C	Degrees Celsius
%	Percent
$\mu g.kg^{-1}$	Microgram per kilogram
$mg.kg^{-1}$	Milligram per kilogram
$m^2.g^{-1}$	Square metres per gram

ABBREVIATIONS

AAS	Atomic absorption spectroscopy
ANOVA	Analysis of variance
AR	Aqua regia
BET	Brunauer–Emmett–Teller
BIC	Bushveld igneous complex
BTRP	Barberton tailings retreatment plant
CIL	Carbon in leach
CRM	Certified reference material
CV	Correlation of variance
DIBK	Diisobutyl ketone
DLLME	Dispersive liquid–liquid microextraction
EDXRF	Energy dispersive X-ray fluorescence
FA	Fire assay
FACT	Fast automated curve fitting
GSB	Greenstone belt
GUM	Guide to uncertainty measurement
HF	Hydroflouric acid
HRCS-GFAAS	High resolution continuum source GF-AAS
ICP–MS	Induced couple plasma mass spectrometry
ICP–OES	Induced couple plasma optical emission spectroscopy
INAA	Instrumental neuron activated analysis
ISO	International standardization organization
KED	Kinetic energy discrimination
LA-ICP–MS	Lase ablation coupled to ICP–MS
LOD	Limit of detection
LOQ	Limit of quantification
MCM	Monte carlo method
MIBK	Methyl isobutyl ketone
MU	Measurement uncertainty
Pb-FA	Lead fire assay
PGE	Precious group elements

PGM	Platinum group metals
PSD	Particle size distribution
PT	Proficiency testing
PTFE	Polytetrafluoroethylene
RAR	Reverse aqua regia
RF	Radio frequency
RMS	Root mean square
RSD	Relative standard deviation
SEM	Scanning electron microscopy
SVDV	Synchronous vertical dual view
TDS	Total dissolved solids
UNC	Uncertainty
VCR	Ventersdorp contact reef
XRD	X-ray diffraction

1 INTRODUCTION

1.1 Background

Gold is one of the most mined minerals in the world and is often referred to as a precious metal (Neingo & Tholana, 2016). It is mostly used for jewellery, investments, to make coins and in dentistry. In Figure 1.1, as of 2023, 50% of gold is utilized in the jewellery industry (Hughes *et al.*, 2021; Carpinteyro *et al*., 2021).

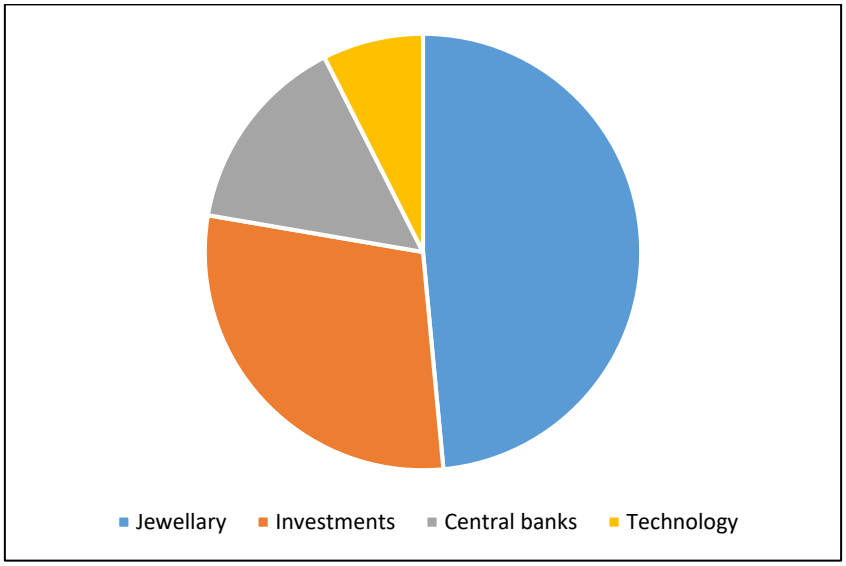

Figure 1.1 Uses of gold (Natural-resources, 2023).

In South Africa, the mining of gold started in the 19th century; thus, a significant amount of land has been mined, with South Africa being the 8th largest producer of gold (Minerals Council, 2023). This has subsequently led to the depletion of the valuable minerals at the level currently being mined and would have to mine deeper into the Earth's surface, which can pose various challenges. South Africa currently has the deepest gold mine, namely, the Mponeng gold mine, which is located along the Ventersdorp contact reef in Carletonville (Scheepers & Malan, 2022). The challenges faced by the mining industry include technology and power to reach lower levels, safety for personnel and the costs that will be incurred, plus the generation of increased mine waste(Neingo & Tholana, 2016) This has led to interest in the recovery of precious metals from mine tailings, which are the residues of the ore that the valuables were extracted from and would often consist of the chemicals used in the processes (Kossoff *et al*., 2014).

With the significant exploitation of gold deposits in South Africa, an increase in the number of tailings produced is inevitable. In Figure 1.2, the distribution of the gold tailings dumps in Gauteng is shown, which is quite significant. A major impact of these tailings on the environment is that they occupy a significant amount of land that could be used for other purposes. This is supported by a report in which it was discovered that in the Johannesburg area, more than 321 km^2 of land is covered by toxic and radioactive tailings (DRDGOLD, 2016). In addition to occupying land, tailings introduce sulfides and pyrite minerals into the soil, which could leach into the ground and surface water (Dold, 2014). Previous studies by Rösner and Van Schalkwyk (2000) on quantifying the impacts of tailings have found that tailings consist of harmful substances such as cyanides, with the concentrations of copper, chromium, cobalt, nickel, and zinc exceeding the threshold concentration for soils.

A further adverse effect of tailings is their ability to cause acid mine drainage, which is a problem that South Africa is trying to solve. Recently, there have been cases in which dams storing tailings collapsed and led to tailings being introduced into nearby communities. This was witnessed in Jaarsfontein in the Free State, South Africa, which led to fatalities and destroying houses (Torres-Cruz and O'Donovan, 2023)

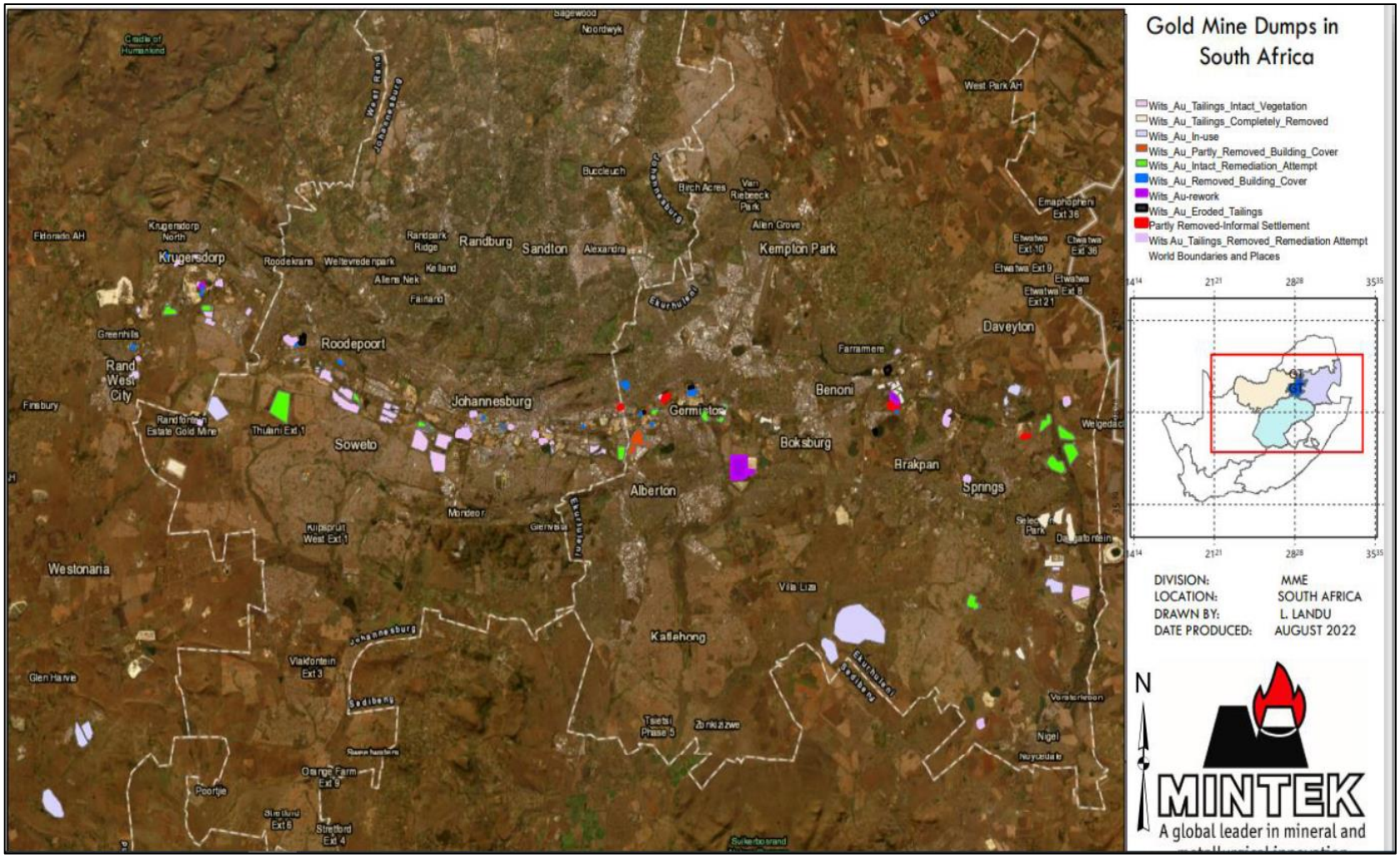

Figure 1.2 Satellite image of gold dumps in South Africa.

Therefore, the possibility of mining deeper into the Earth and the adverse effects of tailings on the environment have led to various studies into the viability of these tailings. Between 2010 and 2015, various projects were launched that were aimed at the reclamation of valuable minerals from tailings. Studies by Ahmari and Zhang (2012), Li *et al*., (2017), Zhu *et al.*, (2017), and Luo *et al.*, (2020) have examined the possible use of tailings in brickmaking for construction purposes and glass manufacturing.

1.2 Gold tailings economics in South Africa

Due to the amount of mining carried out in South Africa, the amount of tailings produced is significant. In Johannesburg, there are approximately 446 mine tailing dumps that cover a total area of 18000 hectares, with the East Rand having the majority of the dumps (Table 1.1).

Table 1.1 Distribution of mine dumps in the Witwatersrand Basin (Mabaso, 2023).

Goldfield	Number of dumps	Total area (ha)
East rand	154	4,893.4
Central rand	127	2,588.5
West rand	69	1,195.1
Carletonville	18	1,710.6
Venterskroon	15	1.941.0
Klerkdorp	17	4,902.0
Welkom	46	1,365.1
Total	**446**	**18,495.17**

Due to the various effects of mine tailings on the environment, processing plants for tailings have been developed by different mining houses to reduce their ecological footprints. Pan African Resources have developed the Elikhulu and Barberton Tailings Retreatment Plant (BTRP), which processes approximately 1.2 Mt historic tailings per month and recovers about 55 000 ounces of gold, as shown in Table 1.2. Another tailings processing plant that has been developed is the Ergo plant by DRDGOLD, which processes 1.7 Mt of tailings and recovers 80 000 ounces of gold. A substantial amount of tailings have already been processed. Figures 1.3 and 1.4 show the tailings dumps before 2016 and after 2016, in which the tailings have been cleared that emanated from a mine in the West Rand. Reprocessing of mine tailings benefits mining houses in terms of finances, the reduced resources needed and their environmental management.

Table 1.2 Various gold tailings treatment plants currently running in South Africa.

Treatment facility	Tailings processed per month (ton)	Gold recovered (ounce)	Grade of gold (g/t)	References
Barberton Tailings Retreatment Plant	100 000	20 000	0.7	(Pan African Resources, 2020)
Elikhulu	1 200 000	60 000	0.1	(Pan African Resources, 2020)
DRDGOLD	1 700 000	80 000	0.3	(DRDGOLD, 2016)
Mine Waste Solutions	-	100 000	0.25	(Harmony, 2016)

Figure 1.3 Tailings dam in West Rand in 2005 (Source: Google Earth).

Figure 1.4 Tailings dam in West Rand in 2016 (Source: Google Earth).

As an example of the financial benefit from reprocessing mine tailings, the Elikhulu project, which is estimated to cost approximately R2 billion, will process 179 million tonnes that were accumulated during Evander's history of gold mining and produce up to 50 000 oz per year from a reserve of 1.7 million oz mine (Pan African Resources, 2020). The BTRP produced 28,590 oz of gold at a remarkably low all-in-sustaining cost of $332 per oz (Pan African Resources, 2020). Additionally, gold production increased by 18% and led to self-sufficiency in a year and a half. Furthermore, the reprocessing of tailings from various plants is forecasted to continue until 2032, as shown in Figure 1.5.

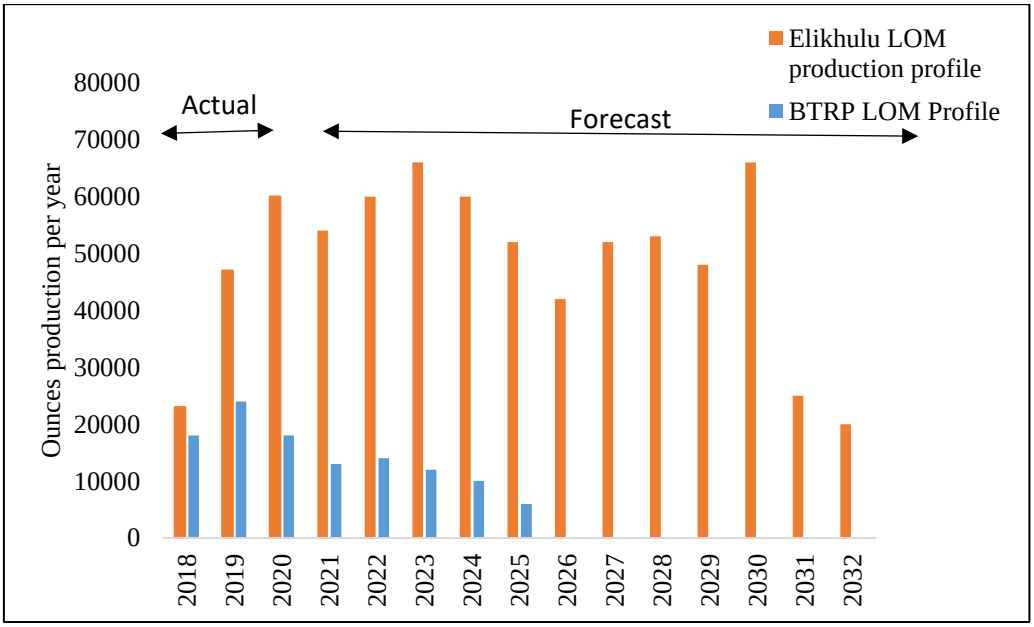

Figure 1.5 Graphical representation of the amount of gold expected to be produced per year at the Elikhulu and BRTP treatment facilities. LOM represents the life of mine (Pan African Resources, 2020).

Based on the information obtained on mine tailings and industry research, analytical techniques are necessary for the quantification of gold with the lowest measurement uncertainties. Additionally, few to no studies describe the outcomes of their method development without the corresponding uncertainties. In the analytical quantification of gold, the methods involved or used have associated errors that can be quantified and calculated as to how much they contribute to the final measurement value. This can lead to the identification of steps or methods that need improvement. This can also benefit the mining industry in reprocessing tailings for the reduction of the ecological footprint and to recover any lost gold. Therefore, this study looked into the quantification of gold from low-grade tailings using various methods together with the evaluation of the statistical measurement uncertainties.

1.3 Problem statement

The continued mining of gold in South Africa contributes significantly to the economy of the country. However, at the same time, it is leading to the increased production of mine waste or tailings, which tend to affect the environment in various ways. For example, they occupy a large amount of land, and toxic minerals can end up in nearby communities via airborne or water transportation. This has then sparked a shift from mining companies to re-mine the tailings in a bid to decrease the land they cover and to cut operation costs, safety concerns and their impact on nearby communities.

Subsequently, the challenge that was then encountered was for methods to extract and quantify the gold in an accurate manner, as it is in low amounts (low grade). Although methods such as fire assays are often problematic for low-grade samples, they can offer high errors. Therefore, this study looked into optimizing various methods and evaluating the uncertainties of these methods. This is important because it stands to lead to a high amount of tailings being recovered, with an accurate method, thereby holistically benefitting different sectors.

1.4 Aim

- The aim of the study was to develop an environmentally friendly, cost-effective and low measurement uncertainty-associated method for the quantification of gold from low-grade tailings.

1.5 Objectives

a. To characterize the mine tailings samples by X-ray diffraction and alkaline fusion to obtain the mineralogy.

b. The purity of the reagents was assessed by analysing the preparation blanks of the various methods by ICP–MS and ICP–OES to determine the purity of the reagents.
c. To determine the optimum method for analysis of gold, the following methods were used:
    - Fire assay
    - Acid dissolution with solvent extraction
    - Wet chlorination using sodium hypochlorite (NaOCl) and hydrochloric acid (HCl)
d. To quantitatively determine the gold in the tailings by employing gravimetric and instrumental determination using ICP–MS and ICP–OES;

- Gravimetric determination
- Instrumental determination using ICP–MS and ICP–OES

e. To evaluate the associated uncertainties in the investigated methods (fire assay and acid digestion.

1.6 Justification of study

With the depth of mining increasing (going deeper into the Earth), it is becoming impractical to mine further. Furthermore, large amounts of tailings are being produced in the process, which is not beneficial for the environment. The impacts or effects are reported to be the introduction of harmful compounds or substances into the environment, the cause of acid mine drainage, and the occupation of land that could be used for other purposes (Dold, 2014).

Therefore, it is important to shift the focus to tailings, as they might be of economic value. Having a practical method of determining gold and other valuable metals from tailings can lead to the optimum recovery of the minerals that were lost during the extraction and concentration process due to ineffective methods at that time. This can be a positive step into the reclamation of land occupied by tailings in South Africa, as there will be greater benefits.

In the analysis of mineral-containing ores, the contribution to the measurement uncertainties comes from all the steps involved, from decomposition to analysis. Usually, the handling and analysis of low-concentration samples often lead to high measurement uncertainties, depending on the tolerance. In the case of low-grade tailings, being able to determine the associated measurement uncertainties from different matrices can offer an improved understanding of the errors involved and the credibility or accuracy of the methods developed.

1.7 Novelty of the study

The variety of gold quantification methods focuses on medium- to high-grade ores, which allows for better recoveries. In this study, the focus was on developing methods for low-grade gold in tailings, as they will contribute significantly to the existing body of knowledge. This included investigating the use of small sample weights, less-invasive acid combinations and assessing the associated measurement uncertainties. The incorporation of the measurement uncertainty will provide guidance as to which method performs satisfactorily, which is important in the analytical chemistry world.

1.8 Structure of thesis

The thesis is structured as outlined.

Chapter 1: Introduction
The backdrop of the current issue and the research design are provided in Chapter 1.

Chapter 2: Literature Review
A review covering the occurrence of gold, mine tailings, and techniques for estimating the amount of gold in geological samples.

Chapter 3: *Statistical analysis*
This consists of a short review of measurement uncertainty and its evaluation.

Chapter 4: Acid digestion (Manuscript)
The methodology and strategy employed for the acid digestion studies as well as the measurement uncertainties were examined in this chapter.

Chapter 5: Fire assay (Manuscript)
In this chapter, the fire assay method by gravimetric analysis will be the focus, and the measurement uncertainties will be addressed.

Chapter 6: Chlorination (Manuscript)
Al look into the chlorination of the gold tailings sample.

Chapter 7: Conclusion and future prospects
A conclusion based on the three experimental chapters and future prospects.

1.9 References

Ahmari, S. and Zhang, L. (2012). Production of eco-friendly bricks from copper mine tailings through geopolymerization. *Construction and Building Materials*, *29*, 323–331. https://doi.org/10.1016/j.conbuildmat.2011.10.048

Dold, B. (2014). Evolution of acid mine drainage formation in sulphidic mine tailings. *Minerals*, *4*(3), 621–641. https://doi.org/10.3390/min4030621

DRDGOLD. (2016). *Sustainability*. https://www.drdgold.com/sustainability/tailings-management. Accessed: 16 September 2021.

Harmony. (2016). *Tailings management*. https://www.harmony.co.za/sustainability/environment/tailings-management/. Accessed: 16 September 2021

Hughes, A.E., Haque, N., Northey, S. A and Giddey, S. (2021). Platinum group metals: A review of resources, production and usage with a focus on catalysts. *Resources*, *10*(9), 1–40. https://doi.org/10.3390/resources10090093

Kossoff, D., Dubbin, W. E., Alfredsson, M., Edwards, S. J., Macklin, M. G and Hudson-Edwards, K. A. (2014). Mine tailings dams: Characteristics, failure, environmental impacts, and remediation. *Applied Geochemistry*, *51*, 229–245. https://doi.org/10.1016/j.apgeochem.2014.09.010

Li, C., Wen, Q., Hong, M., Liang, Z., Zhuang, Z and Yu, Y. (2017). Heavy metals leaching in bricks made from lead and zinc mine tailings with varied chemical components. *Construction and Building Materials*, *134*, 443–451. https://doi.org/10.1016/j.conbuildmat.2016.12.076

Luo, L., Li, K., Weng, F., Liu, C and Yang, S. (2020). Preparation, characteristics and mechanisms of the composite sintered bricks produced from shale, sewage sludge, coal gangue powder and iron ore tailings. *Construction and Building Materials*, *232*, 117250. https://doi.org/10.1016/j.conbuildmat.2019.117250

Mabaso, S. M. (2023). Legacy Gold Mine Sites & Dumps in the Witwatersrand: Challenges and Required Action. *Natural Resources*, *14*(05), 65–77. https://doi.org/10.4236/nr.2023.145005Mia Breytenbach. (2016). Gold tailings retreatment an attractive proposition in current environment. *Mining Weekly*.

https://www.miningweekly.com/print-version/south-africa-has-absolute-potential-for-vibrant-sustainable-tailings-projects-industry-players-2016-10-14. Accessed: 20 May 2023

Mineral Council Siuth Africa (2023). Gold. https://www.mineralscouncil.org.za/sa-mining/gold. Accessed: 15 November 2023.

Natural-resources. (2023). *Platinum facts*. https://natural-resources.canada.ca/our-natural-resources/minerals-mining/minerals-metals-facts/platinum-facts/20520. Accessed: 20 May 2023

Neingo, P. N and Tholana, T. (2016). Trends in productivity in the South African gold mining industry. *Journal of the Southern African Institute of Mining and Metallurgy*, *116*(3), 283–290. https://doi.org/10.17159/2411-9717/2016/v116n3a10

Pan African Resources. (2020). *Barberton Tailings Retreatment Plant*. https://www.panafricanresources.com/btrp/. Accessed: 16 September 2021

Rösner, T and Van Schalkwyk, A. (2000). The environmental impact of gold mine tailings footprints in the Johannesburg region, South Africa. *Bulletin of Engineering Geology and the Environment*, *59*(2), 137–148. https://doi.org/10.1007/s100640000037

Scheepers, L., & Malan, D. F. (2022). A case study of geotechnical conditions affecting mining-induced seismicity in a deep tabular mine. *Journal of the Southern African Institute of Mining and Metallurgy*, *122*(3), 115–124. https://doi.org/10.17159/2411-9717/1511/2022

Torres-Cruz, L. A and O'Donovan, C. (2023). Public remotely sensed data raise concerns about history of failed Jagersfontein dam. *Scientific Reports*, *13*(1), 4953. https://doi.org/10.1038/s41598-023-31633-5

Zhu, M., Wang, H., Liu, L. L., Ji, R and Wang, X. (2017). Preparation and characterization of permeable bricks from gangue and tailings. *Construction and Building Materials*, *148*, 484–491. https://doi.org/10.1016/j.conbuildmat.2017.05.096

2 LITERATURE REVIEW

2.1 Literature review on gold

2.1.1 Gold

In South Africa, gold is mainly mined from the Witwatersrand Basin (Wits basin), which is situated in Johannesburg, Gauteng, the Ventersdorp Reef (VCR), which is situated alongside the Wits basin, and the Greenstone belt (GSB), which is situated in Barberton, Mpumalanga.

Witwatersrand basin

The Witwatersrand basin (Figure 2.1) is the largest gold field in the world, from which over 52 000 tonnes of gold were sourced. It is estimated that approximately 30 000 tonnes of gold remain in the basin. Seven significant conglomerate reefs, including Evander, East Rand, Central Rand, West Rand, West Wits, Klerksdorp, and Welkom, make up the basin. According to reports, the Central Rand Super group holds the majority of the gold (Tucker *et al*., 2016).

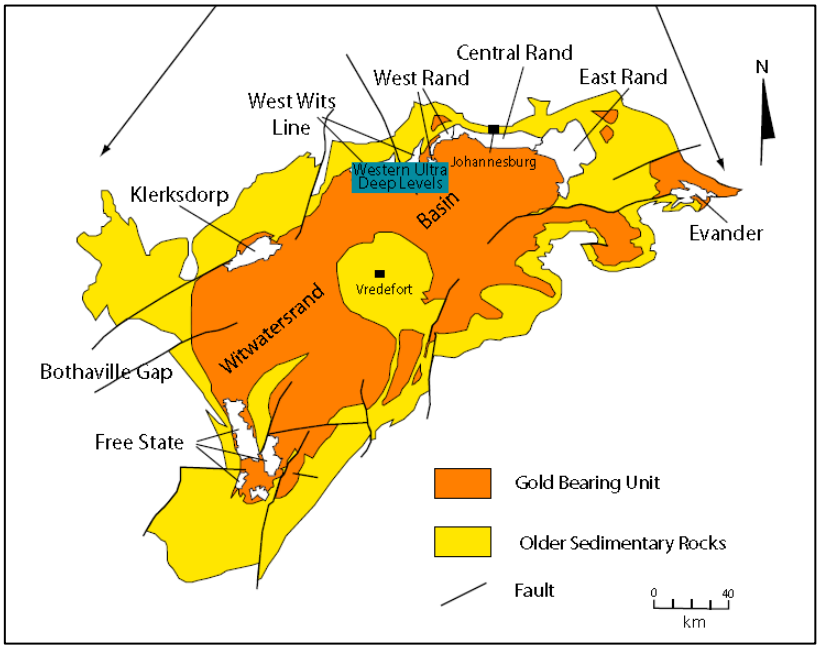

Figure 2.1 Map of the Witwatersrand basin (da Costa *et al.*, 2020).

Ventersdorp Contact Reef (VCR)

This reef is the basal conglomerate of the overlying Ventersdorp formation at the base of the Ventersdorp Supergroup and is identified as part of the Witwatersrand basin. The VCR (Figure

2.2) is one of the major gold-bearing regions in the Witwatersrand, with an estimated gold grade of 5-12 $g.t^{-1}$ (Birch, 2022).

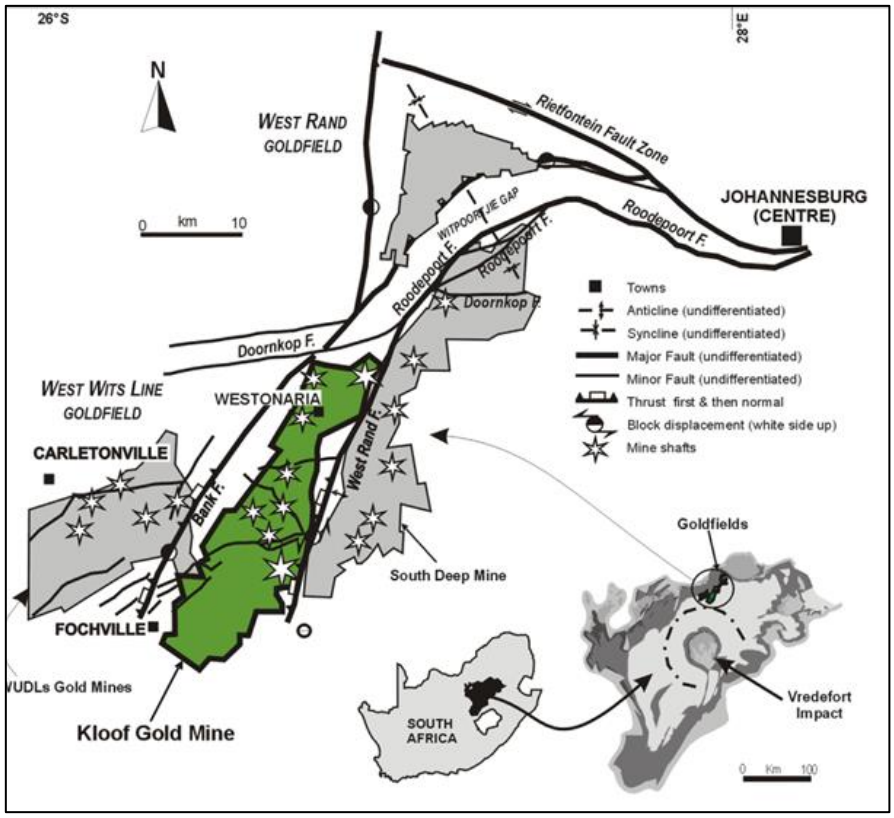

Figure 2.2 Map of the Ventersdorp Contact Reef (Manzi *et al.*, 2014).

2.2 Literature review on tailings

Tailings are defined as the material that remains from the ore after the extraction of various minerals such gold and often consists of the chemicals used during the extraction processes (Hudson, 2001). In most cases, valuable minerals exist in the earth's crust in small concentrations, resulting in many tailings being produced to obtain a low quantity of minerals. Previous studies by Lottermoser (2007) reported that the ratio of gold to gangue material is 10:1. With the grade of minerals such as gold decreasing, it is expected that the ratio will increase in favour of the gangue. In Australia, the grade of copper decreased by 1% from 10% between 1885 and 2005, whereas in Canada, the nickel grade dropped by 1.5% from 5% in the same years (Giurco *et al.*, 2009). For gold, it is reported that the amount of tailings to concentrate is higher than that of base metals because they already exist in parts per million amounts in nature, with the grade expected to fall to 2 $g.t^{-1}$ by the year 2050 (Giurco *et al.*, 2009).

The composition of tailings is dependent on the mineralogical makeup of the ore body, the processing chemicals, and the efficiency of extraction and weathering (Kossoff *et al.*, 2014). The most abundant minerals that are typically found in tailings are quartz and pyrite, along with base metals such as aluminium, calcium, magnesium, manganese, sodium, phosphorus, titanium and sulfur (Table 2.1) (Kossoff *et al.*, 2014). Most studies have looked into quantifying toxic elements such as arsenic, copper, lead and zinc from tailings (Hudson-Edwards *et al.* 2003). In the mineralogical characterization of tailings from AngloGold Ashanti and base metal extraction by Malatse and Ndlovu (2015), it was found that SiO_2 is the major mineral in the gangue fraction and minerals such as calcite and dolomite in the minority. Secondary minerals also form from tailings, and the composition of these minerals depends on the mineralogy of the source and environmental conditions such as pH and climate. Examples of these are geothite, scondite, etc. (Kossoff *et al.*, 2014).

Table 2.1 South African tailings characterization from the literature.

Mine or Matrix	Minerals	Elements	Reference
Louise Moore mine	Dolomite, Mica, Amphibole, Serpentine, Smectite, Quartz	As (277), Au (0.37), Cd (0.4), Cr (359), Fe (40,47), Ni (224)[*]	(Singo & Kramers, 2021)
Gold mine in Krugersdorp		Zn>Ni>Co>As>Pb>Cd	(Omotola Fashola *et al.*, 2020)
East Rand basin	Quartz, Magnetite, Marcasite, Kyanite, Gupeite, Magnesioferrite	Si (45.98), Al (2.35), K (1.29), Fe (0.99), Ti (0.42), Mg (0.27), Ca (0.16)[#]	(Okereafor *et al.*, 2020)
AngloGold Ashanti	SiO_2 (77.7), Al_2O_3 (10.2), Fe_2O_3 (4.51), CaO (1.93), Ti (0.47)[#]		(Malatse & Ndlovu, 2015)
Witwatersrand basin	Quartz (58-82), Mica (3-10), Chlorite (3-10)[#]		(Nengovhela *et al.*, 2006)
West rand basin	SiO_2 (36.6), Al_2O_3 (7.25), Fe_2O_3 (4.27), CaO (0.68), TiO_2 (0.27)[#]		(Gcasamba *et al.*, 2019)

Ventersdorp Contact Reef	Quartz, muscovite, chalmosite, gypsum, pyrite, talc	As (0.088), Si (34), Fe (3.4), Al (3.4), Mg (0.97), Ti (0.23)[#]	(Mashale *et al.*, 2023)

[*]Unit: $\mu g.g^{-1}$, [#]Unit: %

2.2.1 Type of tailings

As mentioned in Section 2.2, tailings are generated as a result of extraction processes applied on the ore, which includes cyanidation, flotation and gravity concentrating. In Table 2.2, the different types of tailings and the processes from which they are generated are shown.

Table 2.2 Types of tailings emanating from different mineral processing techniques.

Type of tailings	**Formation**	**Reference**
Gravity concentration tailings *Gravity concentration: the process by which particles of different sizes, shapes and densities are separated from each other by the force of gravity.*	**Fine gold** is usually too small to be recovered by installed equipment.	(Marsden and House, 2006)
	Flaky gold which presents a large surface area in one plane and carried away with the lighter particles.	
	Hydrophobic gold that adheres to the water–air interface, giving the gold particle an artificially low density.	
	Unliberated gold which is associated with oxides, silicates or sulfide gangue.	
Cyanidation tailings *Cyanidation: a hydrometallurgical technique for extracting or leaching gold from ores by converting the gold to a water soluble complex.*	**Free or exposed gold** that is too coarse to dissolve in the initial process.	(Marsden and House, 2006)
	Gold locked in silicates or oxide gangue	
	Gold encapsulated within unreactive and nonporous sulfide grains such as pyrite.	

	Gold coated with iron-oxides or hydroxides which are formed by dissolution or precipitation reactions.	
Flotation tailings *Flotation: Separates concentrate ores by changing their surface*	Sulfide gold tailings coated in nonfloatable material such as iron oxides and silicates or if associated with nonhydrophobic materials.	(Marsden and House, 2006)

2.2.2 Storage of tailings

Various ways exist in which tailings can be stored, which is extremely important. These include storing as slurries or as dried material in storage dams (Kossoff *et al.*, 2014), with the former being the most used. Most of the impoundments are constructed near water sources to prevent dust from emerging from the tailings surface and possible acid mine drainage (Kossoff *et al.*, 2014). In some cases, due to poor construction, the dams fail, leading to major environmental effects. The most adverse impacts are that the failures lead to the discharge of toxic elements into river systems, which affects water and sediment quality, impacting the ecosystem. In South Africa, gold tailings dams failed in 1994 due to a breach following heavy rains, and 600 000 m^3 of tailings were released into the community of Merriespruit (Fourie *et al.*, 2001). This led to the death of 17 people due to drowning and suffocation. In another failure in Spain in 1998, 1.3 x 10^6 m^3 of Ag, Cu, Pb and Zn tailings were released into a river, and the entire fish and shellfish population was killed (Hudson-Edwards *et al.*, 2003). In a more recent incident, a tailings dam storing mine waste from a diamond mine collapsed in September 2022 in the Free State, South Africa. This led to one death and several injuries with houses destroyed (Torres-Cruz & O'Donovan, 2023). These are examples of fatalities that are a result of tailings dam failures, which shows how dangerous they are. However, once they dry, tailings still pose a threat with dust to surrounding communities and AMD leaching that has toxic metals.

2.3 Sampling methods

In the handling of a small sample from a larger original sample, it is important to have a sample that is a representation of the bulk sample, which will influence the homogeneity. Depending on the method and application, there are various methods for splitting the bulk sample. Splitting

the bulk sample also allows for the assessment of the sample homogeneity across the fractions before proceeding with other methods.

a. Riffle splitting

   This involves the splitting of the sample using chutes that move in alternative directions, resulting in two randomly divided equal-sized fractions (Petersen *et al.*, 2004). This process can be repeated until the preferred size is obtained. The riffle splitting method is reported to have a relative standard deviation (RSD) of 1% (Petersen *et al.*, 2004).

b. Rotary splitting

   In this method, the sample is fed into a feed hopper and split into rotating bins at a uniform rate using a vibratory feeder (Nenuwa *et al.*, 2018). These bins can be set to collect the sample more than once until the preferred sample size is obtained. The percent RSD for the rotary splitting method is 0.1% (Nenuwa *et al.*, 2018).

c. Cone and quarter

   This method is optimum for large samples, whereby the sample is shovelled into a uniform conical shape pile, then flattened and divided into four sections using two boards (Taggart, 2009). As expected, this method has a high percent RSD of 7% (Taggart, 2009).

d. Grab sampling

   In grab sampling, the homogenized sample is placed on a rolling mat, and random portions are taken using a spatula or a shovel, depending on the sample size (Petersen *et al.*, 2004). This method is reported to have a relative standard deviation of 5% (Petersen *et al.*, 2004). Although faster and cheaper, the grab sampling splitting method introduces a significant amount of errors.

e. Slurry splitting

   In slurry splitting, the homogenized sample is mixed with water to form a slurry that is put through a rotary splitter at a slower rate than the dry samples.

2.4 Sample size

When dealing with geological samples, the amount or mass of the sample being sampled for analysis is crucial, as it can severely affect the subsequent analysis. According to the study of Stanley (2007), the sampling error contributes more to the component errors in the determination of gold from various ores than the actual analysis (Stanley, 2007). This is mainly

because gold is inhomogenously distributed in the ore and the gold particles usually form nuggets, which are when the gold particles form clumps (Stanley, 2007). An example of a nugget effect is usually seen when the sample is analysed in duplicate and the results are not comparable. However, such problems are rarely encountered in the analysis of base metals because the ore grains containing them are more abundant than those containing gold (Stanley, 2007).

Various ways exist to try and ensure that, first, the sample is homogenous and that the right amount of the sample is taken, which will guarantee satisfactory homogeneity with the lowest measurement uncertainties. One method used to reduce or avoid large sampling errors is to have a sufficient number of replicates, but this often leads to biases in the interpretation of the data, especially when the sample is unknown (Mao *et al.*, 2013). The other method includes screening the sample for particle size, either using the old sieve analysis method or by using instrumental analysis such as the Malvern Mastersizer. These tests allow for the establishment of the particle sizes, and if the particle size is not satisfactory, the sample is subjected to milling to make it finer. In the literature, it is reported that for the analysis of gold, the finer the material is, the greater the chances of eliminating the nugget effect and obtaining improved homogeneity (Mao *et al.,* 2013).

Furthermore, the homogeneity of the sample after carrying out certain chemical analyses can be quantified using the homogeneity indicator (Equation 2.1). This homogeneity indicator is calculated using the equation below, where *RSD* is the rsd calculated from the repetitive measurements and *m* is the mass that was weighed. A value of less than or equal to 10 indicates that the sample is of satisfactory homogeneity (Mao *et al.,* 2013).

$$H_E = (RSD) \times \sqrt{m} \qquad \textit{Equation 2.1}$$

Upon determining the relative homogeneity, Pauwell's equation (Equation 2.2) can be used to establish the minimum sample mass, which is the smallest accurate fraction of the bulk that may be regarded as representative at a certain measurement uncertainty (Mao *et al.,* 2013).

$$M = \left(\frac{K_2' \times \%RSD)}{UNC}\right) \times m \qquad \textit{Equation 2.2}$$

where K'_2 is a factor for tolerance limits for a 2-sided normal distribution and UNC is the needed uncertainty in that specific chemical analysis.

2.5 Characterization techniques

2.5.1 Mineralogical composition

Mineralogical information was obtained using XRD. When equipped with the X'Pert Highscore plus software and PAN-ICSD, this technique can give the dominant minerals together with the quantitative results.

2.5.2 Elemental composition

Determination of the elemental composition of the samples is important in the characterization stage, as it provides information on what the sample contains. This is mostly important in the selection of the subsequent methods downstream of characterization. In this case, the common methods employed to decompose geological samples are alkaline fusion and acid digestion, which are analysed by ICP–MS, ICP–OES, atomic absorption spectroscopy (AAS) and pressed pellets or fused beads, which are analysed by X-ray fluorescence (XRF).

2.5.2.1 Sample preparation

Alkali fusion

This method includes the fusing of the sample on an open flame in a crucible using flux reagents such as sodium carbonate (Na_2CO_3), sodium peroxide (Na_2O_2), lithium metaborate ($LiBO_2$), lithium borate (LiB_4O_7), potassium borate ($K_2B_4O_7$), potassium hydroxide (KOH) and sodium hydroxide (NaOH) (Liu *et al.*, 2019). Although all the reagents serve their purpose, Na_2CO_3 and Na_2O_2 are the most preferred, as they can readily decompose refractory minerals such as zircon. The alkali fusion method offers advantages such as time efficiency, as it is usually short, works for refractory minerals and has high decomposition efficiencies, as it is at high temperatures (Enzweiler & Potts, 1995). Due to the high flux-to-sample ratio, it often leads to high blanks with high total dissolved solids (TDS), which becomes a problem during instrumental analysis. However, this is often overcome by dilution of the melt in high volumes. For example, a 0.2 g sample plus flux is usually dissolved into a 200 mL volumetric flask. Furthermore, gel-like insoluble silicates can form in the process, which introduces difficulties during analysis (Liu *et al.*, 2019).

Acid digestion

In this method, the samples are digested by acid attack from the use of various acids, such as HCl, nitric acid (HNO_3), perchloric acid ($HClO_4$) and hydrofluoric acid (HF) (Liu *et al.*, 2019). These can be through an open vessel or a closed vessel, which offer different advantages. These acids can be used in their individual form or a mixed form. For example, HCl, HNO_3, $HClO_4$ and HF are often used as a combination, and HF has the added advantage of being able to

decompose silicates (Wang *et al.*, 2016). This decomposition allows for decreased spectral interference and the liberation of minerals that were enclosed in the silicates (Balaram & Subramanyam, 2022). However, other minerals, such as zircon, might be partially digested, as the maximum temperature is determined by the boiling point of the acid combination, in which case, zircon might need high temperatures (Balaram & Subramanyam, 2022). Furthermore, this method can be performed in close vessels, such as microwave-assisted digestion, in which the sample and the acids are added into a microwave vessel and digested for a certain time. This has an advantage of short digestion times and a minimum amount of reagents used (Wang *et al.*, 2016). However, this can also be limiting, as some minerals require longer digestion times.

2.6 Determination of gold in high- and low-grade samples, including mine tailings

In most cases, the valuable metals are deposited in the ore, which needs to be decomposed and concentrated to separate the minerals from it and quantify thereafter. With high-grade ores, the conventional method to use is the fire assay (FA), which has worked for decades. However, other alternatives, such as dry or wet chlorination, thermochemistry and dissolution, have been applied successfully in high-grade ores and a few low-grade ores (Table 2.3). Alternative methods were employed to minimize the errors that FA introduces and to reduce the time needed for FA. However, with tailings, which are expected to be very low grade, there is limited research on whether FA is still the optimum method and whether it can be determined gravimetrically. There is also limited research on whether the characteristics of the ore change significantly after being chemically processed, which subsequently influences the selection of the decomposition and analysis methods.

2.6.1 Fire assay

Fire assay is a decomposition (and concentrating) method that has been used for decades. It involves fusing the sample at temperatures of at least 1100 °C with a flux that contains a collecting medium such as lead oxide (Figures 2.3) (Rao and Reddi, 2000). The fused mixture is then poured into iron molds to allow for cooling and phase separation, upon which the gold-containing button is separated from the slag in a process called deslagging. The button is subsequently put on a cupel and heated at 1000 °C (Figure 2.4), in which the lead and other base metals are removed from the gold as oxides. The prill that is obtained after cupellation is then subjected to further chemical analysis, either instrumental or gravimetric analysis. Lead FA (Pb-FA) is usually used for the collection of gold, platinum and palladium (Rao and Reddi, 2000). FA is the most preferred decomposition method because it can handle large samples and

allows for complete separation of the gold from the gangue material (Rao and Reddi, 2000). In a study by Rabatho *et al.* (2010), before subjecting low-grade tailings to FA, gold was concentrated using magnetic separation, and grades of 0.7 and 0.2 $g.t^{-1}$ were reported for gold and palladium (Pd). Subsequently, the decomposed samples are concentrated using methods such as adsorption and precipitation to gravimetrically or instrumentally determine gold using ICP–OES/MS and AAS, among others (Wang *et al.*, 2016). Many studies prefer instrumental analysis, as it is much easier and multiple elements can be determined, with low detection limits. There is limited information on the gravimetric determination of gold from low-grade tailings.

Since it can handle large samples, it can be assumed that FA can be applied for low-grade ores. However, it also requires an extremely experienced assayer, as errors in the fluxes and masses added can lead to incomplete collection of metals. Common problems encountered with FA include the prolonged time of dissolving the button, which can lead to low recoveries in the case of incomplete dissolution (Rao and Reddi, 2000). However, various studies have looked into using tellurium and stannous chloride to precipitate out the gold, which leads to improved collection efficiencies (Jackson *et al.*, 1990, Morcelli *et al.*, 2004).

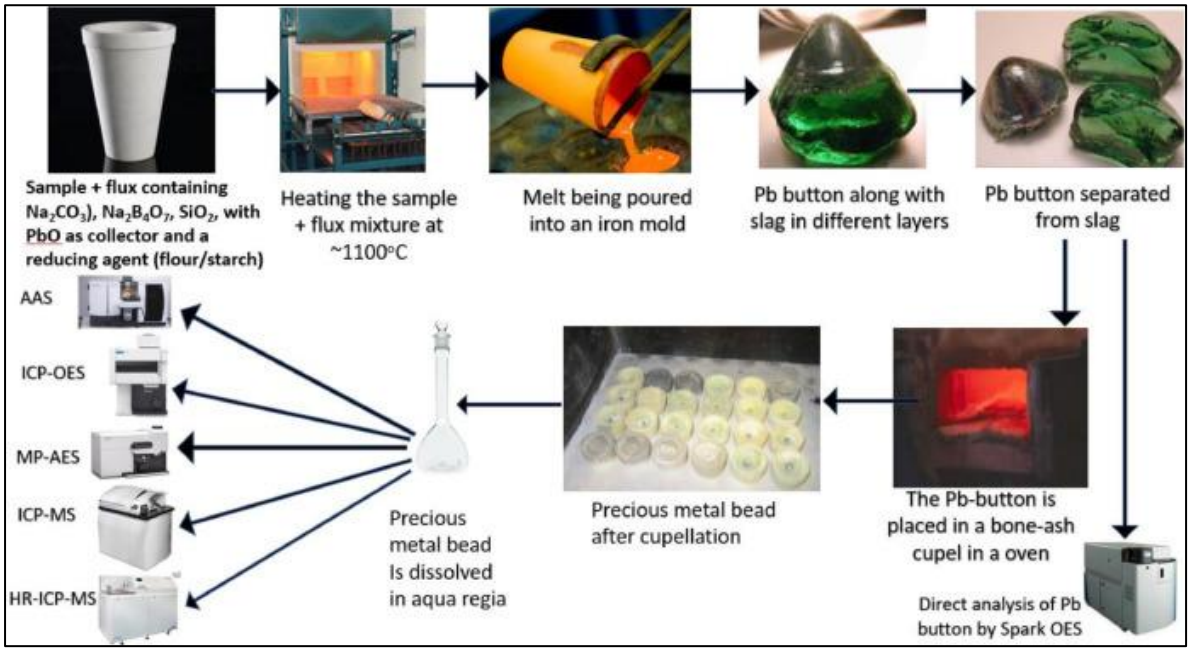

Figure 2.3 Schematic diagram of the fire assay process and its various finishes (Balaram & Subramanyam, 2022).

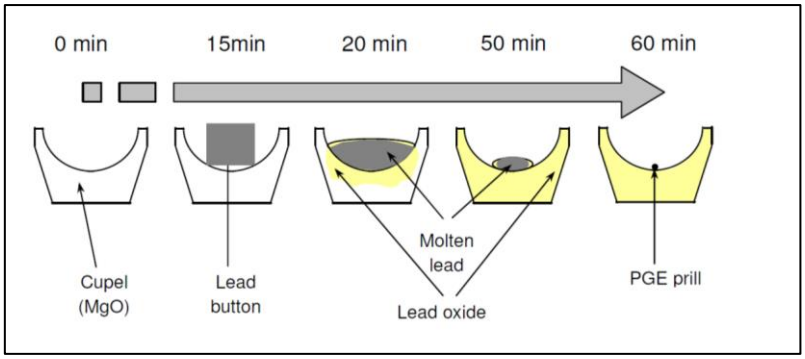

Figure 2.4 Diagram of cupellation during the fire assay (Mcintosh, 2004).

Components of fire assay flux

In the fire assay, the flux is the main component of the process, as it contains reagents that ensure that the process occurs efficiently. The flux assists by leading to the formation of two phases: a liquid borosilicate slag that contains everything except for the noble metals and a liquid lead phase that contains the noble metals.

Litharge (PbO) is the source of the metallic lead that is responsible for collecting gold, which is reduced by carbon from maize or flour (Equations 2.3 to 2.5). This process of reduction occurs in the presence of oxygen, which enters the furnace through an opening, and the reduction follows the following reactions:

$$2C_{(s)} + O_{2(g)} \rightarrow 2CO_{(g)} \qquad \textit{Equation 2.3}$$

$$CO_{(g)} + 0.5O_{2(g)} \rightarrow CO_{2(g)} \qquad \textit{Equation 2.4}$$

$$PbO_{(s)} + C_{(s)} \rightarrow Pb_{(l)} + CO_{(g)} \qquad \textit{Equation 2.5}$$

In addition to being a collector, PbO can destroy any sulfides in the sample and functions as an oxidant, allowing gold encapsulated by sulfides such as pyrite to be liberated, as in Equations 2.6 and 2.7 (Mcintosh, 2006). Furthermore, the litharge reacts with the slag to form lead silicates, which ensure the homogeneity and fluidity of the slag; therefore, the amount of lead started with is not 100% recovered.

$$3PbO_{(s)} + FeS_{(s)} \rightarrow 3Pb_{(l)} + FeO_{(g)} + SO_{2(g)} \qquad \textit{Equation 2.6}$$

$$PbO_{(s)} + SiO_{2(s)} \rightarrow PbSiO_{3(g)} \qquad \textit{Equation 2.7}$$

Most importantly, the targeted analytes must be soluble in the lead collection phase to be quantitatively collected.

The other constituents of the flux that are common;

- Na_2CO_3 is a basic compound that reacts with silica-based minerals to form a fusible sodium silicate. It also acts as a desulfurizing and oxidizing agent. Sodium carbonate also decreases the melting points of the minerals in the samples so that fusion can occur (Mcintosh, 2006). For example, quartz melts at 1700 °C by itself, but when reacted with sodium carbonate, the melting point decreases to 790 °C (Figure 2.5).

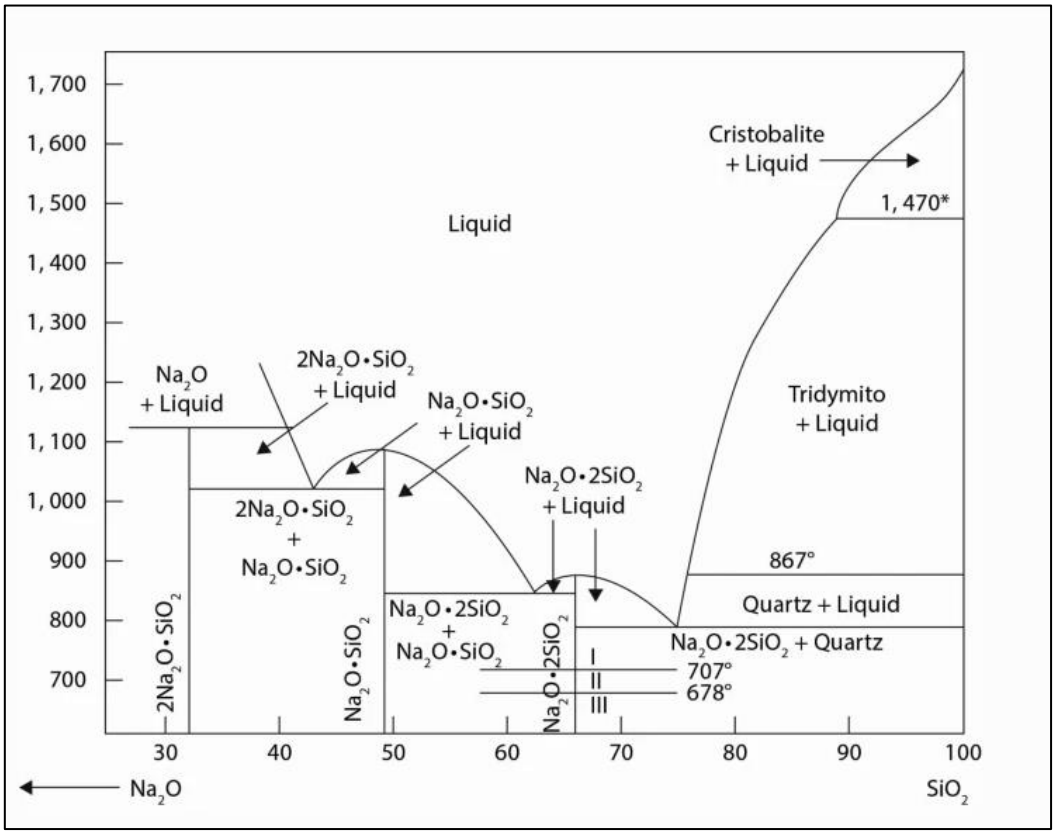

Figure 2.5 Phase diagram of the Na_2O-SiO_2 (mass-%) system (Vadász *et al.*, 2019).

- Quartz (SiO_2): SiO_2 is a strong oxidizing agent that forms silicates, which are the basis for the formation of slag. It can also protect crucibles from the corrosive action of litharge.
- Borax glass or fused borax ($Na_2B_4O_7$): a strong oxidizing agent that lowers the temperature of fusion so that the slag can form and it fluxes metal oxides well (Equation 2.8). It also increases the fluidity of slags, thereby making pouring easier.

$$B_2O_{3(s)} + CaO_{(s)} \rightarrow CaO.B_2O_{3(l)} \qquad \textit{Equation 2.8}$$

- Calcium fluoride (CaF_2): increases fluidity and helps with difficult pours.
- Reducing agent (maize meal or flour): source of carbon that reduces the PbO to Pb to enable it to collect the noble metals.

It has been reported by Rao and Reddi (2000) that the flux constituents have to be in certain amounts concerning each other for maximum collection of the targeted metals. However, the ratio of the litharge to reducing agent (PbO:C) is of utmost importance, as the reaction that occurs, which leads to the production of lead rain, is crucial in the collection of the targeted analytes by lead.

2.6.2 Chlorination

Chlorination of ores is a metallurgical process that involves treating ores with sources of chloride ions, which produces chlorinated metal complexes that are often soluble in most solvents (Atasoy, 2002). Chlorinated metal complexes usually have different properties from their precursor, such as high volatility, low melting point, water solubility and ease of reduction, which leads to the ultimate aim of separating them from gangue or other metals. Chlorination is the preferred leaching method because it is environmentally safer than cyanidation (Baghalha, 2007).

Chlorination can occur in a dry environment (Figure 2.6), whereby chlorine gas is used as the source, or in a wet environment (Figure 2.7), whereby HCl, sodium chloride (NaCl), or ammonium chloride (NH_4Cl) are used as the source of the chloride ions (Atasoy, 2002). Chlorination offers the advantage of being applied to low-grade ores and allows for large sample masses of up to 250 grams (Rao and Reddi, 2000), resulting in detection limits ranging from 0.06 $ng.g^{-1}$ to 0.25 $ng.g^{-1}$ for platinum. In Baghalha (2007), calcium hypochlorite ($Ca(OCl)_2$) vs sodium hypochlorite (NaOCl) were used for a gold sample of 1-2 $g.t^{-1,}$ and the maximum gold recovered was 58% after 48 h of $Ca(OCl)_2$, while with NaOCl, the leaching time was 24 h under acidic conditions. However, in Fu *et al*. (2017), where NaOCl was used, good recoveries of at least 60% were obtained under alkaline conditions. In a study by Matsau and Koch (2003) that looked into a method that excludes FA, it was found that chlorination under specific conditions was able to determine the targeted gold from an ore.

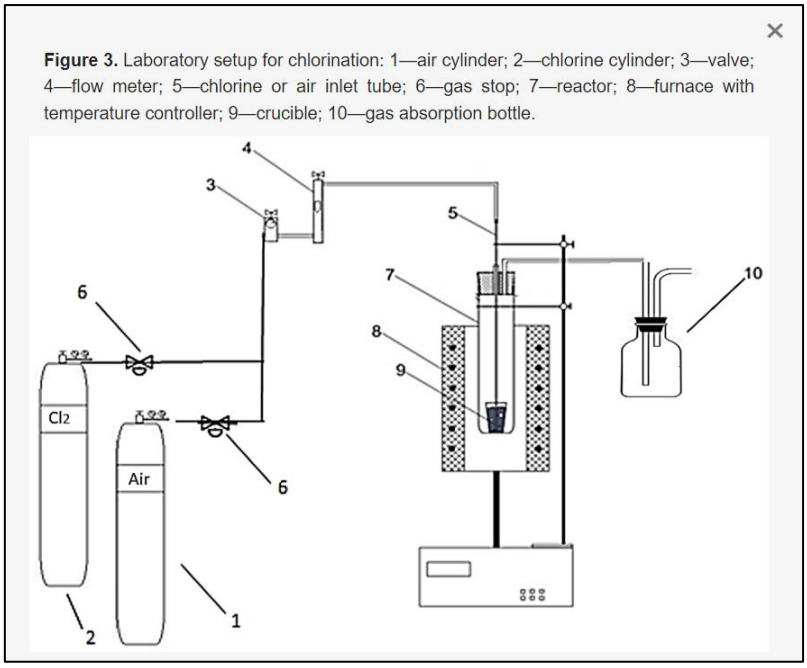

Figure 2.6 Process of dry chlorination (Dosmukhamedov *et al.*, 2022).

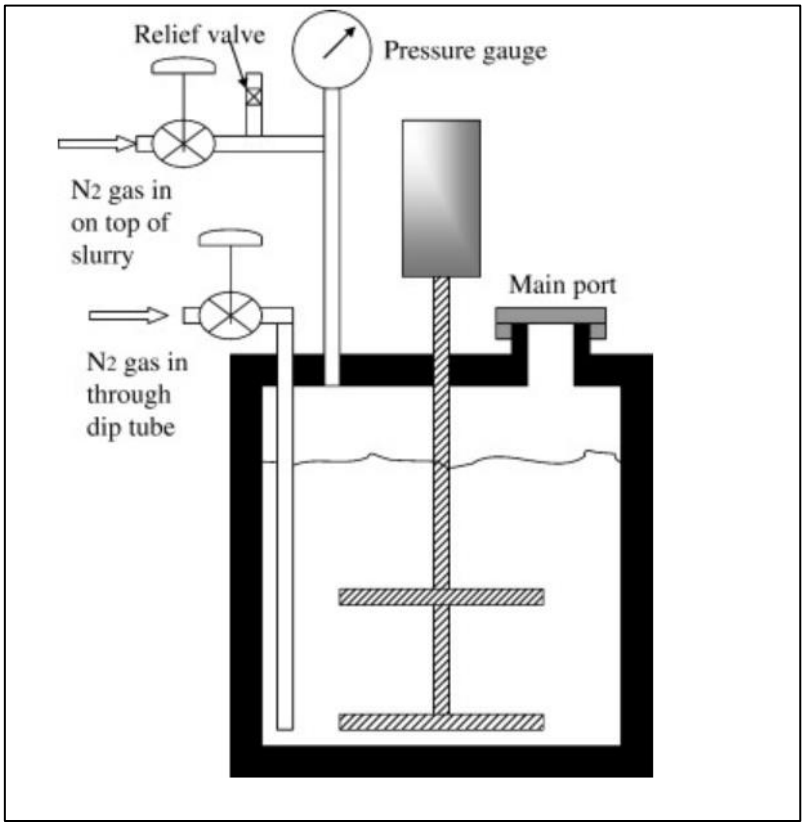

Figure 2.7 Process of wet chlorination. The reaction vessel consists of the sample slurry and NaOCl and HCl (Baghalha, 2007).

2.6.3 Acid dissolution/digestion

This is based on the fact that gold can be digested in acids such as HF, HCl, $HClO_4$, bromide (Br_2) and hydrogen peroxide (H_2O_2) under specific conditions. However, the extraction of gold

from geological samples using acids is often not satisfactory, as minerals such as braggite and copper do not dissolve in HCl and HNO_3, matrices of chromite are also resistant to acid attack, and sulfur-rich samples have fine-sized particles, which hinders high recoveries. A previous study by Matsau and Koch (2003) reported a roasting process that was added before acid dissolution to help with the mentioned problems, and high extractions were obtained.

2.6.4 Solvent extraction

Solvent extraction of gold from solutions as a method of preconcentration has gained popularity because it is easy to carry out and offers high extraction efficiencies (Nguyen *et al.*, 2016). In Nguyen *et al.* (2016), reagents such as tri-butyl phosphate and quaternary ammonium salts such as Aliquat-336 in diisobutyl ketone (DIBK) were used for the selective extraction of Au(II) from an HCl solution. In another study by Radzyminska-lenarcik *et al. (*2021), gold was concentrated and extracted using a new amine derivative, β-diketone, while a greener solvent, diethyl carbonate, was evaluated in Raiguel *et al.* (2020). Both studies reported extraction efficiencies of over 80%. Other extractants reported to offer high recoveries are N-n-octylaniline, amilorie monohydrochloride, etc.

2.6.5 Adsorption

Ion exchange is often used where solvent extraction is lacking, whereby a reversible exchange of ions takes place between a solid and liquid phase of ion exchangers during two sequential processes, namely, adsorption and elution. According to Izatt *et al.* (2012) and Izatt *et al.* (2015), Au, Pd, platinum (Pt), iridium (Ir), and rhodium (Rh) were sequentially separated using Superlig resins with varying affinities, whereas in Komendova (2020), preconcentration of gold was achieved using the Strata SDB-L sorbent. However, it offers the benefits of concentrating selected elements to measurable levels and can also remove sample matrices that often contribute to interferences during instrumental analysis. The drawbacks of this technique are that repetitions are often necessary to achieve complete removal of base metals.

Table 2.3 Methods commonly employed in the decomposition of gold in various ore bodies.

Method	Key reagents	Sample mass, g	Analysis method	Reference
Lead FA	Pb/Na_2CO_3,$Na_2B_4O_7$,SiO_2,flour	10-30	ICP–MS	(Hall & Pelchat, 1994)
Lead FA	Pb/Na_2CO_3,$Na_2B_4O_7$,SiO_2,flour	50	FS-LA-ICP–MS	(Bédard & Barnes, 2002)
Lead FA	Pb/Na_2CO_3,$Na_2B_4O_7$,SiO_2,flour	10-20	HRCS-GFAAS	(Ni *et al.*, 2019)
Lead FA	Pb/Na_2CO_3,$Na_2B_4O_7$,SiO_2,flour	15	ICP–MS	(R. Juvonen *et al.*, 2002)
Precipitation	Hydroxylamine hydrochloride	0.2	Gravimetry	(Singh, 2012)
Alkaline fusion with ion exchange	Na_2O_2	0.5	GF-AAS	(Enzweiler & Potts, 1995)
Alkaline fusion with Se-Te coprecipitation	Na_2O_2/$NaKCO_3$/KOH	1-20	ICP–MS	(Amassé, 1998)
Alkaline fusion with Te precipitation	Na_2O_2	2	ICP–MS	(Jin & Zhu, 2000)
Acid digestion with Te coprecipitation	HF+ HCl+HNO_3	2-5	GF-AAS	(Gupta, 1989)
Acid digestion with Te precipitation	HNO_3+HF+$HClO_4$+HCl	0.3-1.3	INAA	(Elson & Chatt, 1983)
Acid digestion with Hg precipitation	HCl+HNO_3	0.5	GF-AAS	(Niskavaara & Kontas, 1990)
Acid digestion with solvent extraction	HCl+HNO_3 MIBK	0.1-2.0	GF-AAS	(Terashima, 1988)
Acid digestion with solvent extraction	HNO_3+HF+HCl DLLME	0.02	GF-AAS	(Fazelirad *et al.*, 2014)
Acid digestion with solvent extraction	HCl+HNO_3	10	GF-AAS	(Monteiro *et al.*, 2003)
Acid digestion with solvent extraction	HBr +Br_2	5-10	GF-AAS	(Chattopadhyay & Sahoo, 1992)
Acid digestion	HCl+HNO_3	10	GF-AAS	(Liu *et al.*, 2013)
Acid digestion	HNO_3+HF+HCl+AR DIBK-loaded CG71 resin	4	ICP–MS	(Pitcairn *et al.*, 2006)
Acid digestion (MW)	HCl+HNO_3 Single granular carbon	0.2	GF-AAS	(Hassan *et al.*, 2011)
Acid digestion (MW)	HCl+HNO_3 Modified carbon nanotubes	0.5	SS-HR-CS-GF-AAS	(Dobrowolski *et al.*, 2017)

Acid digestion	$HCl+HNO_3$ Magnetic nanoparticles	5-10	FI-column-GF-AAS	(Ye *et al.*, 2014)

#Based on determining the purity of the gold

2.7 Quantitative determination of gold

Following the procedures above, the gold can be quantitatively determined using techniques such as instrumental and gravimetric analysis.

2.7.1 Instrumental analysis

For decades, gold has been and still is determined mainly on instruments such as ICP–OES or ICP–MS, AAS, LA-ICPMS. The common advantage of instrumental analysis is that multiple elements can be determined simultaneously; hence, most studies use this technique (Jarvis *et al*., 1995; Juvonen *et al*., 2004; Morcelli *et al.,* 2004). Instruments such as ICP–OES and ICP–MS have detection limits as low as 10 µg. L^{-1} (Komendova, 2020). For F-AAS, the detection limits range from 3 to 500 µg. L^{-1} (Komendova, 2020). Disadvantages of instrumental analysis include the costs associated with performing the analysis and the expertise of the analyst, which is important in the correct interpretation of the results. Table 2.4 shows the various instrumental techniques and their limits of detection.

2.7.2 Gravimetric analysis

Gravimetric analysis, whereby it is determined by weight, is an easy and cost-effective procedure. However, it can be challenging in regard to the determination of gold that is in association with platinum group metals (PGMs). Studies such as Vasekina *et al.* (2014) and Singh (2012) have quantified gold using gravimetry through the use of hydroxylamine hydrochloride. In Singh (2012), gold was gravimetrically quantified from a gold metal by reduction in a zero-valent state by hydrolamine hydrochloride, and it was found to be a rugged and precise method, offering low uncertainties. The biggest challenge with gravimetric analysis is the increase in the work that must be carried out. Another disadvantage of this method is that it cannot be carried out on low-grade samples, such as tailings. However, gravimetric analysis or determination offers direct measurement traceability to the physical units.

These two quantification techniques have been used in various studies for the longest times, thus leaving few gaps. However, a gap that was identified was that they were rarely associated with measurement uncertainty. Incorporating the measurement uncertainty with these techniques strengthens their capabilities and provides a bigger picture into the accuracy and limitations of the results they produce

Table 2.4 Various instrumental analysis techniques for the quantification of gold in geological matrices.

Technique	Advantages	Disadvantages	Typical LOD	References
ICP–OES	Fast analysis, simultaneous detection of analytes.	Suffers from a great deal of interferences and method development can be time-consuming	0.01-0.1 ng.L^{-1*}, 10 µg.L^{-1*}	(Juvonen *et al.,* 2004; Komendova, 2020)
ICP–MS	Low detection limits, wide linear range	Intensive spectral interferences for geological samples	0.053 ng.g^{-1*}, 0.90 ng.g^{-1*}, 0.71 µg.L^{-1*}, 0.0068 ng.$L^{-1\#}$, 0.007 µg.$L^{-1!}$	(Cadar *et al.,* 2021; Jackson *et al.,* 1990; Juvonen *et al.,* 2004; Oguri *et al.,* 1999; Wang *et al.,* 2016)
GF-AAS	Require low sample volume, complex organic matrices can be eliminated proper to atomization of sample	Expensive, low sample throughput and requires highly skilled operators	0.3 ng.$L^{-1\#}$, 0.5 µg.$L^{-1@}$, 0.1 µg.$L^{-1\#}$	(Balaram *et al.,* 2012; Medved' *et al.,* 2004; Niskavaara & Kontas, 1990; Todand *et al.,* 1995)
LA-ICP–MS	Minimal sample preparation, access to isotopic information	Ions detected following m/z separation are not typical of the original sample's makeup.	0.007 µg.$L^{-1!}$	(Limbeck *et al.,* 2015)
INAA	It is not affected by problems arising from digestion due to difficult matrices.	Can analyse a limited number of analytes.	2 µg.L^{-1*}, 0.7 µg.$L^{-1\#}$	(Asif *et al.,* 1992; Elson & Chatt, 1983)

*= *fire assay,* [#]*=digestion,*[!]*= fusion,* [@]*=ion exchange resins*

2.7 References

Amassé, J. (1998). Determination of platinum-group elements and gold in geological matrices by Inductively Coupled Plasma-Mass Spectrometry (ICP-MS) after separation with selenium and tellurium carriers. *Geostandards Newsletter*, *22*(1), 93–102. https://doi.org/10.1111/j.1751-908X.1998.tb00548.x

Asif, M., Parry, S. J and Malik, H. (1992). Instrumental neutron activation analysis of a nickel sulfide fire assay button to determine the platinum group elements and gold. *The Analyst*, *117*(8), 1351–1353. https://doi.org/10.1039/an9921701351

Baghalha, M. (2007). Leaching of an oxide gold ore with chloride/hypochlorite solutions. *International Journal of Mineral Processing*, *82*, 178–186. https://doi.org/10.1016/j.minpro.2006.09.001

Balaram, V., Mathur, R., Satyanarayanan, M., Sawant, S. S., Roy, P., Subramanyam, K. S. V., Kamala, C. T., Anjaiah, K. V., Ramesh, S. L and Dasaram, B. (2012). A Rapid Method for the Determination of Gold in Rocks, Ores and Other Geological Materials by F-AAS and GF-AAS After Separation and Preconcentration by DIBK Extraction for Prospecting Studies. *Mapan - Journal of Metrology Society of India*, *27*(2), 87–95. https://doi.org/10.1007/s12647-012-0012-2

Balaram, V and Subramanyam, K. S. V. (2022). Sample preparation for geochemical analysis: Strategies and significance. *Advances in Sample Preparation*, *1*, 100010. https://doi.org/10.1016/j.sampre.2022.100010

Bédard, L. P and Barnes, S. J. (2002). A comparison of the capacity of FA-ICP–MS and FA-INAA to determine platinum-group elements and gold in geological samples. *Journal of Radioanalytical and Nuclear Chemistry*, *254*(2), 319–329. https://doi.org/10.1023/A:1021632118200

Birch, C. C. (2022). Optimizing cut-off grade considering grade estimation uncertainty - A case study of Witwatersrand gold-producing areas. *Journal of the Southern African Institute of Mining and Metallurgy*, *122*(7), 337–346. https://doi.org/10.17159/2411-9717/1403/2022

Cadar, O., Mocan, T., Roman, C and Senila, M. (2021). Analytical performance and validation of a reliable method based on graphite furnace atomic absorption spectrometry for the determination of gold nanoparticles in biological tissues. *Nanomaterials*, *11*(12).

https://doi.org/10.3390/nano11123370

Chattopadhyay, P and Sahoo, B. N. (1992). Modified decomposition procedure for the determination of gold in geological samples by atomic absorption spectrometry. *The Analyst*, *117*(9), 1481–1484. https://doi.org/10.1039/an9921701481

da Costa, G., Hofmann, A and Agangi, A. (2020). A revised classification scheme of pyrite in the Witwatersrand Basin and application to placer gold deposits. *Earth-Science Reviews*, *201*(July 2019), 103064. https://doi.org/10.1016/j.earscirev.2019.103064

Dobrowolski, R., Mróz, A., Dąbrowska, M and Olszański, P. (2017). Solid sampling high-resolution continuum source graphite furnace atomic absorption spectrometry for gold determination in geological samples after preconcentration onto carbon nanotubes. *Spectrochimica Acta - Part B Atomic Spectroscopy*, *132*, 13–18. https://doi.org/10.1016/j.sab.2017.03.011

Dosmukhamedov, N., Kaplan, V., Zholdasbay, E., Argyn, A., Kuldeyev, E., Koishina, G and Tazhiev, Y. (2022). *Chlorination Treatment for Gold Extraction from Refractory Gold-Copper-Arsenic-Bearing Concentrates*. 1–14.

Elson, C. M and Chatt, A. (1983). Determination of gold in silicate rocks and ores by coprecipitation with tellurium and neutron activation-γ-spectrometry. *Analytica Chimica Acta*, *155*, 305–310. https://doi.org/10.1016/S0003-2670(00)85610-X

Enzweiler, J and Potts, P. J. (1995). The separation of platinum, palladium and gold fromsilicate rocks by the anion exchange separation of chloro complexes after a sodium peroxide fusion: an investigation of low recoveries. *Talanta*, *42*(10), 1411–1418. https://doi.org/10.1016/0039-9140(95)01577-X

Fazelirad, H., Taher, M. A and Nasiri-Majd, M. (2014). GFAAS determination of gold with ionic liquid, ion pair based and ultrasound-assisted dispersive liquid–liquid microextraction. *Journal of Analytical Atomic Spectrometry*, *29*(12), 2343–2348. https://doi.org/10.1039/c4ja00272e

Fourie, A. B., Blight, G. E and Papageorgiou, G. (2001). Static liquefaction as a possible explanation for the Merriespruit tailings dam failure. *Canadian Geotechnical Journal*, *38*(4), 707–719. https://doi.org/10.1139/t00-112

Gcasamba, S. P., Ramasenya, K., Ekolu, S and Vadapalli, V. R. K. (2019). A laboratory investigation on the performance of South African acid producing gold mine tailings and its possible use in mine reclamation. *Journal of Environmental Science and Health - Part A Toxic/Hazardous Substances and Environmental Engineering*, *54*(13), 1293–1301. https://doi.org/10.1080/10934529.2019.1642694

Gupta, J. G. S. (1989). Determination of trace and ultra-trace amounts of noble metals in geological and related materials by graphite-furnace atomic-absorption spectrometry after separation by ion-exchange or co-precipitation with tellurium. *Talanta*, *36*(6), 651–656. https://doi.org/10.1016/0039-9140(89)80257-7

Hall, G. E. M and Pelchat, J. C. (1994). Analysis of geological materials for gold, platinum and palladium at low ppb levels by fire assay-ICP mass spectrometry. *Chemical Geology*, *115*(1–2), 61–72. https://doi.org/10.1016/0009-2541(94)90145-7

Hassan, J., Shamsipur, M and Karbasi, M. H. (2011). Single granular activated carbon microextraction and graphite furnace atomic absorption spectrometry determination for trace amount of gold in aqueous and geological samples. *Microchemical Journal*, *99*(1), 93–96. https://doi.org/10.1016/j.microc.2011.04.003

Jackson, S. E., Fryer, B. J., Gosse, W., Healey, D. C., Longerich, H. P and Strong, D. F. (1990). Determination of the precious metals in geological materials by inductively coupled plasma–mass spectrometry (ICP–MS) with nickel sulfide fire-assay collection and tellurium coprecipitation. *Chemical Geology*, *83*(1–2), 119–132. https://doi.org/10.1016/0009-2541(90)90144-V

Jin, X and Zhu, H. (2000). Determination of platinum group elements and gold in geological samples with ICP–MS using a sodium peroxide fusion and tellurium coprecipitation. *Journal of Analytical Atomic Spectrometry*, *15*(6), 747–751. https://doi.org/10.1039/b000470g

Juvonen, M. R., Bartha, A., Lakomaa, T. M., Soikkeli, L. A., Bertalan, E., Kallio, E. I and Ballók, M. (2004). Comparison of recoveries by lead fire assay and nickel sulfide fire assay in the determination of gold, platinum, palladium and rhenium in sulfide ore samples. *Geostandards and Geoanalytical Research*, *28*(1), 123–130. https://doi.org/10.1111/j.1751-908X.2004.tb01048.x

Juvonen, R., Lakomaa, T and Soikkeli, L. (2002). Determination of gold and the platinum group elements in geological samples by ICP–MS after nickel sulfide fire assay: Difficulties

encountered with different types of geological samples. *Talanta*, *58*(3), 595–603. https://doi.org/10.1016/S0039-9140(02)00330-2

Komendova, R. (2020). Recent advances in the preconcentration and determination of platinum group metals in environmental and biological samples. *TrAC - Trends in Analytical Chemistry*, *122*, 115708. https://doi.org/10.1016/j.trac.2019.115708

Kossoff, D., Dubbin, W. E., Alfredsson, M., Edwards, S. J., Macklin, M. G and Hudson-Edwards, K. A. (2014). Mine tailings dams: Characteristics, failure, environmental impacts, and remediation. *Applied Geochemistry*, *51*, 229–245. https://doi.org/10.1016/j.apgeochem.2014.09.010

Latypov, R., Chistyakova, S and Mukherjee, R. (2017). A novel hypothesis for origin of massive chromitites in the Bushveld igneous Complex. *Journal of Petrology*, *58*(10), 1899–1940. https://doi.org/10.1093/petrology/egx077

Limbeck, A., Galler, P., Bonta, M., Bauer, G., Nischkauer, W and Vanhaecke, F. (2015). Recent advances in quantitative LA-ICP–MS analysis : challenges and solutions in the life sciences and environmental chemistry. *Analytical and Bioanalytical Chemistry*, *407*, 6593–6617. https://doi.org/10.1007/s00216-015-8858-0

Liu, X. I., Wen, T., Sun, W., Yao, W., Wang, T and Wu, J. (2013). Determination of Au and Pt in geological samples by graphite furnace atomic absorption spectrometry with concentrate and extraction by foam plastics and thiourea. *Rock and Mineral Analysis*, *32*(4), 576–580.

Liu, Y. H., Wan, B and Xue, D. S. (2019). Sample digestion and combined preconcentration methods for the determination of ultralow gold levels in rocks. *Molecules*, *24*(9). https://doi.org/10.3390/molecules24091778

Malatse, M and Ndlovu, S. (2015). The viability of using the Witwatersrand gold mine tailings for brickmaking. *Journal of the Southern African Institute of Mining and Metallurgy*, *115*(4), 321–327. https://doi.org/10.17159/2411-9717/2015/v115n4a8

Manzi, M. S. D., Hein, K. A. A., Durrheim, R. J and King, N. (2014). The Ventersdorp Contact Reef model in the Kloof Gold Mine as derived from 3D seismics, geological mapping and exploration borehole data sets. *International Journal of Rock Mechanics and Mining Sciences*, *66*, 97–113. https://doi.org/10.1016/j.ijrmms.2013.12.015

Mao, X., Liu, J., Huang, Y., Feng, L., Zhang, L., Tang, X., Zhou, J., Qian, Y and Wang, M.

(2013). Assessment of Homogeneity and Minimum Sample Mass for Cadmium Analysis in Powdered Certi fi ed Reference Materials and Real Rice Samples by Solid Sampling Electrothermal Vaporization Atomic Fluorescence Spectrometry. *Journal of Agricultural and Food Chemistry*, *61*, 848–853. https://doi.org/10.1021/jf3045473

Mashale, K., May, B., Sehata, J and Tshilongo, J. (2023). Statistical evaluation of the uncertainties in the characterization of South African mine tailings. *South African Journal of Chemistry*, *77*, 42–47. https://doi.org/10.17159/0379-4350/2023/v77a07

Mcintosh, K. S., Auer, D., Koch, K. R and Eksteen, J. J. (2006). *Integrating pyrometallurgy and robotic systems engineering : Fully automated fire assay laboratory for rapid PGE analysis*. *19*, 219–231. https://doi.org/10.1016/j.mineng.2005.05.012

Medved', J., Bujdoš, M., Matúš, P and Kubová, J. (2004). Determination of trace amounts of gold in acid-attacked environmental samples by atomic absorption spectrometry with electrothermal atomization after preconcentration. *Analytical and Bioanalytical Chemistry*, *379*(1), 60–65. https://doi.org/10.1007/s00216-004-2538-9

Monteiro, M. I. C., Lavatori, M. P. A and De Oliveira, N. M. M. (2003). Determination of gold in ores by isobutyl methyl ketone extraction and electrothermal atomic absorption spectrometry: A stability study of the metal in organic media. *Geostandards Newsletter*, *27*(3), 245–249. https://doi.org/10.1111/j.1751-908X.2003.tb00725.x

Morcelli, C. P. R., Figueiredo, A. M. G., Enzweiler, J., Sarkis, J. E. S., Jorge, A. P. S and Kakazu, M. (2004). Determination of platinum-group elements in geological reference materials by high resolution-ICP–MS after nickel sulfide fire-assay collection and Te Coprecipitation. *Geostandards and Geoanalytical Research*, *28*(2), 305–310. https://doi.org/10.1111/j.1751-908X.2004.tb00745.x

Nengovhela, A. C., Yibas, B and Ogola, J. S. (2006). Characterization of gold tailings dams of the Witwatersrand Basin with reference to their acid mine drainage potential, Johannesburg, South Africa. *Water SA*, *32*(4), 499–506. https://doi.org/10.4314/wsa.v32i4.5290

Ni, W., Mao, X., Zhang, H., Liu, L., Gao, X and Xiao, F. (2019). Lead fire assay preconcentration and high resolution continuum source graphite furnace atomic absorption spectrometry for the determination of ultratrace amounts of Au, Ir, Pd, Pt and Rh in rocks and minerals. *Spectrochimica Acta - Part B Atomic Spectroscopy*, *158*(June), 105643. https://doi.org/10.1016/j.sab.2019.105643

Niskavaara, H and Kontas, E. (1990). Reductive coprecipitation as a separation method for the determination of gold, palladium, platinum, rhodium, silver, selenium and tellurium in geological samples by graphite furnace atomic absorption spectrometry. *Analytica Chimica Acta*, *231*(C), 273–282. https://doi.org/10.1016/S0003-2670(00)86426-0

Oguri, K., Shimoda, G and Tatsumi, Y. (1999). Quantitative determination of gold and the platinum-group elements in geological samples using improved NiS fire-assay and tellurium coprecipitation with inductively coupled plasma–mass spectrometry (ICP–MS). *Chemical Geology*, *157*(3–4), 189–197. https://doi.org/10.1016/S0009-2541(98)00205-8

Okereafor, U., Makhatha, M., Mekuto, L and Mavumengwana, V. (2020). Gold mine tailings: A potential source of silica sand for glass making. *Minerals*, *10*(5). https://doi.org/10.3390/min10050448

Omotola Fashola, M., Mpode Ngole-Jeme, V and Oluranti Babalola, O. (2020). Physicochemical properties, heavy metals, and metal-tolerant bacteria profiles of abandoned gold mine tailings in Krugersdorp, South Africa. *Canadian Journal of Soil Science*, *100*(3), 217–233. https://doi.org/10.1139/cjss-2018-0161

Pitcairn, I. K., Warwick, P. E., Milton, J. A and Teagle, D. A. H. (2006). Method for ultralow-level analysis of gold in rocks. *Analytical Chemistry*, *78*(4), 1290–1295. https://doi.org/10.1021/ac051861z

Radzyminska-lenarcik, E., Pyszka, I and Kosciouszko, A. (2021). Separation and Recovery of Gold(III), Palladium(II) and Platinum(IV) by Solvent Extraction Using a New β-Diketone Derivative from Acidic Solutions. *Materials*, *14*, 1–12. https://doi.org/https://doi.org/10.3390/ma14164436

Raiguel, S., Gijsemans, L., Van Den Bossche, A., Onghena, B and Binnemans, K. (2020). Solvent Extraction of Gold(III) with Diethyl Carbonate. *ACS Sustainable Chemistry and Engineering*, *8*(36), 13713–13723. https://doi.org/10.1021/acssuschemeng.0c04008

Rao, C. R. M and Reddi, G. S. (2000). Platinum group metals (PGM); occurrence, use and recent trends in their determination. *TrAC- Trends in Analytical Chemistry*, *19*(9), 565–586. https://doi.org/10.1016/S0165-9936(00)00031-5

Singh, N. (2012). A rugged, precise and accurate new gravimetry method for the determination of gold: An alternative to fire assay method. *SpringerPlus*, *1*(1), 1–6. https://doi.org/10.1186/2193-1801-1-14

Singo, N. K and Kramers, J. D. (2021). Feasibility of tailings retreatment to unlock value and create environmental sustainability of the Louis Moore tailings dump near Giyani, South Africa. *Journal of the Southern African Institute of Mining and Metallurgy*, *121*(7), 361–367. https://doi.org/10.17159/2411-9717/1138/2021

Stanley, C. (2007). The Fundamental Relationship Between Sample Mass and Sampling Variance in Real Geological Samples and Corresponding Statistical Models The Fundamental Relationship Between Sample Mass and Sampling Variance in Real Geological Samples and Corresponding Stat. *Exploration and Mining Geology*, *16*(1–2), 109–123. https://doi.org/10.2113/gsemg.16.1-2.109

Terashima, S. (1988). Determination of Gold in Sixty Geochemical Reference Samples by Flameless Atomic Absorption Spectrometry. *Geostandards Newsletter*, *12*(1), 57–60. https://doi.org/10.1111/j.1751-908X.1988.tb00042.x

Todand, M. M., Jarvis, I and Jarvis, K. E. (1995). Microwave digestion and alkali fusion procedures for the determination of the platinum-group elements and gold in geological materials by ICP–MS. *Chemical Geology*, *124*(1–2), 21–36. https://doi.org/10.1016/0009-2541(95)00021-D

Torres-Cruz, L. A and O'Donovan, C. (2023). Public remotely sensed data raise concerns about history of failed Jagersfontein dam. *Scientific Reports*, *13*(1), 4953. https://doi.org/10.1038/s41598-023-31633-5

Tucker, R. F., Viljoen, R. P and Viljoen, M. J. (2016). A review of the witwatersrand basin - The World's greatest goldfield. *Episodes*, *39*(2), 105–133. https://doi.org/10.18814/epiiugs/2016/v39i2/95771

Vadász, P., Plešingerová, B., Briančin, J., Sučik, G and Medveď, D. (2019). Interactions in Two – Phase Systems of MgO (s)–(Na 2° – SiO 2)(l). *Research and Development*, *3*, 32–39.

Wang, Y., Baker, L. A and Brindle, I. D. (2016). Determination of gold and silver in geological samples by focused infrared digestion: A re-investigation of aqua regia digestion. *Talanta*, *148*, 419–426. https://doi.org/10.1016/j.talanta.2015.11.019

Ye, J., Liu, S., Tian, M., Li, W., Hu, B., Zhou, W and Jia, Q. (2014). Preparation and characterization of magnetic nanoparticles for the on-line determination of gold, palladium, and platinum in mine samples based on flow injection microcolumn preconcentration coupled with graphite furnace atomic absorption spectrometry. *Talanta*, *118*, 231–237.

https://doi.org/10.1016/j.talanta.2013.10.018

3 STATISTICAL ANALYSIS

Given that the work in this thesis consists of the collection of numerical data, there had to be statistical analysis of the data. The analysis assessed whether there were significant differences in the means of experiments using tests such as paired t tests and analysis of variance (ANOVA). Therefore, the statistical analysis carried out in this work combined both descriptive and inferential statistics. The data that were assessed were collected by means of experiments and from documents and records such as calibration certificates.

3.1 Basic statistical evaluations

These include concepts such as the mean, standard deviation and relative standard deviations and were calculated using Equations 3.1, 3.2 and 3.3.

$$\bar{x} = \frac{\Sigma x}{n} \qquad \textit{Equation 3.1}$$

where the *x bar* is the mean, *x* is the measurement and *n* is the number of measurements made.

$$s^2 = \sqrt{\frac{\Sigma(x-\bar{x})^2}{n-1}} \qquad \textit{Equation 3.2}$$

where *x* is the value point in the data set, *x bar* is the mean and *n* is the number of data points in the data set.

$$\%RSD = \frac{s^2}{\bar{x}} \times 100\% \qquad \textit{Equation 3.3}$$

where s^2 is the standard deviation and the *x bar* is the mean of the data set.

3.2 Paired t test and Analysis of Variance (ANOVA)

3.2.1 Paired t test

The paired t test is used to determine whether there is a significant difference between two means of the same population. For example, one experiment (population) was performed, with the solutions analysed on the ICP–MS (mean 1) and ICP–OES (mean 2), there would be an assessment to check if the results obtained are statistically significant or not. The paired t test follows these assumptions made about the data:

- The dependent variable is distributed normally
- There is an independent sampling of the observations
- There is a continuous measurement of the dependent variable
- The independent variable must consist of two related groups or matched pairs.

This follows the construction of the null (H_0) and alternative (H_1) hypotheses as shown below:

$$H_0: mean_1 = mean_2 \text{ Or} H_0: mean_2 - mean_1 = 0$$

$$H_1: mean_1 \neq mean_2$$

The test statistic that is used to decide on the significance of the means is calculated as:

$$t_{stat} = \frac{\bar{d}-0}{\frac{\hat{\sigma}}{\sqrt{n}}} \qquad \textit{Equation 3.4}$$

where *d bar* is the sample mean of the differences, σ bar is the sample standard deviation of the differences and *n* is the sample size. The decision rule is then to reject the null hypothesis of $t_{stat}>t_{crit}$ or a p value lower than 0.5. The t_{crit} is obtained from the t test distribution table, which is at different confidence intervals.

3.2.2 ANOVA

ANOVA was used to assess the means of three or more populations. It follows the following assumptions:

- The means being compared are of independent groups.
- Most preferable when there are 3 or more groups
- There is 1 independent variable
- The independent variable should have 3 or more levels.
- It uses the F-distribution for the calculation

ANOVA assesses the source of the variation in the means and the variation within and between groups using Equations 3-5 to 3-8. The following hypothesis is proposed:

$$H_0: mean_1 = mean_2 = mean_3$$

$$H_1: mean_1 \neq mean_2 \neq mean_3$$

$$SSW = \sum_{i=1}^{k} \sum_{j=1}^{i} \left(X - \bar{X}_j\right)^2 \qquad \textit{Equation 3.5}$$

$$MSW = \frac{SSW}{df_w} \; where \; df_w = K - 1 \qquad \textit{Equation 3.6}$$

and

$$SSB = \sum_{j=1}^{k} \left(X - \bar{X}_j\right)^2 \qquad \textit{Equation 3.7}$$

$$MSB = \frac{SSB}{df_b} \; where \; df_b = n - 1 \qquad \textit{Equation 3.8}$$

3.3 Measurement uncertainty

The statistics in Sections 3.1-3.2 can only provide statistical information to a certain extent. In this case, the measurement uncertainty can be incorporated. The parameter linked with a measurement's result that characterizes the dispersion of the values that could properly be attributed to the measurand is therefore known as measurement uncertainty in the GUM (Ellison & Williams, 2012).

It is crucial to convey the measurement uncertainty linked to a measurement result since it shows how confidently a measurement technique is used (Barwick *et al.,* 1999). It is important to understand that measurement uncertainty and error are distinct concepts. Whereas measurement uncertainty takes the shape of an interval within which the measured value falls, error refers to the difference between the measured value and its true value (Lee *et al.,* 2022). Furthermore, the magnitude of error can be used to correct the measured result, whereas the measurement uncertainty value cannot. The evaluation of measurement uncertainty is also one of the parameters that is needed in the validation of a method because there is a strong link between method validation, measurement uncertainty of measurement and metrological traceability, which are also referred to as the three cornerstones of measurements. Metrological traceability refers to a measurement's capacity to be related to specific reference standards and not institutions through a series of calibrations and accompanied by measurement uncertainty (Ellison & Williams, 2019). In a review by Sajnóg, Hanć and Barałkiewicz (2018), it was determined that the three cornerstones of measurements need to be established to guarantee correct measurement results. A measurement result should, in an ideal world, provide the estimated quantity of the measurand, an SI unit for the unit, and the accompanying measurement. measurement uncertainty (Ellison & Williams, 2019).

Measurement uncertainty results from various factors that make up an analytic method. Such methods include temperature variations, purity of reagents, weighing of solid reagents and stability. Hence, it is important to determine the magnitude by which they affect the measurement result.

3.3.1 Approaches to determining measurement uncertainty

The two main approaches for the determination of measurement uncertainty are the guide to the expression of uncertainty in measurement (GUM) and the Monte Carlo method (MCM).

Both methods lead to the evaluation of the measurement uncertainty by using different mechanisms.

GUM

The Gum framework utilizes the law of propagation of measurement uncertainty and the characterization of the output quantity (measurand) by a Gaussian distribution or a scaled and shifted t-distribution to assess measurement uncertainty (Witkovsky *et al.*, 2017) (Figure 3.1). The GUM framework follows the steps outlined below:

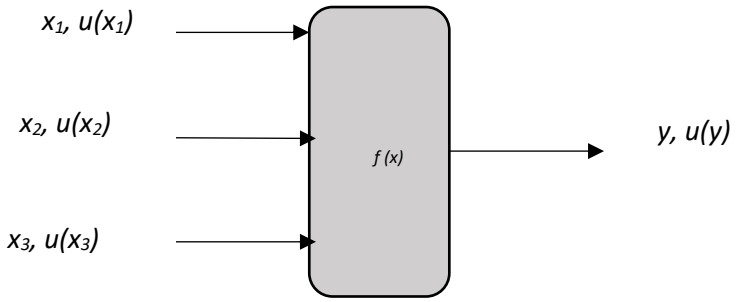

Figure 3.1 GUM framework operation.

a. *Specification of the measurand Y, identification of the input qualities X_i and modelling of the function relationship (Equation 3.9).*

$$Y = f(X_1, X_2, X_{3,} \dots \dots X_N) \qquad \textit{Equation 3.9}$$

In this case, the parameters of the equation would be measurement uncertainty contributors in their individual form, and in turn, they will have their measurement uncertainty components.

b. *Determine each input estimate of X_i based on whether it is a Type A or Type B*

In this step, it is important to distinguish between the two types of uncertainties, namely, Type A and Type B. In Type A, the measurement uncertainty by the contributor is calculated from a series of repeated measurements using variables such as the mean, standard deviation and degrees of freedom (Farrance & Frenkel, 2012). The standard uncertainty is therefore given by the standard deviation of the repeated measurements. In contrast, for Type B, the measurement uncertainty information is obtained from sources such as calibration certificates, journal articles and proficiency test scheme reports (Farrance & Frenkel, 2012).

c. *Using the preceding evaluation, convert each input quantity into standard measurement uncertainty.*

This is done by taking the quotient of the estimated measurement uncertainty and the divisor, multiplied by the sensitivity coefficient. The divisor depends on whether the measurement uncertainty is a Type A or B, if Type B, whether it is a normal, rectangular, triangular or uniform distribution (Table 3.1).

Table 3.1 Divisors for various distributions of data for Type B measurement uncertainty.

Distribution	Divisor
Normal	1
Rectangular	$\sqrt{3}$
Triangular	$\sqrt{6}$
Uniform	$\sqrt{2}$

d. *Use Equation 3.10 to find the covariance between any two input estimations.*

$$r(x_i, x_j) = r(x_j, x_i) = \frac{s(x_i, x_j)}{s(x_j)s(x_i)} \qquad \textit{Equation 3.10}$$

e. *Calculate Y, an estimate of the measurand*

f. *Calculate the combined measurement uncertainty using Equation 3.11.*

$$u_c(y) = \sqrt{u_c^2(y)} \qquad \textit{Equation 3.11}$$

g. *Determine the expanded measurement uncertainty*

An interval surrounding a measurement's result that is anticipated to contain a significant portion of the distribution values that could reasonably be assigned to the measurand is defined by the expanded measurement uncertainty (Farrance & Frenkel, 2012). This is calculated by multiplying the measurement uncertainty with the coverage factor (k), which is based on the degree of confidence, by the total measurement uncertainty. The coverage factor for a 95% confidence interval is k=2.

Monte Carlo Method (MCM)

The MCM operates by taking the measurement uncertainty distribution for each variable, and an equation for calculating the desired quantity is input into the MCM (Witkovsky *et al.*, 2017).

The needed quantity is then determined by selecting at random from the input variables' defined measurement uncertainty distributions (Witkovsky *et al.*, 2017) (Figure 3.2). This approach is often used in evaluations in which the GUM framework is not applicable, which is in this case;

- There is a nonlinear functional relationship between the input characteristics and the measurand.
- The contributions to measurement uncertainty are not roughly equal.
- The probability distribution of the input quantities is not symmetric or normal.
- The output quantity's probability distribution is asymmetrical.

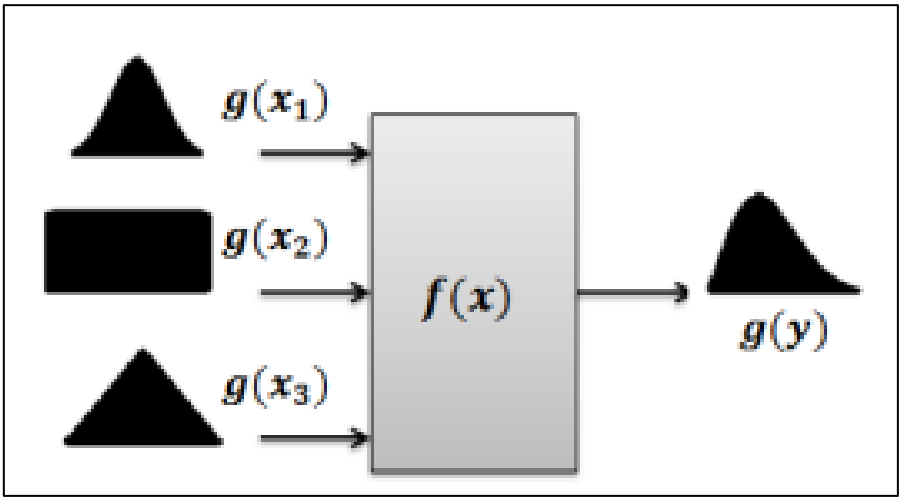

Figure 3.2 Propagation of distributions by the Monte Carlo method (Couto *et al.*, 2013).

Because it employed pseudorandom values from each input quantity probability distribution to be processed in the mathematical function M times, the MCM has an advantage over the GUM framework in that it avoids the difficult partial derivatives from GUM. The standard deviation of the simulations, using the M model values for ym, is then used to calculate the standard measurement uncertainty (Equation 3.12).

$$u(y) = \sqrt{\frac{1}{M^{-1}\Sigma_{r=1}^{M}(y_r - y)}} \qquad \textit{Equation 3.12}$$

3.4 Quantification of measurement uncertainty

3.4.1 Bottom-up approach

In the bottom-up approach, all the sources of measurement uncertainty of the analysis are evaluated (Figure 3.3). It also involves a clear explanation of the measurand, the relationship between the measurand and the source, and how it affects the measurand (Martinello *et al* ., 2020). This relationship can be shown through the use of a fishbone or cause and effect

diagram, such as in Figure 3.4, in which the measurand is the nickel content to be determined by ICP–MS. The effect is then represented by the main horizontal branch, which is the Ni result, and the causes that affect the results are presented as the branches.

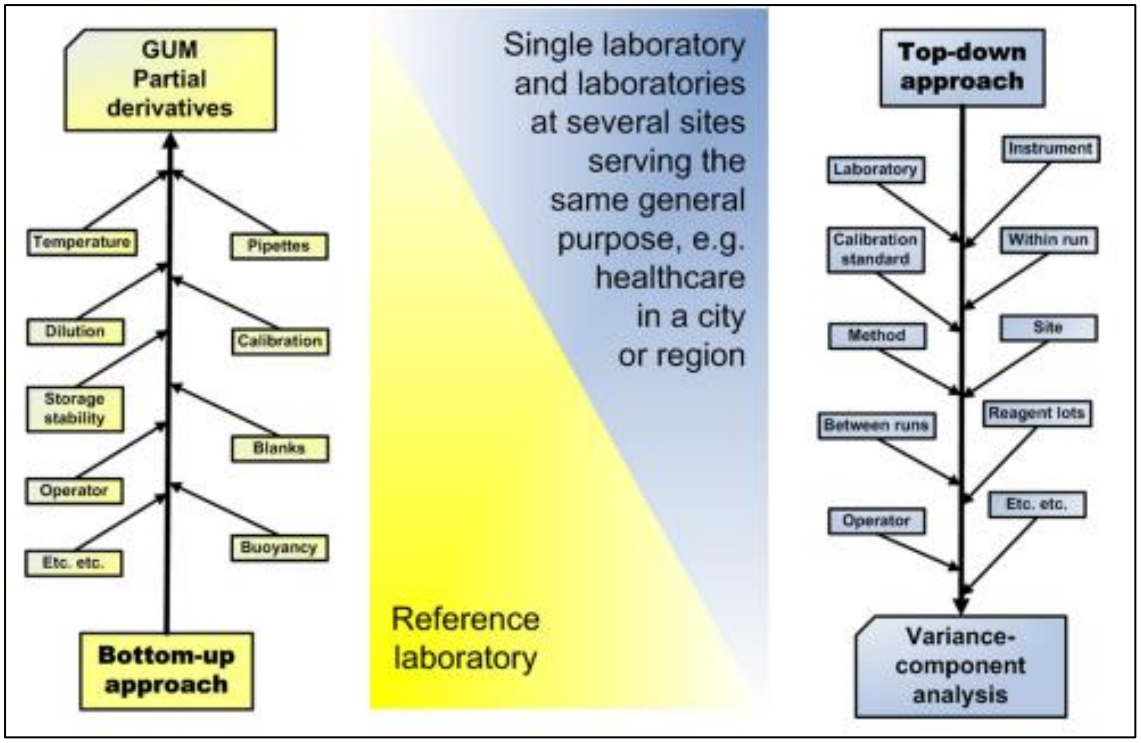

Figure 3.3 The primary methods used by GUM to evaluate measurement uncertainty (Magnusson *et al.*, 2012).

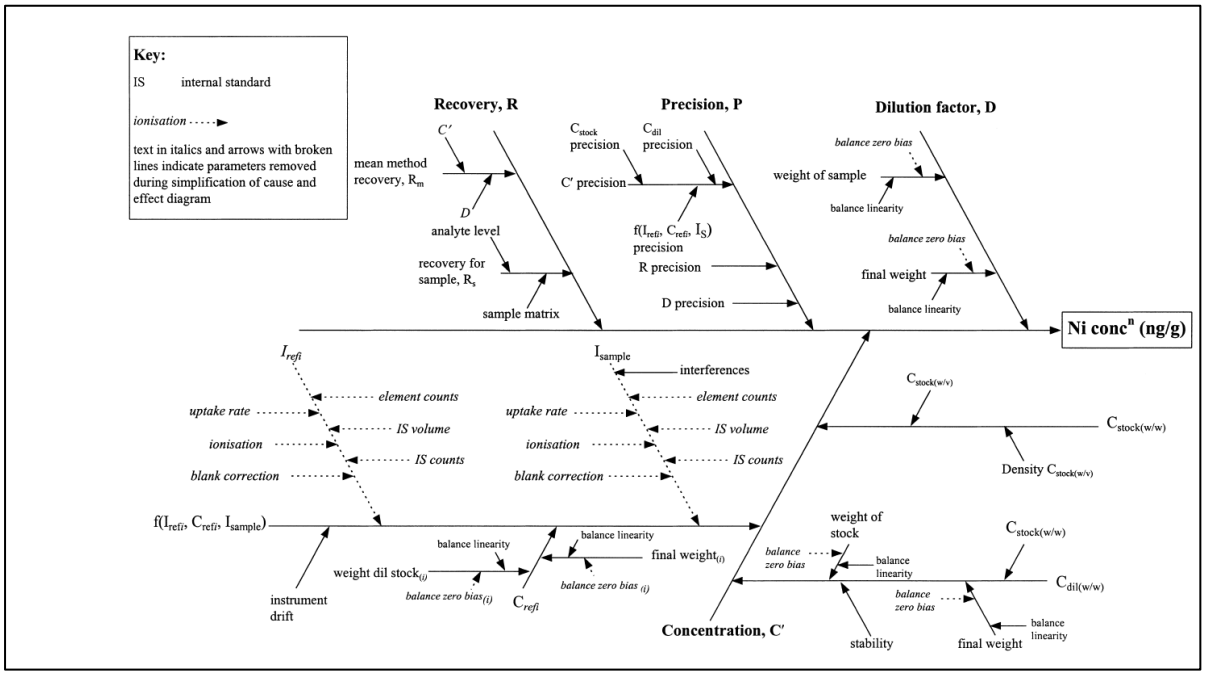

Figure 3.4 A cause and effect diagram (fishbone diagram) is typically used for a bottom-up approach (Barwick *et al.*, 1999).

After the fishbone diagram has been constructed, the 'causes' are then populated in the budget table (Table 3.2), which consists of various parameters, such as the sources of the measurement uncertainty, type of measurement uncertainty and standard measurement uncertainty.

Table 3.2 Example of a measurement uncertainty budget table.

Sources of measurement uncertainty	Quantified value	Unit	Sensitivity coefficient	Type of measurement uncertainty	Probability distribution	Divisor	Standard measurement uncertainty
Homogeneity	0.009405	$mg.L^{-1}$	1	A	Normal	1	0.009405
Mass balance (sample)	0.03	mg	1	B	Rectangular	$\sqrt{3}$	0.0173
Method repeatability	0.00032	$mg.L^{-1}$	1	A	Normal	1	0.00032
Instrument stability	0.000503	$mg.L^{-1}$	1	B	Triangular	$\sqrt{6}$	0.0000205
Linearity	0.003579	$mg.L^{-1}$	1	A	Normal	1	0.003579
Glassware calibration	0.04	$mg.L^{-1}$		B	Triangular	$\sqrt{6}$	0.063
				Combined measurement uncertainty			
				Coverage factor			
				Expanded measurement uncertainty			

The combined measurement uncertainty is calculated by taking the root sum of the squared individual uncertainties, as shown in Equation 3.14 for model equations containing subtractions and additions and Equation 3.15 for those containing quotients and products.

$$u_c = \sqrt{u(s_1)^2 + u(s_2)^2 + u(s_3)^2 + u(s_4)^2} \qquad \textit{Equation 3.13}$$

$$u_c = y.k\sqrt{\left(\frac{u(s_1)}{s_1}\right)^2 + \left(\frac{u(s_2)}{s_2}\right)^2} \qquad \textit{Equation 3.14}$$

From the combined measurement uncertainty, the expanded measurement uncertainty is then calculated. This is performed to obtain the range in which the measurand values are practically likely to lie. Although time-consuming, the bottom-up approach allows for the identification of critical stages in the method, which can be used for method development and optimization (Martinello *et al.*, 2020).

3.4.2 Top-Down approach

In the top-down approach, MU is directly estimated by evaluating quality control and method verification experimental data (Martinello *et al.*, 2020). This method is cost effective, and the data can be updated when more data are available from quality control and proficiency testing

schemes. This approach is based on the performance of certified reference materials in that particular method and how the method performs during proficiency testing (PT) schemes. The bias (Equation 3.16) and precision (CV, coefficient of variation) are then calculated from these two factors and are used to calculate the measurement uncertainty. The advantage of this method is that it is less time-consuming and it shows the measurement uncertainty in real time. There are various methods used to calculate the measurement uncertainty due to the bias from the CRMs and the PT schemes. These methods include the Nordest approach, Eurolab approach and the Cofrac approach, which calculates the bias from PT and interlaboratory testing. It is worth noting that these three methods give comparable results, as evidenced in Martinello *et al*. (2020).

$$RMS_{Bias} = \sqrt{\frac{(Bias_1^2 + Bias_2^2 + Bias_3^2 \ldots}{n}} \qquad \textit{Equation 3.15}$$

3.4.2.1 Nordest approach

This approach uses bias from CRMs, PTs and interlaboratory testing. The measurement uncertainty contributed from PT schemes is calculated using Equation 3.17, where CV_{PT} is the CV of each PT round, n_{lab} is the number of participating labs in each round and n is the number of PT rounds. The measurement uncertainty from the CRMs and interlaboratory internal quality control (IQCS) is also calculated using the same equation, but using the CV among the CRM measurements for each analytical series and n_m as the number of CRM measurements and n as the number of CRMs used.

$$u(PT) = \frac{(\frac{CV_{PT1}}{\sqrt{n_{lab}}} + \frac{CV_{PT2}}{\sqrt{n_{lab}}} + \frac{CV_{PT3}}{\sqrt{n_{lab}}})}{n} \qquad \textit{Equation 3.16}$$

The measurement uncertainty from the bias is then determined using Equation 3.18 for all the parameters, replacing the last term with the appropriate term, in which RMS bias is determined from Equation 3-16.

$$u(Bias_{PT}) = \sqrt{RMS_{Bias}^2 + u(PT)^2} \qquad \textit{Equation 3.17}$$

3.4.2.2 Eurolab approach

The Eurolab approach uses bias from the CRM and PT scheme results. The measurement uncertainty resulting from biases from the mean deviation, measurement uncertainty of the target value, and imprecision of the mean value of the repeated measurements are all calculated using Equation 3.19.

$$u(Bias_{PT}) = \sqrt{RMS_{Bias}^2 + u(PT)^2 + \frac{CV_{repPT}^2}{n_{repPT}}} \qquad \textit{Equation 3.19}$$

Equation 3.19 can also be applied using u(PC_{IQCS}), the CV among the replications of the IQCS measurements and the number of replications. For measurement uncertainty due to CRM bias, Equation 3.19 is used, replacing PT with CRM.

3.4.2.3 Cofrac approach

This method bases the evaluation of measurement uncertainty on the measurement uncertainty of the external evaluations, which is determined by the divergence from the uniform distribution law and the bias coefficient of variation, as given in Equation 3.20.

$$u(Bias_{PT}) = \sqrt{(\frac{RMS_{Bias}}{\sqrt{3}}) + CV_{Bias}^2} \qquad \textit{Equation 3.18}$$

3.5 Evaluation of measurement uncertainty literature

Various fields ranging from medicine to the geological field have reported on measurement uncertainty evaluations. Most of the studies employed the bottom-up approach, as it would allow for the identification of the step that contributes the most to the measurement uncertainty and is subsequently optimized (Table 3.3). In Senila *et al.* (2014), the measurement uncertainty was evaluated as part of the method validation of various elements from medicinal plants, and in the cause and effect diagram, they focused on the CRM analysis, repeatability and concentrations of the materials as the main components. Barwick, Ellison and Fairman (1999) estimated the uncertainties associated with Ni quantification on the ICP–MS by doing an extensive cause-and-effect diagram (Figure 3.3). From the parameters that were assessed, it was discovered that sample recovery had an insignificant contribution to measurement uncertainty, while measurement uncertainty due to precision was the largest for samples less than 3 $ng.g^{-1}$. Another important parameter that had a large contribution was instrumental drift, which supports or emphasizes the need to carry out continuous quality checks during analysis.

Table 3.3 Evaluations of measurement uncertainty from different matrices in different fields.

Matrix	Instrumental analysis	Approach	Reference
Medicinal plants	ICP–OES	Bottom-up	(Senila *et al.*, 2014)
Geological samples	INAA	Bottom up	(Zahn *et al.*, 2015)
Geological samples	XRF	Bottom up	(Morgenstern *et al.*, 2005)
Gold	Gravimetry	Bottom up	(Singh, 2012)
Geological samples	ICP–MS	Bottom up	(Barwick *et al.*, 1999)
Cosmetics	ICP–MS	Top-down	(Jia *et al.*, 2017)
Medicine	-	Top down	(Martinello *et al.*, 2020)
Dietary exposure	-	Top down	(Hart *et al.*, 2003)
Rocks	-	Bottom-up	(Voit *et al.*, 2023)

The evaluation of measurement uncertainty can be a time-consuming exercise, especially when there are multiple steps involved in chemical analysis. Furthermore, it involves dealing with complex equations, as seen with the GUM or MCM simulations. However, it is a worthy exercise as it strengthens the measurements performed and can serve as guidance for subsequent analysis.

3.6 References

Barwick, V. J., Ellison, S. L. R and Fairman, B. (1999). Estimation of uncertainties in ICP-MS analysis: A practical methodology. *Analytica Chimica Acta*, *394*(2–3), 281–291. https://doi.org/10.1016/S0003-2670(99)00302-5

Ellison, S. L. R and Williams, A. (Eds.). (2012). *Eurachem/CITAC Guide: Quantifying Uncertainty in Analytical Measurement* (3rd ed.).

Ellison, S. L. R and Williams, A. (Eds.). (2019). *Eurachem/CITAC Guide: Metrological Traceability in Chemical Measurement* (2nd ed.). www.eurachem.org

Farrance, I and Frenkel, R. (2012). Uncertainty of measurement: A review of the rules for calculating Uncertainty components through functional relationships. *Clinical Biochemist Reviews*, *33*(2), 49–75.

Guimaraes Couto, P., Damasceno, J and de Oliviera, S. (2013). Monte Carlo Simulations Applied to Uncertainty in Measurement Monte Carlo Simulations Applied to Uncertainty in Measurement. In *Theory of applications of Monte Carlo Simulations*, 28–51. Intech. https://doi.org/10.5772/53014

Hart, A., Smith, G. C., Macarthur, R and Rose, M. (2003). Application of uncertainty analysis in assessing dietary exposure. *Toxicology Letters*, *140–141*(v), 437–442. https://doi.org/10.1016/S0378-4274(03)00040-7

Jia, Y., Chen, M., Hu, W and Liu, T. (2017). Evaluation of the Uncertainty in the Determination of Arsenic in Cosmetics by Inductively Coupled Plasma–mass Spectrometry (ICP–MS). *Esse 2017*, 539–550. https://doi.org/10.1515/9783110540048-055

Lee, J. W., Hwang, E and Kacker, R. N. (2022). True value, error, and measurement uncertainty: two views. *Accreditation and Quality Assurance*, *27*(4), 235–242. https://doi.org/10.1007/s00769-022-01508-9

Magnusson, B., Ossowicki, H and Rienitz, O. (2012). Routine internal- and external-quality control data in clinical laboratories for estimating measurement and diagnostic uncertainty using GUM principles Routine internal- and external-quality control data in clinical laboratories for estimating measurement. *Scandinavian Journal of Clinical and Laboratory Investigation*, *00*, 1–9. https://doi.org/10.3109/00365513.2011.649015

Martinello, Flávia, Snoj, N., Skitek, M and Jerin, A. (2020). The top-down approach to measurement uncertainty: Which formula should we use in laboratory medicine? *Biochemia Medica*, *30*(2), 1–9. https://doi.org/10.11613/BM.2020.020101

Morgenstern, P., Brüggemann, L and Wennrich, R. (2005). Effect of the sample matrix on measurement uncertainty in X-ray fluorescence analysis. *Spectrochimica Acta - Part B Atomic Spectroscopy*, *60*(9–10), 1373–1379. https://doi.org/10.1016/j.sab.2005.08.005

Sajnóg, A., Hanć, A and Barałkiewicz, D. (2018). Metrological approach to quantitative analysis of clinical samples by LA-ICP–MS: A critical review of recent studies. *Talanta*, *182*(February), 92–110. https://doi.org/10.1016/j.talanta.2018.01.050

Senila, M., Drolc, A., Pintar, A., Senila, L and Levei, E. (2014). Validation and measurement uncertainty evaluation of the ICP–OES method for the multielemental determination of essential and nonessential elements from medicinal plants and their aqueous extracts. *Journal of Analytical Science and Technology*, *5*(1), 1–9. https://doi.org/10.1186/s40543-014-0037-y

Singh, N. (2012). A rugged, precise and accurate new gravimetry method for the determination of gold: An alternative to fire assay method. *SpringerPlus*, *1*(1), 1–6. https://doi.org/10.1186/2193-1801-1-14

Voit, K., Zeman, O., Gappmaier, P., Wriessnig, K and Adamcova, R. (2023). Influence of Measurement Uncertainty in the Determination of Selected Rock Parameters—A Realistic Approach. *Materials*, *16*(8). https://doi.org/10.3390/ma16083045

Witkovsky, V., Wimmer, G., Durisova, Z., Duris, S and Palencar, R. (2017). Brief overview of methods for measuremnt uncertainty analysis: GUM uncertainty framework, Monte Carlo method, characteristi function approach. *2017 11th Inetrnational Conference on Measurement*. https://doi.org/10.23919/MEASUREMENT.2017.7983530

Zahn, G. S., Ticianelli, R. B., Lange, C. N and Deborah, I. T. F. (2015). Uncertainty Analysis in Comparative Naa Applied To Geological and Biological Matrices. *International Nuclear Atlantic Conference*.

http://repositorio.ipen.br/bitstream/handle/123456789/25171/21161.pdf?sequence=1&isAllowed=y

4 ANALYSIS OF GOLD FROM TAILINGS AFTER GOLD DEPORTMENT, SIZE FRACTIONATION AND ACID DIGESTION BY ICP–MS AND THE ASSOCIATED UNCERTAINTIES

Kedibone Nicholine Mashale[1,2], Napo Goodwill Ntsasa[1], Majimi James Sehata[1], James Tshilongo[1,2] and Luke Chimuka[2]

[1]*Analytical Chemistry Division, Mintek, 200 Malibongwe Drive, Praegville, 2194, South Africa.*

[2]*Molecular Sciences Institute, School of Chemistry, University of the Witwatersrand, Braamfontein, 2000, South Africa.*

[*]*Corresponding author: kedibonema@mintek.co.za; Tel: 011 709 4050.*

ABSTRACT

The growing interest in reprocessing mine tailings for gold recovery requires a suitable quantification method that is accurate, rapid, and environmentally friendly. Acid digestion is often used for the determination of gold; however, it often faces challenges of incomplete digestion due to the presence of minerals such as quartz (SiO_2) and iron (II) chromite ($FeCr_2O_4$). The homogeneity of the sample is further compromised due to small sample masses, which can result in high bias. This study, therefore, investigated a shorter acid digestion method employing reverse aqua regia, both in the presence and absence of hydrofluoric acid (HF). Prior to acid digestion, the sample was subjected to gold depot analysis, which showed that 78% was recovered through direct cyanidation and that only 0.8% was associated with pyrite. Furthermore, the size screening test showed that the majority of the gold can be recovered in the fraction that passed through the 38 µm screen. This proposed method provided good linearity (5-100 µg. L^{-1}) and low limits of detection (0.14-0.33 µg.kg^{-1}). The recoveries obtained from the methods were 50-79% for aqua regia, 81-83% for reverse aqua regia, 63-83% for aqua regia with HF and 81-111% for reverse aqua regia with HF. The method also worked well for the certified reference materials (CRM), AMIS 610 (accurate value of 0.068 g.t^{-1}) and AMIS 646 (accurate value of 0.166 g.t^{-1}), which are of a similar matrix. The method was also evaluated for measurement uncertainty using the bottom-up approach, and the expanded uncertainty at a coverage factor of 2 (k=2) was reported to be 0.258 ± 0.092 g.$t^{-1,}$ which was comparable to that offered by the fire assay with the ICP–OES finish, which was 0.28 ± 0.10 g.t^{-1}. This implies that the acid digestion method is suitable for quantifying the gold from mine tailings without large measurement uncertainties.

Keywords: Gold tailings, Acid digestion, Measurement uncertainty, Fire assay

4.1 Introduction

Recently, there has been an increased interest in the reprocessing of mine tailings for the extraction of any valuable minerals lost due to inefficient processes. This is a great initiative that benefits the environment and mining companies in that less energy is needed, as the material has already been removed from the earth's crust, decreases the number of mine-related deaths, and has financial benefits (Araujo *et al.* 2022). This, however, means that the methods used for quantifying minerals such as gold need to be improved, or new methods need to be developed. This is because, for a typical gold mine tailing sample, the ratio of the gold to the gangue material is approximately 1:10 (Lottermoser, 2007).

For decades, the fire assay (FA) has been used as the conventional method for the quantification of gold from various ores and is usually coupled to gravimetric analysis or instrumental analysis, atomic absorption spectroscopy (AAS), inductively coupled plasma–mass spectrometry (ICP–MS), inductively coupled plasma optical emission spectroscopy (ICP–OES), etc. The challenge with fire assay is that due to the ratio of gold to gangue material, a large sample mass must be used to obtain a prill that can be accurately weighed and is easy to subject to other procedures; it requires highly skilled assayers and uses lead, which is toxic to humans (Reddy and Rao, 1999). Additionally, the amount of the sample used versus the amount of gold that will be determined, is it economically and environmentally beneficial?

For the quantification of gold, various methods exist other than fire assays, namely, acid digestion, direct analysis using instrumental neuron activation analysis (INAA), or laser ablation techniques; however, the grade of the gold is always a limitation. In terms of acid digestion, which has been studied mostly for medium- to high-grade gold ores, which includes the digestion or decomposition of the sample using acids assisted by heat, various challenges have been reported (Zhang & Hu, 2019). The challenges include the presence of minerals such as pyrite, quartz and chromite, which can hinder the digestion process, especially when a large amount of gold is enclosed in those minerals (Ghosh *et al.* 2019). Acid digestion usually uses a combination of various acids to obtain a synergistic effect, such as perchloric acid ($HClO_4$), hydrofluoric acid (HF), hydrochloric acid (HCl), sulfuric acid (H_2SO_4) and nitric acid (HNO_3) (Pitcairn *et al.* 2006). Because of the incomplete digestion of the material due to encapsulation of the gold grains, the digestion time and acid quantities need to be increased, and the possible use of HF decomposes the quartz in the sample and removes it as SiF_4 (Pitcairn *et al.* 2006; Dong *et al.* 2020). However, environmentally, it is not beneficial, as it requires higher amounts of energy. Since tailings have already been processed, the assumption is that it might be easier

to digest the tailings with mild conditions (acid combinations and time) and still be able to accurately quantify the gold (Dong *et al.* 2020).

Apart from the incomplete acid digestion that occurs, another challenge is the distribution of the gold in the sample and the relation of the small sample mass to homogeneity. This is mainly because the grains that contain gold are heterogeneously distributed in the ore, which eventually leads to the formation of gold nuggets (Stanley, 2007) and is often seen in the analysis of replicates. For fire assays, this problem is often overcome by using large sample masses (> 50 g for a tailings sample), which then also improves the accuracy and precision of the analysis. In acid digestion, the typical masses used are less than 20 g, some going as low as 5 g (Monteiro *et al.* 2003; Pitcairn *et al.* 2006; Liu, Wan and Xue, 2019). In this case, it is recommended that the majority of the particles in the sample pass the 35 µm screen. Upon chemical analysis, the level of homogeneity in the sample can be calculated using the homogeneity indicator (Equation 4.1) and Pauwel's equation (Equation 4.2) to calculate the minimum amount of sample needed to give homogenous results at a certain measurement uncertainty level (Mao *et al.* 2013). In the equations below, H_E is the homogeneity indicator, RSD is calculated from repetitive measurements and m is the sample mass.

$$H_E = (RSD) \times \sqrt{m} \qquad \textit{Equation 4.1}$$

$$M = \left(\frac{K_2' \times \%RSD)}{UNC}\right) \times m \qquad \textit{Equation 4.2}$$

Furthermore, the suitability of acid digestion for the quantification of low gold can be assessed by the measurement uncertainties that arise from chemical analysis. This would strengthen the quantification if there is a level of confidence attached to the analytical results. Although there are various ways to assess this uncertainty, the bottom-up approach would be more advantageous, as it will show the parameters that contribute to larger uncertainties and will allow for that parameter to be assessed and improved. Therefore, in this study, an acid digestion method that offers shorter digestion times and uses the simplest acid combination was explored and compared to the existing fire assay. The comparison was performed based on the measurement uncertainties that each method produces.

4.2 Methods and methods

4.2.1 Materials

The reagents used in this study were of high purity and were used as received. Anhydrous sodium carbonate (Na_2CO_3), sodium peroxide (Na_2O_2), hydrogen peroxide (H_2O_2) and sodium cyanide (NaCN) were purchased from Associated Chemical Enterprises Pty Ltd.

(Johannesburg, South Africa). Hydrochloric acid (HCl, 37%) and nitric acid (HNO_3, 65%) were purchased from Sigma Aldrich (Missouri, United States of America). The tuning solution for ICP–MS analysis was purchased from Thermo Fischer Scientific (Massachusetts, United States of America). For ICP–OES, the tuning solutions were purchased from Agilent Technologies (California, United States of America). African Mineral Standards (Modderfontein, South Africa) provided the certified reference materials (CRM), AMIS 610, and AMIS 646. The gold and base metal stock solutions (1000 mg. L^{-1} and 10 000 mg. L^{-1}) were purchased from LGC Standards (Middlesex, United Kingdom). All solutions were prepared using Millipore water from a Milli-Q system from Sigma Aldrich (Missouri, United States of America). The custom-made lead-based flux for the fire assay was purchased from PureChem (Douglasdale, South Africa). Two mine tailing samples of 25 kg, which were of a processed nature, were sourced from the Ventersdorp Contact Reef (VCR) and the Green Stone Belt (GSB) in Barberton. The technique used for sampling was grab sampling.

4.2.2 Particle size distribution, homogeneity, and purity analysis

The ground sample was divided into smaller portions using a rotary separator with 24 portions obtained with an average weight of 1 kg each. A Malvern hydroEV instrument and Mastersizer 3000 software (Malvern Pan Analytical Ltd, Worcestershire, UK) were used to measure the particle size distribution (PSD). Additional screening was performed by physical sieves (1180, 600, 425, 300, 212, 150, 106, 75, 53, 38 µm), starting with a wet sieve to remove the finer fraction (termed -38 µm). This slurry was then dried in an oven overnight at 60 °C, ground to a powder and then passed through a series of sieves. The homogeneity of the fractions was assessed by selecting random fractions and chemically analysing them; mineralogical, elemental composition and fire analysis. Blank samples from techniques were analysed to determine reagent purity.

4.2.3 Mineralogical analysis

The material was analysed by a backloading preparation process after being pulverized in a swing mill to -50 µm. The diffractogram was produced using a Malvern Panalytical Aeris diffractometer (Malvern Pan Analytical Ltd, Worcestershire, United Kingdom) equipped with a PIXcel detector, fixed slits, and Fe-filtered Co-K radiation. The diffractometer has a scanning range of 5-80° 2 and a step scan of 0.022° 2 with a measurement time of 48 s. PAN-ICSD and the X'Pert Highscore plus software were used to identify the phases. Using the Rietveld method, the relative phase quantities (wt%) were calculated, with the method detection limit being specified as 0.5-3 wt%.

4.2.4 Elemental composition

The elemental composition was determined by alkaline fusion (Guo *et al.*, 2014), in which 0.2 g of the sample was mixed with 0.7 g of $NaCO_3$ and 1.5 g of Na_2O_2. This mixture was fused on an open flame (200 °C) until a red melt was obtained. The melt was allowed to cool prior to leaching with 100 mL of water and 40 mL of HCl. The leached solution was then transferred into a 200 mL volumetric flask and brought to the mark with deionized water for an ICP–OES finish. The matrix of the sample contained scandium as an internal standard and HCl.

4.2.5 Determination of the head grade

For the fire assay, 350 g of the flux consisting of $NaCO_3$ (39.14%), fused borax (21.50%), reducing agent (cake flour) (2.08%), paraffin (0.01%), silica (12.75%), and litharge (21.70%) was weighed into a large crucible and mixed with 100 g of the tailings sample. This combination was then mixed with a spatula until homogenous, and 5 drops of concentrated silver nitrate ($AgNO_3$) were added to enrich the extraction of the gold from the matrix. A scoop of silica was added to protect the crucible. The mixture was then placed in a furnace at 1400 °C for one hour to allow for fusion. After the time had elapsed, the fused melt was poured into iron molds and allowed to cool before deslagging the sample. The button obtained after deslagging was placed on a cupel and heated at 1000 °C for one hour (Blyth *et al*. 2004). The prill obtained was digested with 3 mL of 65% HNO_3 and then 9 mL of 37% HCl and transferred into a 25 mL volumetric flask with scandium as an internal standard. This solution was analysed by ICP–MS for gold content.

4.2.6 Gold depot study

Due to the low-grade nature of the gold in the tailings sample, the deportation of gold was analysed using chemical methods, which was a 3-stage diagnostic leach. The process involved leaching the sample with cyanide using 10 $g.t^{-1}$ NaCN for 24 h on a rolling bench (a), a second cyanide leaching with carbon in leach (CIL) whereby carbon granules are added to the slurry during the 24 h of leaching (b), a leach using 2.5 M HCl (c), a leaching step with 27% HNO_3 (d), roasting at 850 °C for 1 hour (e). The gold content obtained from the filtrates and residues was used to calculate the deposition of gold on various minerals, such as quartz, pyrite, and calcites. The content of gold associated with the minerals was then calculated as follows:

- Cyanide soluble gold (free milling) = Head –a
- Preg-robbed (carbonaceous) gold= a-b
- Calcite locked gold= b-c

- Sulfide locked gold= c-d
- Gold locked in roastables= d-e
- Gold locked in gangue (base metals, quartz)= Head – (a+b+c+d+e)

4.2.7 Acid digestion

A sample of 1 g was weighed into a Teflon beaker and wet with deionized water. The acid mixtures used were reverse aqua regia (3 HNO_3: 1 HCl) and aqua regia (3HCl:HNO_3), with and without HF addition, totaling four experiments. The ratio of the acids was kept at 3:1, as it has been reported in the literature that it is optimum for gold samples (Wang & Brindle, 2014). After the sample was wet, 10 mL of the acid mixture was added and allowed to digest on a hot plate (200 °C) for 20 min under reflux. After the initial step, 10 mL of nitric acid (and 10 mL HF for the experiments with HF addition) was added to further aid the digestion and allowed to heat until dryness. The residue was then dissolved and reconstituted with HCl, and drops of H_2O_2 were added to dissolve any remaining residues. The samples were transferred into 50 mL Class A volumetric flasks containing 10% HCl and 10 mg. L^{-1} scandium. The experiments were repeated three times on the four samples (VCR, GSB, AMIS 610, and AMIS 646), including blanks.

4.2.8 Instrumental analysis

ICP–MS

Samples from acid digestion were analysed on the Thermo Fischer Scientific iCap Q with data processing on the Qtegra (Version: 2.10.3324.62). The samples were introduced into the system using an ASX-520 autosampler, polytetrafluoroethylene (PTFE) nebulizer, and a double-pass cyclonic spray chamber. The operating conditions of the instrument are shown in Table 4.1. Performance checks and autotuning were carried out daily to ensure the optimum functioning of the instrument. These included mass calibrations, optimizations of the nebulizer flow rate, torch position, and overall system performance. The tuning solution used was a 1 µg. L^{-1} standard containing Be, Ce, Fe, In, Li, Mg, Pb, and U in 1% HNO_3. A six-point external calibration curve at 5, 10, 20, 40, 50, and 100 µg. L^{-1} was prepared from a 1 mg. L^{-1} working solution, which was prepared from a 1000 mg. L^{-1} stock solution. The analysis was carried out in both the standard and kinetic energy discrimination (KED) modes to compare the two modes of interference correction. To avoid oversaturation of the detector, the samples were diluted using a MicroLab 600 auto dilutor to a final volume of 10 mL.

Table 4.1 ICP–MS operating conditions

Parameter	Detail	**Parameter**	Detail
RF power (kW)	1.5	**Nebulizer gas flow ($L.min^{-1}$)**	0.99
Plasma gas	Argon	**Pirani pressure (mbar)**	1.49
Plasma flow ($L.min^{-1}$)	14	**Penning pressure (mbar)**	3.52×10^{-7}
Auxiliary gas flow ($L.min^{-1}$)	0.79	**Pump speed (rpm)**	40.0
Interface temperature (°C)	33.63	**Isotopes**	197Au 185Re and 115In
Water flow ($L.min^{-1}$)	0.4	**Measurement mode**	Standard and KED mode

ICP–OES

An Agilent 5900 ICP–OES (Agilent Technologies Inc., California, United States of America) equipped with ICP-Expert software (version: 7.5.4.11997) and a charged coupled device detector (CCD) was used for the analysis of the base metal solutions. The operating conditions (see Table 4.2) used were RF power 1.25 kW, plasma current 12 L min^{-1}, auxiliary current 1.3 L min^{-1} and sample absorbance of 0.3 mL min^{-1}. Analysis was performed in radial mode for the base metal and in axial mode for gold, with high purity argon used as the plasma and carrier gas source. The wavelengths of the analytes are chosen according to their intrinsic strength and proximity to possible interferences. Calibration standards for base metals in the 0.050 to 50% range, including calibration blanks, are prepared from mono-element stock solutions. To enable analysis to cover a concentration range of 0.05 to 50%, a concentration factor of 1000 was added when creating standards. For gold, the calibration standards ranged from 0.03 to 1 $mg.L^{-1}$. Calibration was verified using 5% and 25% quality control standards for base metals and 0.1, 1 and 2 mg. L^{-1} for gold, certified reference materials included in the analysis.

Table 4.2 Operating conditions for the ICP–OES.

Parameter	Detail	**Parameter**	Detail
Model	Agilent SVDV 5900	**Plasma gas**	Argon
Reading mode	Axial and radial	**Plasma flow (L.min^{-1})**	12
Viewing height (mm)	8	**Pump speed (rpm)**	12
Read time (s)	5	**Sample uptake (s)**	25
RF Power (kW)	1.2	**Stabilization time (s)**	15
Rinse time (s)	30	**Selected wavelengths (Intrinsic intensity)**	Au: 267.694 (10266.7) 242.774 (8573.1) 211.068 (1302.3) 208.207 (1731.0)
Base metals wavelengths (nm)	Al (396.152), As (188.980), Ca (317.933), Cr (267.716) Fe (234.350), Mg (285.213), Mn (257.610), Ni (216.555), Pb (283.305), Ti (334.188), Si (288.185), V (292.464), Zn (206.200)		

Criteria

In Table 4.3, the criteria to assess the calibration curves are outlined.

Table 4.3 Criteria set for the calibration of the ICP–OES and ICP–MS.

Parameter	**ICP–OES**	**ICP–MS**
Allowable error	10% for <0.1 mg.L^{-1} 5% for >0.1 mg.L^{-1}	10% for < 20 µg.L^{-1} 5% for > 20 µg.L^{-1}
Correlation coefficient	0.999	0.999

4.2.9 Statistical evaluations

All samples and tests were performed in triplicate to obtain a good representation of the analysis and for continued assessment of the homogeneity. Since the sample was split into smaller fractions, the number of fractions to be used to test for homogeneity was calculated following Equations 4.3a and b (ISO guide 35, 2017), whereby N is the number of fractions after splitting the bulk sample:

$$min = \sqrt[3]{N_{fraction}} \quad \textit{Equation 4.3a}$$

$$max = 3 \times \sqrt[3]{N_{fraction}} \quad \textit{Equation 4.3b}$$

The uncertainty evaluations were approached with the bottom-up method, which included looking at the factors that can affect the quantification of the gold using a fire assay and acid digestion with an ICP–MS finish. The results of these two tests were treated to see if their means were significantly different using a paired t test using Microsoft Excel (Microsoft Office Professional Plus 2016). Based on the following model equation (Equation 4.4), the factors that were incorporated into the uncertainty analysis were glassware calibration, mass balance, instrument stability, homogeneity, method repeatability, reproducibility, dilution factor, and dilution of the working standard. For measurements that were repeated, the standard deviation was used as the standard uncertainty. For mass balance and instrument uncertainty, the uncertainty was obtained from the calibration data (BIPM, 2008) and propagated (Equation 4.5) to give the combined uncertainty at a coverage factor of 2 (k=2) or 95% confidence interval.

$$C = \frac{C_0 \times V}{W \times 1000} \times D \quad \textit{Equation 4.4}$$

$$u(y) = \sqrt{(a)^2 + (b)^2 + (c)^2 \ldots\ldots} \quad \textit{Equation 4.5}$$

where *C* is the concentration of the element in the sample, C_0 is the concentration of the element in the sample concentration, V is the sample solution volume, *D* is the dilution factor, and *W* is the mass of the sample.

4.3 Results and discussion

4.3.1 Instrumental analysis

The calibration showed linear relationships (Figure 4.1) with the R^2 value reading greater than 0.999 for both the ICP–OES and ICP–MS. Expressions at 3 s/m and 10 s/m, where s is the standard deviation of 10 blanks and m is the slope of the calibration curve, were used to estimate the instrumental limit of detection (LOD) and quantification (LOQ). The LOD for gold was determined to be 0.0245 mg. L^{-1} and 0.337 µg. L^{-1} for ICP–OES and ICP–MS, while the LOQ was 0.065 mg. L^{-1} and 1.123 µg.L^{-1}.

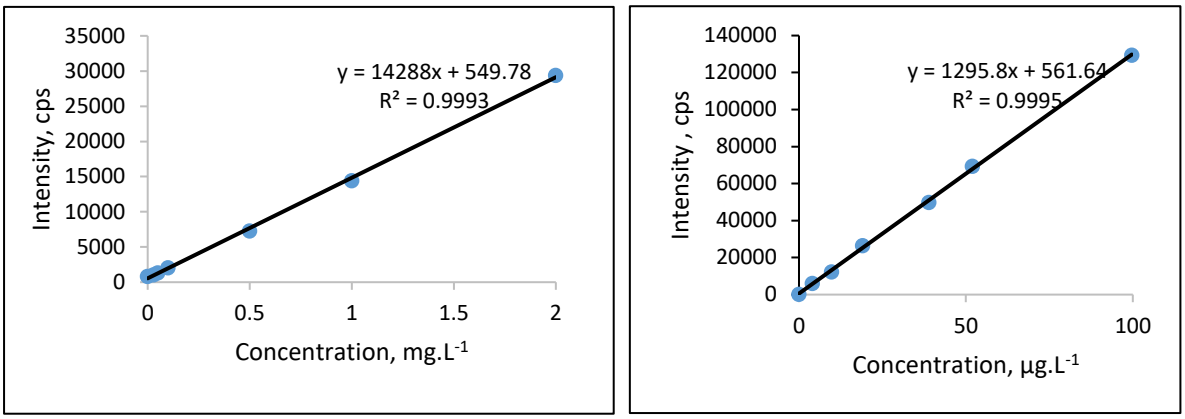

Figure 4.1 External calibration curves for Au on the ICP–OES (a) and ICP–MS (b).

According to the criteria set out in Section 4.2.8, the calibrations performed satisfactorily, with the highest error being 8.28% for a 0.03 mg. L^{-1} standard. The errors are shown in Table 4.4.

Table 4.4 Calibration errors for ICP–OES and ICP–MS

	Method concentration ($mg.L^{-1}$) ICP–OES	**Error (%)**	**Method concentration ($\mu g.L^{-1}$) ICP–MS**	**Error (%)**
Standard 1	0.03	8.28	5	3.2
Standard 2	0.05	2.64	10	2.42
Standard 3	0.1	1.91	20	4.52
Standard 4	0.5	0.94	40	2.71
Standard 5	1	0.68	50	3.98
Standard 6	2	0.063	100	0.31

4.3.2 Mineralogical composition

The predominant minerals are shown in Table 5.5, with quartz (SiO_2) being the most dominant at approximately 80% by weight and calcite as the minor phase at 0.2% by weight, as expected for the matrix. VCR and GSB (Tabelin & Igarashi, 2009; Tomiyama *et al.* 2019). The presence of quartz at this percentage indicates the possibility that gold encapsulation may interfere with acid decomposition, while the presence of pyrite (FeS_2) may interfere with the fire assay and further chemical analysis. Previous studies have shown a similar trend in terms of the major

and minor minerals being detected, which included quartz (58-82%), mica (3-10%), chlorite (3-10%) for a Wits basin (Nengovhela *et al.* 2006) and quartz, magnetite and magnesioferrite for the East Rand Basin (Okereafor *et al.* 2020), both of which were quantified by XRD. In terms of mineralogical comparisons of the sample and the CRMs (AMIS 610 and AMIS 646) used in the study, the amounts of quartz were quite similar.

Table 4.5 Mineralogical information of the original tailings sample and the certified reference material in %wt.

Mineral	**Chemical formula**	**VCR sample**	**GSB sample**	**AMIS 610**	**AMIS 646**
Quartz	SiO_2	78.1 ± 2.7	67.5 ± 3.90	82	62
Pyrite	FeS_2	0.8 ± 0.21	0.4 ± 012	n.d	1
Muscovite	$KAl_2(AlSiO_{10})(F,OH)_2$	11.4 ± 0.60	13.8 ± 0.35	n.d	10
Dolomite	$MgCO_3.CaCO_3$	1.4 ± 0.53	0 ± 0	n.d	n.d
Chlorite	$(X,Y)_{4\text{-}6}(SiAl)_4O_{10}(OH,O)_8$	6.9 ± 1.33	7.6 ± 0.70	2	1
Gypsum	$CaSO_4.2H_2O$	0.2 ±0.10	0.6 ± 0.12	n.d	1
Talc	$Mg_3Si_4O_{10}(OH)_2$	0.9 ± 0.06	0.8 ± 0	5	n.d
Calcite	$CaCO_3$	0.2 ± 0.12		<1	n.d
Chloritoid	$(Fe,Mg,Mn)Al_2SiO_5(OH)_2$	n.d	11.6 ± 2.05	n.d	n.d

X and Y can represent ions of Fe, Mn, Ni, Zn, Al, Li and Ti. n.d denotes not detected as it is below the detection limit.

The mineralogical analysis of the screened fractions showed that quartz is still dominant in each of the screens, with a decreasing behaviour from the finer screen to the coarser screen (Figure 4.2). However, for analytes such as gold, this would be a different story, as it is usually enclosed in minerals such as pyrite and arsenopyrite. Therefore, recovering the gold in the finer fractions would be optimal as the surface area for reactions to occur could have increased and minerals such as quartz would have decreased in concentration. Similar observations were reported in a previous study by Beyuo & Agorhom (2021), whereby the 300 and minus 75 µm screens reported 39% and 15%, respectively. This is considered to be beneficial as quartz is often known to be a hindrance during acid dissolutions as it can encapsulate the gold, but in this case, extraction of the gold from the finer screen with a low amount of quartz is expected to yield better results. In Table 4.6 and Figure 4.2, the elemental composition from the screened fractions also correlates with the mineralogical data in which Si is most abundant in the coarser fractions.

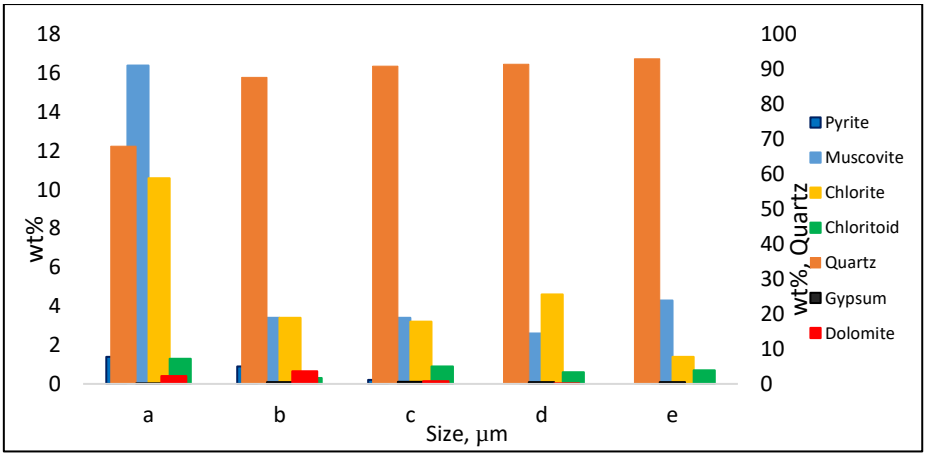

Figure 4.2 Mineralogical data of the fractions screened by XRD (n=3). Screen sizes, a= -38 µm (finer screen), b= +38 µm, c= +53 µm, d=+75 µm and e= +106 µm

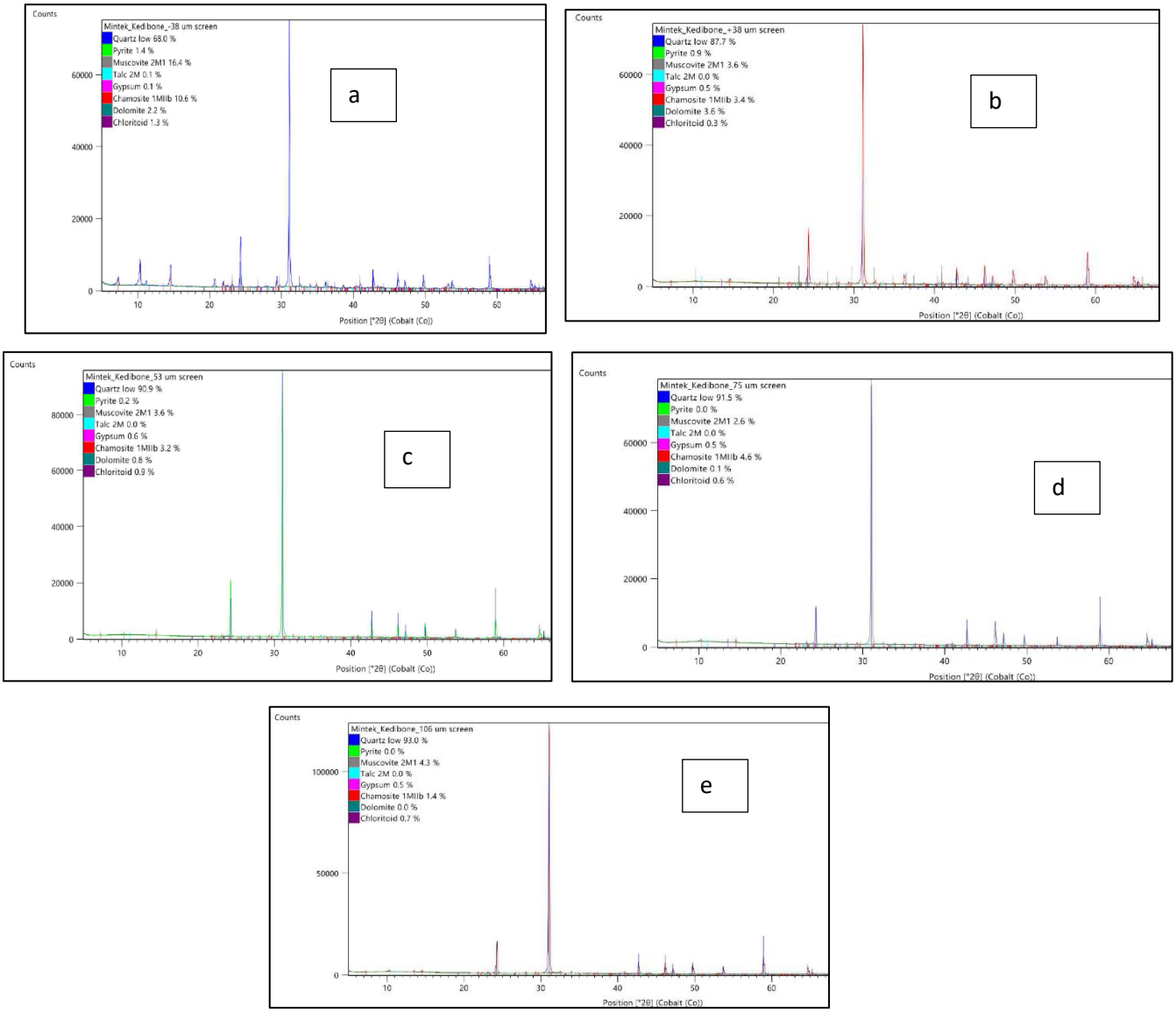

Figure 4.3 Diffractograms of the screened fractions. a= -38 µm, b= +38 µm, c= +53 µm, d= +75 µm, e= +106 µm. The prominent peak belongs to quartz.

Table 4.6 Elemental composition (%) of the screened fractions by ICP–OES (n=3).

Screen (µm)	Al	Ca	Cr	Mg	Mn	Si	V	Zn	Fe
+600	3.56	2.93	0.05	0.79	0.04	27.22	0.21	0.03	4.24
+425	3.65	2.75	0.07	0.75	0.039	30.28	0.02	0.033	3.88
+300	3.08	2.6	0.04	0.65	0.035	28.77	0.09	0.03	3.21
+212	2.89	3.00	0.04	0.67	0.035	34.36	0.07	0.02	2.89
+150	4.51	0.93	0.02	1.06	0.048	34.38	0.04	0.04	4.19
+106	1.58	0.57	0.04	0.37	0.016	40.1	0.07	0.02	0.91
+75	1.87	0.66	0.02	0.48	0.018	40.92	0.10	0.02	1.16
+53	2.02	0.78	0.02	0.6	0.025	42.1	0.08	0.02	1.78
+38	1.81	0.78	0.03	0.57	0.025	27.84	0.09	0.03	2.90
-38	1.94	1.33	0.08	0.48	0.025	27.29	0.053	0.023	1.5655

4.3.3 Purity analysis and homogeneity

The analysis of the blanks from the different techniques showed that the impurities in the reagents were negligible. For the purity analysis of the alkaline fusion blanks, which contained $NaCO_3$ and Na_2O_2, 0.08% (Table 4-7) of Al was obtained, which is only 2.35% of the amount of Al in the sample. A significant impurity is one that is 10% of that analyte in the sample. This was the behaviour observed for all the base metals and for the fire assay flux (Table 4.8) that were quantified, implying that the errors due to impurities will not be significant.

Table 4.7 Purity analysis of the flux for alkaline fusion by ICP–OES (n=5) in %.

	Al	Ca	Cr	Cu	Fe	Mg	Mn	Ni	Pb	Si	Ti	V	Zn
Blank 1	n.d	0.00	n.d	n.d	0.01	n.d	n.d	n.d	n.d	n.d	n.d	n.d	n.d
Blank 2	n.d	0.00	n.d	n.d	0.01	n.d	n.d	n.d	n.d	n.d	n.d	n.d	n.d
Blank 3	n.d	0.007	n.d	n.d	0.02	n.d	n.d	n.d	n.d	n.d	n.d	n.d	n.d
Blank 4	n.d	n.d	n.d	n.d	0.01	n.d	n.d	n.d	n.d	n.d	n.d	n.d	n.d
Blank 5	n.d	n.d	n.d	n.d	0.01	n.d	n.d	n.d	n.d	n.d	n.d	n.d	n.d

n.d. denotes not detected

Table 4.8 Purity analysis of the flux for the fire assay by ICP–OES (n=5) in %.

	Al	Ca	Cr	Cu	Fe	Mg	Mn	Ni	Pb	Si	Ti	V	Zn
Flux 1	0.08	0.33	0.01	n.d	0.04	n.d	0.002	0.003	0.00	n.d	0.0004	0.085	0.0069
Flux 2	0.08	0.32	0.01	n.d	0.04	n.d	0.002	0.003	0.00	n.d	0.0001	0.084	0.0066
Flux 3	0.08	0.33	0.01	n.d	0.04	n.d	0.002	0.003	0.00	n.d	0.0005	0.085	0.0073
Flux 4	0.08	0.32	0.01	n.d	0.05	n.d	0.002	0.003	0.00	n.d	n.d	0.085	0.0071
Flux 5	0.08	0.33	0.01	n.d	0.05	n.d	0.002	0.003	0.00	n.d	0.0001	0.085	0.0071

n.d. denotes not detected

Upon chemical analysis, the homogeneity of the split samples was assessed by calculating the homogeneity indicator (H_E) and the minimum mass that would give satisfactory homogeneity at an uncertainty level of 5 and 25%. The homogeneity indicator was calculated as shown in Example 4.1.

Example 4.1: H_E for aluminium at a weighed mass of 0.2 g:

$$H_E = (RSD) \times \sqrt{m}$$

$$= (0.97150 \times \sqrt{0.2}$$

$$H_E = 0.43\%$$

$$\mathrm{M} = \left(\frac{\mathrm{K}_2' \times \%\mathrm{RSD})}{\%\mathrm{UNC}}\right) \times \mathrm{m}$$

$$M = \left(\frac{2.459 \times 0.97150}{5}\right) \times 0.2$$

$$M = 0.007518\ g = 7.5\ mg$$

In the calculation of the homogeneity indicator, a value of less than 10% would indicate satisfactory homogeneity. In Table 4.9, the majority of the elements showed good homogeneity, with the exceptions of chromium and copper giving 11 and 12%, respectively. In terms of the gold with an H_E of 8.8%, it was expected that the distribution of gold grains in the ore would be less homogeneous than that of base metals. Furthermore, this behaviour is also supported by the large mass that would be needed to obtain an uncertainty of 5%, which is 1439 g. For the base metals, the mass needed at that uncertainty ranged from 0.0075-5.94 g.

Table 4.9 Homogeneity indicators for base metals and gold at uncertainties of 5 and 25%.

Element	**Mean (%)**	**Standard deviation (%)**	**Relative standard deviation (%)**	**H_E (%)**	**M (g) 5%**	**M (g) 25%**
Al	3.44	0.033	0.97	0.43	0.0075	0.0004
As	0.01	0.00083	9.40	4.20	0.70	0.037
Ca	1.11	0.034	3.09	1.38	0.076	0.0040
Cr	0.03	0.0074	24.62	11.01	4.83	0.2520
Cu	0.01	0.0026	27.31	12.21	5.94	0.31
Fe	3.36	0.048	1.42	0.64	0.016	0.0008
Mg	0.97	0.018	1.82	0.82	0.026	0.0014
Mn	0.04	0.0010	2.44	1.09	0.048	0.0025
Pb	0.02	0.0039	17.97	8.03	2.57	0.13
Si	33.57	0.51	1.52	0.68	0.018	0.0010
Ti	0.23	0.0035	1.51	0.68	0.018	0.0010
Zn	0.01	0.00025	4.84	2.16	0.19	0.0097
Au*	0.29	0.0031	1.06	8.89	1439	57.54

**The weighed sample mass for gold was 100 g, and the unit is $g.t^{-1}$.*

Additionally, the homogeneity of the fractions was assessed by carrying out a one-way ANOVA, and the results are shown in Table 4.10. The results indicated that there was no significant difference ($F_{crit} > F_{stat}$) between the results of the various fractions, therefore leading to the acceptance of the null hypothesis. This analysis supports the data obtained by calculation of the homogeneity indicator.

Table 4.10 Homogeneity evaluation employing ANOVA.

Element	SS		F_{stat}	F_{crit}	P_{value}	Decision rule
	Between	within				
Al	0.014521	0.042533	0.80	4.35	0.53	Accept null
As	7.58E-08	2.96E-07	0.60	4.35	0.64	Accept null
Ca	0.001207	0.000884	3.19	4.35	0.094	Accept null
Fe	0.005114	0.01365	0.87	4.35	0.50	Accept null
Mg	0.000303	0.000348	2.03	4.35	0.20	Accept null
Mn	1.03E-06	7.75E-06	0.31	4.35	0.82	Accept null
Ni	2.45E-07	5.39E-07	1.06	4.35	0.42	Accept null
Ti	7.01E-06	5.98E-05	0.27	4.35	0.84	Accept null
V	4.04E-09	4.48E-08	0.21	4.35	0.89	Accept null

4.3.4 Gold deportment

To quantify the gold that is associated with minerals such as pyrite, magnetite, and quartz, a gold deposition study was carried out. A suitable pre-treatment technique can be selected to release gold from minerals based on the findings. The results of this study indicated that 78% of the gold was recoverable by direct cyanidation, implying its free gold, 9.4% was locked in the HCl digestible minerals such as magnetite, chlorites, and carbonates, and 3% locked in minerals such as pyrite (Table 4.11). This correlates with the XRD analysis, in which chlorite is one of the dominant minerals at 6.9 wt%, while pyrite is one of the lowest at 0.8%. Previous studies have reported 89%, 83%, and 79-86% for gold recoverable by direct cyanidation and 7.4%, 10.3%, and 13-53% for locked-in pyrites (Goodall, 2008; Coetzee *et al.* 2011; Beyuo and Agorhom, 2021). The amount of gold locked in the pyrites indicates that the recovery of gold from the ore will have minimal challenges that are associated with locked gold. Based on these results, no major chemical pre-treatment method was needed.

Table 4.11 Distribution of gold in various minerals by gold deposition.

	Residue	
Au deportment	**Au grade, $g.t^{-1}$**	**Au distribution, %**
Cyanide soluble	0.25	78
Preg-robbed	0.01	3
HCl digestible minerals	0.03	9.4
HNO_3 digestible minerals	0.01	3
Carbonaceous matter	0.01	3
Gangue locked	0.05	15
Total	0.33	100

4.3.5 Size-based fire assay

The recovery of gold from various matrices can be a challenge when gold is not freely occurring and when it is associated with minerals that are difficult to penetrate through. During the analysis of the various screens from the tailings sample, it was observed that the finer screen (-38 µm) gives the highest recovery of gold at 106% (Figure 4.4). This can be attributed to the fact that the coarser material, which could have been a hindrance during chemical analysis, has been sieved into another fraction, therefore opening up the finer particles and subjecting them to increased surface contact. Furthermore, it was observed that in the five screens that were analysed, all of them give an optimum recovery of gold with recoveries starting from 72%. In a previous study by Coetzee *et al.* (2011), it was reported that the gold recovery indeed increased with the decrease in particle size, with a 90% < 106 µm giving a recovery of 93%. It was further discovered that at particle sizes lower than or equal to 106 µm, the percent of particles passing that screen did not affect the gold recovery significantly. Based on these results and the literature, the ultrafine screen of -38 µm was used for further chemical analysis.

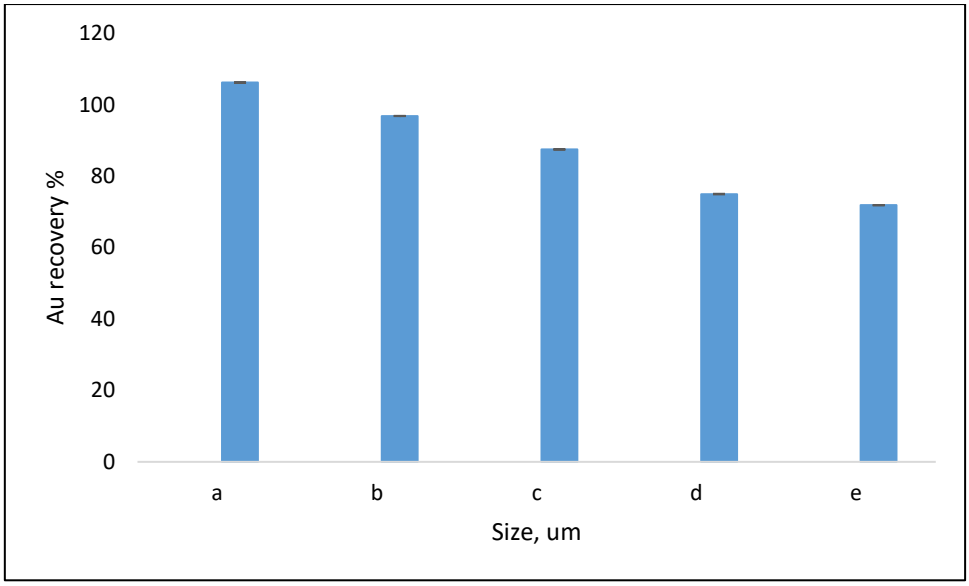

Figure 4.4 Gold recoveries of the screened fractions (n=3). a= -38 µm, b= +38 µm, c= +53 µm, d=+75 µm and e= +106 µm. Standard deviation is represented by error bars.

4.3.6 Acid digestion

As previously mentioned, the main objective of the study was to investigate a digestion method that can accurately quantify gold from a tailings sample with high precision using a fine particle-sized sample. Although various methods exist, most of the methods use large sample masses, use acid combinations that pose various safety hazards, and often require long digestion times (Pitcairn *et al.*, 2006; Tang *et al.*, 2020). In this study, two acid combinations were considered, namely, aqua regia (3HCl:1HNO_3) and reverse aqua regia (1HCl:3HNO_3), with and without the addition of HF, with a sample mass of 1 g and digestion time of 20 min. The mechanism of gold extraction from the sample is based on the formation of a tetranitroaurate ion ($AuNO_3^-$) complex that forms when the nitrate ions are more than the chloride ions, Equations 4.6 and 4.7 (Wang *et al.*, 2016). This ion complex is reported to be more stable than the tetrachloroaurate ion ($AuCl_4^-$) complex. In that sense, aqua regia is expected to recover a part of the gold; however, the reverse aqua regia is likely to give higher recoveries.

$$Au_{(s)} + 3HNO_{3(l)} + 4HCl_{(l)} \rightarrow AuCl^-_{4(l)} + H_3O^+_{(g)} + 3HNO_{2(g)} + 2H_2O_{(l)} \qquad \textit{Equation 4.6}$$

$$Au^{3+}_{(l)} + 4NO^-_{3(g)} \rightarrow Au(NO_3)^-_{4\,(l)} \qquad \textit{Equation 4.7}$$

In Figure 4.5, the recoveries of the experiments are shown for two matrices, VCR and GSB, and the CRMs. It is important to note that all the experiments gave recoveries of greater than 50%. As expected, the experiment with the reverse aqua regia had recoveries starting from

76%, while that with only aqua regia started at 54%. An interesting observation was that in both the presence and absence of HF with the acid combination, the recoveries were satisfactory. The addition of HF aids the decomposition of quartz when gold is encapsulated, which hinders optimum recoveries. This suggests that for tailings samples, the gold is less likely to be encapsulated by the quartz grains. This is also supported by the gold depot analysis (Table 4.11), which showed that the amount of gold associated with quartz was low at 0.05 $g.t^{-1}$. Similar observations were made with the CRMs that were used, which are lower in grade than the sample. With regard to the CRMS, AMIS 610 (certified value of 0.068 $g.t^{-1}$) showed better recoveries compared to the other samples, which had a higher grade. This means that the method was suitable even for a sample with a low amount of gold. Furthermore, the *z* scores of the CRMs were calculated, as shown in Table 4.12, and the *z* scores ranged from 0.017-3.08. In statistical terms, this was a good performance of the methods, as the data it generated indicated average deviation from the certified value. In a study by Wang and Bridle (2014), an acid combination of HCl:HBr was used for tailings, and although it worked as the mixture is good for attacking sulfides, there is a risk of losing the bromine ions in the solution through vaporization, while in Helmeczi *et al*. (2018), aqua regia was used to digest the sample assisted by sonication in a warm water bath. The shortcoming of this method is that because the temperature is 60 °C, most of the material will not be decomposed, meaning it will have to be filtered off.

In terms of having a residue left behind after digestion due to incomplete digestion, the constant additions of HNO_3 compensated for that as the nitrate ions were always in excess, thereby being available to digest the residues over time. It could have also been because of the nature of the tailings, whereby most of the minerals are already in small quantities and since it has been processed before, it makes subsequent chemical analysis much easier.

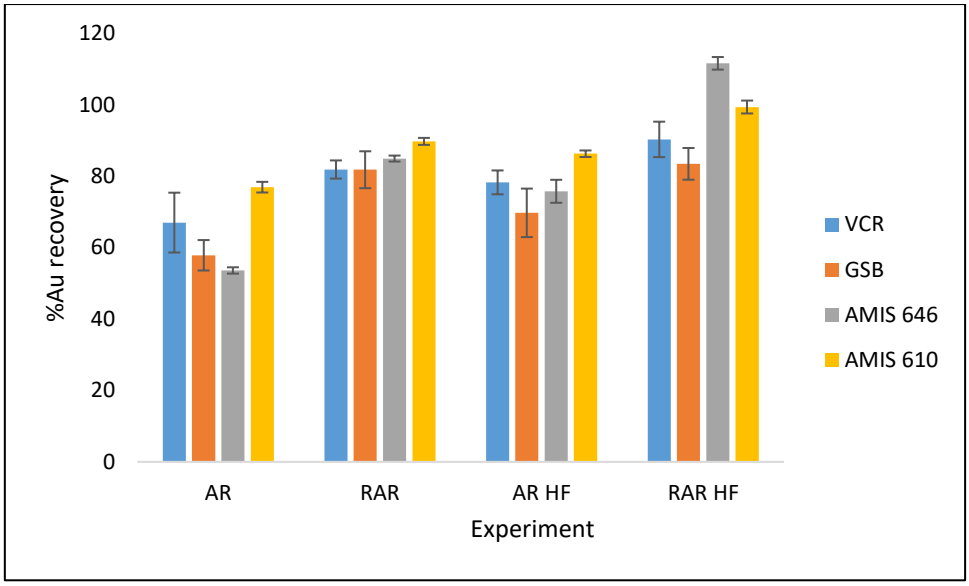

Figure 4.5 Gold recoveries obtained from the four experiments (n=3). The standard deviation is represented by the error bars. AR=aqua regia, RAR=reverse aqua regia, AR=aqua regia with HF, RAR=reverse aqua regia with HF.

Table 4.12 Gold recovery results for the certified reference materials determined by ICP–MS (n=3).

CRM	Experiment	Certified value ± standard deviation ($g.t^{-1}$)	Recovered value ± standard deviation ($g.t^{-1}$)	%Recovery	*z* score
AMIS 610	AR	0.068 ± 0.014	0.061± 0.015	76.9	0.5
	RAR		0.052 ± 0.0041	77	3.8
	AR HF		0.058 ± 0.023	85.3	0.017
	RAR HF		0.059 ± 0.049	87	0.5
AMIS 646	AR	0.166 ± 0.028	0.14 ± 0.0089	54	3.07
	RAR		0.14± 0.012	85	2.2
	AR HF		0.19 ± 0.038	76	0.5
	RAR HF		0.13 ± 0.017	74	2.5

In the analysis of the acid digestion samples, all the wavelengths selected for gold analysis by ICP–OES suffered considerable interference from the base metals in the samples. Although the instrument can deconvolute interfering peaks using the Agilent Fast Automated Curve-fitting Technique (FACT), this could not be possible for the samples, as the interferences were too

close to the analyte. This serves as a limitation for the analysis of gold in acid digestion samples by ICP–OES.

In Table 4.13, a comparison of the various acid digestion methods for gold analysis and the LODs is shown. Various LODs were obtained with Monteiro *et al.* (2003), obtaining 0.002 $\mu g.kg^{-1}$ with analysis on GF-AAS, and Pitcairn *et al.* (2006), with the same LOD on ICP–MS. Both of these methods used larger sample masses and aqua regia as the main reagents; however, they were coupled with other methods, such as solvent extraction. This means that an extra step was added after acid digestion to extract the gold into the organic phase, which often requires special instrumental compartments. Based on the results of this study, acid digestion was sufficient to extract the majority of the gold and analyse the ICP–MS. This is supported by the limits of detection shown in Table 4.13, which ranged between 0.14 and 0.334 $\mu g.kg^{-1}$, with lower LODs obtained from the reverse aqua regia. It is noted that some of the reported literature methods have lower LODs than this study; however, the advantages that this method offers are that it uses a low sample mass and a minimum volume of acids and does not require further sample enrichment, such as solvent extraction, to enrich the gold concentration. This is beneficial for laboratories that process a significant number of samples daily.

Table 4.13 Comparison of proposed methods to published methods for the quantification of gold from geological samples, including tailings.

Method	Key reagents	Sample mass (g)	Analysis method	LOD, ($\mu g.kg^{-1}$)	Reference
Acid digestion with solvent extraction	HNO_3+HF+HCl DLLME	10	GF-AAS	0.0020	(Monteiro *et al.*, 2003)
Acid digestion	Aqua regia	10	GF-AAS	0.23	(Liu *et al.*, (2019)
Acid digestion	HNO_3+HF+HCl+ aqua regia DIBK-loaded CG71 resin	4	ICP–MS	0.0020	(Pitcairn *et al.*, (2006)
Acid digestion	Reverse aqua regia	1	ICP–MS	-	(Wang, Baker and Brindle, 2016)
Acid digestion	Aqua regia	1	ICP–MS	0.334	This study
Acid digestion	Reverse aqua regia	1	ICP–MS	0.18	This study
Acid digestion	Aqua regia with HF	1	ICP–MS	0.292	This study
Acid digestion	Reverse aqua regia with HF	1	ICP–MS	0.14	This study

4.3.7 Statistical evaluations

Measurement uncertainty studies were carried out to compare the acid digestion method with the reverse aqua regia without the addition of HF to the conventional fire assay method. In Table 4.14, the quantified uncertainty contributors are shown together with the combined and expanded uncertainties. For Type B uncertainty, the standard uncertainty was determined by taking the quotient of the expanded uncertainty on the certificate and the coverage factor. For

Type A uncertainty, the standard deviation was taken as the standard uncertainty for repetitive measurements such as for homogeneity and repeatability (precision).

Uncertainty due to weighing

The calibration certificate reported an expanded uncertainty of 0.0003 g at a coverage factor of 2; therefore, the uncertainty due to weighing of the sample is given by:

$$u_s = \frac{Expanded\ uncertainty}{coverage\ factor} = \frac{0.0003}{2} = 0.00015$$

Uncertainty due to the use of volumetric glassware

A 50 mL volumetric flask was used (at 23 °C), which has an uncertainty of 0.05 mL at 20 °C and follows a triangular distribution ($k = \sqrt{3}$). The uncertainty is then given by:

$$u_1 = \frac{0.05}{\sqrt{3}} = 0.02041$$

Due to the temperature variation, the uncertainty contributed by the variation is calculated as:

$$u_2 = \frac{volume \times expansion\ factor \times temperature\ difference}{coverage\ factor}$$

$$u_2 = \frac{50 \times (2.1 \times 10^{-4}) \times 3}{1.96}$$

$$u_2 = 0.160714$$

The combined uncertainty contributed by the use of volumetric glassware:

$$u_{glassware} = \sqrt{(0.02041)^2 + (0.160714)^2} = 0.16$$

$$u_{glassware}relative = \frac{0.16}{50} = 0.0032$$

Uncertainty to dilution of the working standard

A working standard of 1 µg.mL^{-1} was prepared from a 1000 µg.mL^{-1} stock solution, with an uncertainty of 5 µg.mL^{-1}, which follows a rectangular distribution (k=$\sqrt{3}$). The uncertainty due to dilution of stock solution is:

$$u_{stock} = \frac{5}{\sqrt{3}} = 2.88675$$

The working standard was diluted to make calibration standards in the range of 0.005-0.1 µg.mL^{-1}. Repetitive dilutions of the lower and upper standards gave standard deviations of 0.000387 (u_{v1}) and 0.000936 mL (u_{v2}), respectively. The overall uncertainty as a result of the dilution of the working standard is calculated by:

$$u_{working\ standar}relative = \sqrt{\left(\frac{u_{stock}}{[stock]}\right)^2 + \left(\frac{u_{v1}}{dispensed\ volume}\right)^2 + \left(\frac{u_{v2}}{dispensed\ volume}\right)^2}$$

$$u_{working\ standard}relative = \sqrt{\left(\frac{2.88675}{1000}\right)^2 + \left(\frac{0.000387}{0.5}\right)^2 + \left(\frac{0.000936}{5}\right)^2}$$

$$u_{working\ standard}relative = 0.5 \times 3.44 \times 10^{-3} = 0.0017215$$

Uncertainty due to dilution factor

A dilution factor of 5 was used for all the acid digestion samples with a final volume of 10 mL; therefore, a volume of 2 mL was taken from each sample. The standard deviation associated with the repetitive dispensing of 2 mL and 10 mL was calculated as 0.000237 and 0.000103 mL, respectively. These standard deviations are then used in the equation below to calculate the uncertainty arising from the dilution factor.

$$= 5 \times \sqrt{\left(\frac{0.000237}{2}\right)^2 + \left(\frac{0.000103}{10}\right)^2}$$

$$u_{dilution\ factor}relative = 0.0001189$$

As per the data obtained (Table 4.14), the uncertainties between the two techniques are comparable. The major contributors to the uncertainty are the method repeatability (0.031 and 0.038 g.t^{-1}) and reproducibility (0.014 and 0.0093 g.t^{-1}) for both techniques. This was expected because although the fire assay is good for the quantification of gold, it does suffer from minimal repeatability issues, which is due to the nature of the process. Homogeneity contributes more to errors in chemical analysis, especially when there are nugget effects to consider (Stanley, 2007). In terms of this experiment and calculations, it contributed approximately 12% to the overall uncertainty. This is satisfactory considering that a sample mass of 1 g was used in the acid digestion.

Table 4.14 Quantification of the uncertainties from various parameters from acid digestion and fire assay with ICP–MS finish.

Contributor	Acid digestion	Fire assay
Mass balance	0.00015	0.00015
Glassware calibration	0.0032	0.0032
Homogeneity	0.031	0.034
Repeatability	0.031	0.038
Reproducibility	0.014	0.0093
Instrument stability	0.00038	0.00054
Concentration of dilute working standard	0.0017	0.0017
Dilution factor	0.00012	0.00012
Combined uncertainty	*0.046*	*0.052*
Expanded uncertainty	*0.092*	*0.10*
Quantified value and uncertainty	*0.258 ± 0.092 g.t^{-1}*	*0.26 ± 0.10 g.t^{-1}*

Data is represented in two significant figures, except for the quantified value, which is expressed using uncertainty rules.

The data in Table 4.14 are further supported by a paired t test, which showed that in the comparison of the means of the two techniques, there is no significant difference, with a $t_{statistic}$ calculated as -1.59 and $t_{critical}$ calculated as 0.15. Subsequently, the challenge is, if both methods result in similar uncertainties, which method is then to be chosen for routine analysis. Based on the method's simplicity, less time needed, and no use of toxic reagents such as lead, acid digestion would be best recommended, and it does not require intensive skills such as fire assays.

4.4 Conclusion

The purpose of this current study was to assess the suitability of acid digestion using reverse aqua regia and normal aqua regia with and without the addition of HF for the quantification of gold from mine tailings and to compare its uncertainty with those obtained from the conventional fire assay. The study has identified that by using the finer screen (-38 µm) in terms of particle size, satisfactory homogeneity is obtained, which means that in terms of using a sample mass of 1 g, the analysis should not be affected by homogeneity. Furthermore, gold recoveries of >50% were obtained regardless of the presence or absence of HF, implying that encapsulation of the gold grains by minerals such as quartz was not a hindrance. The

uncertainty evaluation performed ranged between 0.092 and 0.10 $g.t^{-1}$ for the acid digestion and fire assays, respectively. This was impressive, as it implies that the acid digestion method is comparable with the fire assay. Overall, the reverse aqua regia method, used on the finer screen, showed great performance and can be used successfully with low uncertainties for the quantification of gold in mine tailings. The major advantage of this method is that it is able to address the challenges that are often encountered in the acid digestion of mineral ores. Such challenges include homogeneity and incomplete dissolution. A majority of the studies that have been carried out use sample masses of at least 10 g and harsh chemical conditions; however, this study used 1 g of sample under easy conditions. Therefore, it is a method that can be recommended for gold analysis, which is also further strengthened by the evaluation of the measurement uncertainties.

4.5 References

Araujo, F. S. M., Taborda-llano, I and Nunes, E. B. (2022). Recycling and Reuse of Mine Tailings : A Review of Advancements and Their Implications. *Geo*, *12*(319), 1–16. https://doi.org/10.3390/geosciences12090319

Beyuo, M and Agorhom, E. (2021). Gold Deportment and Mineralogical Characterization Studies Gold Deportment and Mineralogical Characterization Studies for Improved. *4th UMaT Biennial International Mining and Mineral Conference*, *March*, 1–11.

BIPM, IEC, IFCC, ILAC, ISO, IUPAC, IUPAP, O. (2008). Evaluation of measurement data — Guide to the expression of uncertainty in measurement. *Joint Committee for Guides in Metrology*, *JCGM*, *100*, 134. https://www.bipm.org/documents/20126/2071204/JCGM_100_2008_E.pdf/cb0ef43f-baa5-11cf-3f85-4dcd86f77bd6

Blyth, K. M., Phillips, D. N and van Bronswijk, W. (2004). Analysis of gold ores by fire assay. *Journal of Chemical Education*, *81*(12), 1780–1782. https://doi.org/10.1021/ed081p1780

Coetzee, L. L., Theron, S. J., Martin, G. J., Merwe, J. D. Van Der and Stanek, T. A. (2011). Modern gold deportments and its application to industry. *Minerals Engineering*, *24*(6), 565–575. https://doi.org/10.1016/j.mineng.2010.09.001

Dong, X., Xiong, Y., Wang, N., Song, Z., Yang, J., Qiu, X and Zhu, L. (2020). Analytica Chimica Acta Determination of trace elements in high-purity quartz samples by ICP- OES and ICP–MS : A normal-pressure digestion pretreatment method for eliminating unfavorable substrate Si. *Analytica Chimica Acta*, *1110*, 11–18. https://doi.org/10.1016/j.aca.2020.03.006

Ghosh, P., Mandal, H., Sirisha, B., Sen, U., Goswami, S and Kiran, N. V. R. (2019). A Modified Acid Digestion Method for Analysis of Gold in Geological Samples: A Comparative Study. *Mapan - Journal of Metrology Society of India*, *34*(4), 551–558. https://doi.org/10.1007/s12647-019-00326-8

Goodall, W. R. (2008). Characterization of mineralogy and gold deportment for complex tailings deposits using QEMSCAN®. *Minerals Engineering*, *21*(6), 518–523. https://doi.org/10.1016/j.mineng.2008.02.022

Guo, Z., Bai, Y., Cui, J., Mei, Y and Ma, Z. (2014). Determination of multielement contents in gypsum by ICP–AES. *Guang Pu Xue Yu Guang Pu Fen Xi*, *34*(8), 2250–2253.

Helmeczi, W., Helmeczi, E., Baker, L. A., Wang, Y and Brindle, I. D. (2018). Development of a general acid method for the digestion of gold ore samples together with a comparison of extraction solvents for gold and determination by microwave-induced plasma-atomic emission spectrometry (MIP-AES). *Journal of Analytical Atomic Spectrometry*, *33*(8), 1336–1344. https://doi.org/10.1039/c8ja00136g

Liu, Y. H., Wan, B and Xue, D. S. (2019). Sample digestion and combined preconcentration methods for the determination of ultralow gold levels in rocks. *Molecules*, *24*(9). https://doi.org/10.3390/molecules24091778

Lottermoser, B. (2007). *Mine waste: Characterization, treatment, environmental impact* (2nd ed.). Springer International Publishing:New York.

Mao, X., Liu, J., Huang, Y., Feng, L., Zhang, L., Tang, X., Zhou, J., Qian, Y and Wang, M. (2013). Assessment of Homogeneity and Minimum Sample Mass for Cadmium Analysis in Powdered Certified Reference Materials and Real Rice Samples by Solid Sampling Electrothermal Vaporization Atomic Fluorescence Spectrometry. *Journal of Agricultural and Food Chemistry*, *61*, 848–853. https://doi.org/10.1021/jf3045473

Monteiro, M. I. C., Lavatori, M. P. A and De Oliveira, N. M. M. (2003). Determination of gold in ores by isobutyl methyl ketone extraction and electrothermal atomic absorption spectrometry: A stability study of the metal in organic media. *Geostandards Newsletter*, *27*(3), 245–249. https://doi.org/10.1111/j.1751-908X.2003.tb00725.x

Nengovhela, A. C., Yibas, B and Ogola, J. S. (2006). Characterization of gold tailings dams of the Witwatersrand Basin with reference to their acid mine drainage potential, Johannesburg, South Africa. *Water SA*, *32*(4), 499–506. https://doi.org/10.4314/wsa.v32i4.5290

Okereafor, U., Makhatha, M., Mekuto, L and Mavumengwana, V. (2020). Gold mine tailings: A potential source of silica sand for glass making. *Minerals*, *10*(5). https://doi.org/10.3390/min10050448

Pitcairn, I. K., Warwick, P. E., Milton, J. A and Teagle, D. A. H. (2006). Method for ultralow-

level analysis of gold in rocks. *Analytical Chemistry*, *78*(4), 1290–1295. https://doi.org/10.1021/ac051861z

Stanley, C. (2007). The Fundamental Relationship Between Sample Mass and Sampling Variance in Real Geological Samples and Corresponding Statistical Models. *Exploration and Mining Geology*, *16*(1–2), 109–123. https://doi.org/10.2113/gsemg.16.1-2.109

Tabelin, C. B and Igarashi, T. (2009). Mechanisms of arsenic and lead release from hydrothermally altered rock. *Journal of Hazardous Materials*, *169*(1–3), 980–990. https://doi.org/10.1016/j.jhazmat.2009.04.049

Tomiyama, S., Igarashi, T., Tabelin, C. B., Tangviroon, P and Ii, H. (2019). Acid mine drainage sources and hydrogeochemistry at the Yatani mine, Yamagata, Japan: A geochemical and isotopic study. *Journal of Contaminant Hydrology*, *225*(January), 103502. https://doi.org/10.1016/j.jconhyd.2019.103502

Wang, Y., Baker, L. A and Brindle, I. D. (2016). Determination of gold and silver in geological samples by focused infrared digestion: A reinvestigation of aqua regia digestion. *Talanta*, *148*, 419–426. https://doi.org/10.1016/j.talanta.2015.11.019

Wang, Y and Brindle, I. D. (2014). Rapid high-performance sample digestion for ICP determination by ColdBlock™ digestion: Part 2: Gold determination in geological samples with memory effect elimination. *Journal of Analytical Atomic Spectrometry*, *29*(10), 1904–1911. https://doi.org/10.1039/c4ja00189c

Zhang, W and Hu, Z. (2019). Recent advances in sample preparation methods for elemental and isotopic analysis of geological samples. *Spectrochimica Acta - Part B Atomic Spectroscopy*, *160*. https://doi.org/10.1016/j.sab.2019.105690

5 THE EFFECTIVENESS OF IRON AND TIN IN THE GRAVIMETRIC QUANTIFICATION OF GOLD FROM LOW-GRADE TAILINGS

Kedibone Nicholine Mashale[1,2], Napo Godwill Ntsasa[1], Majimi James Sehata[1], James Tshilongo[1,2] and Luke Chimuka[2]

[1]*Analytical Chemistry Division, Mintek, 200 Malibongwe Drive, Praegville, 2194, South Africa.*

[2]*Molecular Sciences Institute, School of Chemistry, University of the Witwatersrand, Braamfontein, 2000, South Africa.*

[*]*Corresponding author: kedibonema@mintek.co.za; Tel: 011 709 4050.*

Abstract

In the Gauteng region, mine tailings cover a vast area (400-600 km^2) and still contain rich minerals such as gold and other precious metals. The gold that was first lost due to ineffective methods is now being recovered by a number of tailings retreatment units. The necessity for an industrial and analytical procedure that can be used to quantify the gold with the highest degree of precision and the fewest measurement uncertainties is thus made clear. The characterization tests by X-ray diffraction (XRD) showed the presence of high quartz (78-82%), talc (1%), gypsum (0.5%), calcite (0.3%), pyrite (0.4-0.8%), dolomite (1.4%), muscovite (11.4-13.8%) and chloritoid (11.6), which were also consistent with the pH (7-9) and the elemental composition. Before any chemical analysis, a 0.32 $g.t^{-1}$ tailings sample was leached with cyanide to reduce the grade to approximately 0.1 $g.t^{-1}$, which was the sample used for further analysis. The quantification method was based on a fire assay with a gravimetric finish. To optimize the formation of lead rain during the fire assay, the PbO:C ratio in the fire assay flux was varied between 8 and 12, and the sample mass was between 50 and 120 g. Subsequently, the correlation between the initial lead and that recovered after the fire assay was studied by measuring the lead in the button by X-ray fluorescence (XRF). It was observed that varying the flux influenced the gold recovery in both matrices, with a ratio of 10 producing higher recoveries (>85%) and a mass of 100 g being the optimum. An analysis of variance (ANOVA) test showed that the data produced by the three fluxes and masses are significantly different, implying that it was necessary to incorporate variations. In terms of the co-collectors, Sn resulted in higher recoveries than Fe because Sn has a melting point and density of 232 °C and 7.31 $g.cm^{-3}$, respectively, which is significantly lower than that of Fe at 1538 °C and a

density of 7.78 $g.cm^{-3}$. This is because the formation of slag and its separation from precious metals depend highly on these two properties. Quantification of gold by gravimetry is a rather straightforward process, with weighing balances being the only sources of uncertainty. Therefore, the measurement uncertainty associated with the quantification was determined to be ± 0.00432 $g.t^{-1}$. This is lower compared to that obtained from acid digestion.

Keywords: Fire assay, Co-collectors, Measurement uncertainty

5.1 Introduction

There is currently a movement and an interest in the reprocessing of mine tailings to recover left-over gold from the initial process. This is because mine tailings are reported to occupy a large amount of land, with 400-600 km^2 of land being occupied in the Johannesburg area (Bureau and Géologiques, 2008; Olobatoke and Mathuthu, 2016). Furthermore, mine tailings have the potential to be environmental hazards, as some minerals can leach into ground and surface water, and they also contribute to the formation of acid mine drainage (Kossoff *et al.*, 2014). Due to the various effects of mine tailings on the environment, processing plants for tailings have been developed by various mining houses to reduce their ecological footprints. Pan African Resources have developed the Elikhulu and Barberton Tailings Retreatment Plant (BTRP), which processes approximately 1.2 Mt historic tailings per month and recovers about 55 000 ounces of gold (Pan African Resources, 2020). Another tailings processing plant that has been developed is the Ergo plant by DRDGOLD, which processes 1.7 Mt of tailings and recovers 80 000 ounces of gold (DRDGOLD, 2016). These tailings treatment plants are forecasted to last for approximately 10 years, which means a significant amount of tailings would have been processed by then. The average amount of gold that is reported to be recovered in the 10 years is 0.5 $g.t^{-1}$, with the grade decreasing as reprocessing continues.

To support this tailings reprocessing industry, a more sensitive, easy and commercial method is needed that can accurately quantify the gold from the tailings, irrespective of the tailings matrix. It is known that the fire assay (FA) is the best technique for the recovery of precious metals (gold, palladium, platinum, ruthenium, rhodium, osmium, and iridium) from metallurgical and geological samples (Rao and Reddi, 2000). In the fire assay, there is an option of having an instrumental finish by inductively coupled plasma optical emission spectroscopy (FA-ICP–OES) or a gravimetric finish (FA-G). A gravimetric finish offers advantages such as direct traceability to the mass unit, placing more confidence in the results obtained, while instrumental analysis offers fast analysis and can indicate when there are interfering elements.

Additionally, FA-G is less complicated, making it preferable in the fire assay industry. Furthermore, in terms of measurement uncertainty, there are minimal factors that contribute. However, some challenges exist with a gravimetric finish, especially for a low-grade sample. Such challenges include difficult metals that cannot be removed before weighing and producing a prill that can be accurately weighed. In general, the shortcomings of fire assays include that they require a specialized assayer and use lead, which is toxic to the environment.

Apart from fire assay, other decomposition and preconcentration methods that have been tested for the quantification of gold include electrochemistry (Baghalha, 2007), potentiometric titration (Caporali *et al.,* 2010), acid digestion with solvent extraction (Ghosh *et al.,* 2019), nanoparticles (Haiss *et al.,* 2007; Ye *et al.,* 2014) and acid digestion with precipitation (Yin *et al., 2017)*. The various studies have produced good recoveries with high accuracies, with limits of detection being in the parts per trillion range. However, for most of the methods, their shortcomings are the possibility of interfering analytes being extracted with gold and the requirement for specialized equipment. For example, solutions from methyl isobutyl ketone (MIBK) solvent extraction require specialized compartments to be analysed by ICP–OES or MS. Therefore, FA is the optimal method to optimize for commercial purposes.

To make the fire assay method more sensitive and efficient, other metals have been investigated for the possibility of replacing lead during collection. Such metals include bismuth (Bi), antimony (Sb), iron (Fe), copper (Cu) and cobalt (Co), individually or as alloys such as in the case of Sn-Cu (Ni *et al.,* 2021), (Ni *et al.,* 2021), (Ni *et al.,* 2022), (Ni *et al.,* 2020), (Masasire *et al.,* 2022). The characteristics that are looked at in these alternative metals are the ability to melt at low fusion temperatures and the ability to form a button with the gold, which must be dense enough to enable separation from the slag and must be removable as oxides. For example, lead has a melting point and density of 327.5 °C and 11.4 $g.cm^{-3}$, respectively, compared to copper, which has a melting point and density of 1 085 °C and 8.96 $g.cm^{-3}$. This implies that lead would be a better collector than copper. Lead is mostly chosen due to its low melting temperature of 327.5 °C, and the gap between the density of the lead and a typical fire assay slag (2-3 $g.cm^{-3}$) is significant, implying that once the lead has collected the gold, it will be easy to separate it from the slag material.

The investigation of the use of these metals showed that they do have the capabilities to be gold collectors; however, they presented other challenges. In Ni *et al.* (2022), the use of Sn was studied, and it was noted that Sn suffers from selectivity and cannot be removed during cupellation. In Ni *et al.* (2020), Sn and Cu were combined as an alloy to bypass the problems that they experience individually. The problems were that molten Sn can also trap base metals, making it difficult for a matrix that has high base metal content, while Cu is difficult to dissolve in acids and its cupellation cannot be efficiently controlled (Ni *et al.*, 2020). In order studies, instead of changing the collector altogether, they investigated ways that it can be enhanced by the addition of those metals to the lead before fusion. The common metals added are usually precious group elements (PGE), such as gold (Au), palladium (Pd), and silver (Ag). For example, Pd is added to the collection of rhodium (Rh) using Pb-FA in quart, while Ag is added to the basic Pb-FA collection. However, it is quite expensive to use these as co-collectors when other base metals can be used. In Masasire *et al.* (2022), Fe, Cu, and Co were investigated for this purpose, and it was found that the metals individually enhance the collection of precious metals. Therefore, in this study, the possibility of quantifying low-grade gold at levels below 1 $g.t^{-1}$ by gravimetric analysis was investigated. This included the derivation of the basic fire assay method by looking at the flux composition and the addition of Fe and Sn as co-co-collectors. Thereafter, measurement uncertainties in the method were evaluated.

5.2 Materials and methods

5.2.1 Materials

No alterations were made to the analytical grade of any of the compounds or reagents used. From Associated Chemical Enterprises Pty Ltd. (Johannesburg, South Africa), sodium cyanide (NaCN) and sodium hydroxide (NaOH) were acquired. Nitric acid (HNO_3) and hydrochloric acid (HCl) were purchased from Sigma Aldrich in Missouri, United States of America. The 1000 mg. L^{-1} gold stock solution was purchased from LGC Standards in Middlesex, England. PureChem, situated in Douglasdale, South Africa, provided the specially formulated lead-based flux for the fire assay. The certified reference materials AMIS 610 and AMIS 646 were purchased from African Mineral Standards in Modderfontein, South Africa (based on matrix and gold quality). Only deionized water from a Milli-Q system from Sigma Aldrich (Missouri, United States of America) was used in the experiments.

5.2.2 Sample information

Two mine tailing samples of 25 kg were sourced from the Ventersdorp Contact Reef (VCR) of the Witwatersrand Basin and the Green Stone Belt (GSB) in Barberton. The tailings samples

consist mainly of quartz (SiO_2) as the major mineral, muscovite ($KAl_2(AlSiO_{10})(F,OH)_2$), chlorite ($(Fe,Mn)_{4\text{-}6}(SiAl)_4O_{10}(OH,O)_8$), dolomite ($MgCO_3$. $CaCO_3$), chloritoid ($(Fe,Mg,Mn)Al_2SiO_5(OH)_2$) with pyrite as a minor mineral. The sulfur content of the samples obtained by combustion ranged between 1 and 1.5%, while the specific gravity was obtained as 2.79 dimensionless. The surface area by BET analysis of the original sample was 3.3 $m^2.g^{-1}$.

5.2.3 Cyanide leaching for higher grades

A cyanide gold leach was carried out to reduce the grade in the tailings samples, which was at an average of 0.32 $g.t^{-1}$, whereas the desired grade needed for the method development was below 0.1 $g.t^{-1}$. In duplicate, 200 g was weighed and added into a 2 L reactor bottle along with 400 mL of water to make a slurry. The slurry was placed on a roller bench and allowed to mix for at least an hour before taking the pH. The pH of the slurry was taken and adjusted to a final pH >10.5 using NaOH. Once the pH was stable, 0.2 g of NaCN was added to the slurry and placed on the roller bench for 24 h. Subsequently, the slurry was removed from the roller bench, and the pH was checked and adjusted to at least 10.5. The pH, mass and volume of the slurry are recorded in Table 5.1. The slurry was filtered using vacuum filtration, incorporating two washes of the residue. The residues were then collected and dried overnight at 60 °C, whereas the filtrate and wash solutions were collected in plastic bottles and analysed by atomic absorption spectroscopy (AAS).

Table 5.1 Experimental parameters for cyanide leaching.

Parameter	Experiment 1		Experiment 2		Experiment 3		
Ore mass (g)	200.03	200.01	199.75	216.96	197.59	197.83	208.59
Water mass (g)	393.08	393.08	385.86	396.58	415.46	401.94	397.56
Slurry mass (g)	592.83	592.80	587.38	613.07	613.05	599.77	616.15
Slurry volume (mL)	415	412	450	450	408	400	407
pH before NaOH	8.55	8.83	8.17	8.86	7.66	7.75	7.75
NaOH addition (g)	0.3	0.3	0.2	0.2	0.4	0.4	0.4
pH after lime	11.40	11.5	11.70	11.72	11.60	11.12	11.41
NaCN ($kg.t^{-1}$)	1	1	1	1	2	3	5
Mass of slurry after test (g)	591.01	591.39	583.06	612.67	609.02	597.88	603.95
Wet cake (g)	248.23	251.59	236.69	269.91	260.24	255.63	265.57
Dry cake (g)	197.46	196.29	189.34	203.69	198.89	196.99	205.71
Mass loss (%)	1.3	1.9	5	6	0.9	0.42	1.4
Filtrate (mL)	325	340	306	343	350	360	350
pH final	10.82	10.87	10.60	10.67	10.65	10.21	10.71

5.2.4 Fire assay

In fire assay, the varied parameters were the ratio of the litharge (PbO) to the reducing agent (C), the mass of the tailings samples and the addition of co-collectors during fusion. In this method, 350 g of the flux was weighed into a large crucible and mixed with the tailings sample. This combination was then mixed with a spatula until homogenous. A scoop of silica was added to cover the surface of the sample mixture to protect the crucible. The mixture was placed in a furnace at 1400 °C for one hour for fusion. After the time had elapsed, the red melt was poured into iron molds and allowed to cool before deslagging the sample (Figure 5.1). The button obtained after deslagging was placed on a cupel and cupellated at 1000 °C for one hour (Blyth *et al.* 2004). The prill obtained was then washed with dilute HNO_3 to remove the silver as silver nitrate. The prill was placed on a hot plate for drying and annealed by placing it under a flame. The gold was then weighed on a sensitive mass balance, and the grade was calculated using Equation 5.1.

$$Au\ \left(\frac{g}{t}\right) = \frac{weighed\ prill\ (mg)}{Sample\ mass\ (g)} \times 1000 \qquad \textit{Equation 5.1}$$

Figure 5.1 Pouring of the fused sample into iron molds.

Three flux formulations were obtained in which the ratio (PbO:C) was 12 (Flux A), 10 (Flux B) and 8 (Flux C). The complete components are shown in Table 5.2. In terms of the sample mass variation, three masses were tested, which were 50, 100 and 120 g.

Spiking standards of Fe and Sn (5, 10 and 20 mg. L^{-1}) were prepared from a 1000 mg. L^{-1} stock solution. The volume of the co-collectors added was kept constant at 20 mL per sample. These solutions were then added to the samples and mixed into the sample before fusion.

Table 5.2 Components of the three fluxes employed.

Component	Flux A	Flux B	Flux C
Litharge	21.70	21.50	25.80
Sodium carbonate	38.4	39.14	51.70
Fused borax	24.8	24.52	9.80
Silica powder	12.8	12.75	
Reducing agent	Flour-1.8	Flour- 2.08	Maize-3.10
Paraffin	0.5	0.01	-
Kerosol	-	-	0.30
PbO:C	12	10	8

5.2.4.1 Lead determination

Before cupellating the buttons to obtain the prills, the deslagged buttons were flattened to obtain a flat surface. The button was then analysed on an energy dispersive X-ray fluorescence (EDXRF) for lead content. The expectation was that for an initial lead content of 25.8% in 350 g, 90.3 g of lead was started with, and close to that amount should be recovered after the fusion, as per Equation 5.2.

$$PbO_{(s)} + C_{(s)} \rightarrow Pb_{(l)} + CO_{(g)} \qquad \textit{Equation 5.2}$$

Since the reaction is a 1:1 basis, the amount of lead in the flux before fusion is what should be recovered after the fusion, with minimal losses. After the lead has been determined, the buttons are then processed as in Section 5.2.4.

5.2.5 Instrumental analysis

AAS

A Perkin Elmer PinAAcle 900H AAS was used with a 10 cm air-acetylene burner assembly. Method development and data acquisition were performed using Winlab AA flame software (Version: 7.4.1.073). The background correction was performed using a deuterium arc continuum source system. The wavelength for the gold was set at 242.8 nm at a slit of 0.7 nm. The flow rates of the gases were 2.06 $L.min^{-1}$ for acetylene and 12 $L.min^{-1}$ for air, while the current was set at 10 mA. The analysis was performed using manual sampling. The highest standard from the calibration curve was used to set the burner at a position that would result in an absorbance of between 0.3 and 0.4. Thereafter, the samples were diluted according to the reading that the highest standard gave. The AAS was calibrated in the linear range of 0.05-5 $mg.L^{-1}$. Since the samples analysed on this instrument were emanating from cyanidation leach, the calibration standards were prepared in a NaCN matrix. The criteria for the calibration performance are shown in Table 5.3.

Table 5.3 Criteria for calibration of AAS for gold analysis.

Performance parameter	Criteria
Calibration linearity	Must correlate 0.99 to 1
Method recoveries	< 10%
LOD	>Blank reading
LOQ	Must be clearly above the blank reading
Calibration error	<5% for concentrations above 3 $mg.L^{-1}$ <10% for concentrations below 3 $mg.L^{-1}$

5.3 Results and Discussion

5.3.1 Instrumental analysis

In Table 5.4, the performance of the instrument during calibration is shown. AAS gave satisfactory linearity at 0.05 to 5 mg. L^{-1} with a correlation coefficient of 0.9972 (Figure 5.2). In terms of the calibration errors, the instrument performance was satisfactory, as they were within the set limits as stated in Table 5.3.

Table 5.4 Calibration information showing the calculated concentrations and calibration errors.

Standard	Mean signal (Abs)	Entered concentration $mg.L^{-1}$	Calculated concentration $mg.L^{-1}$	%RSD	Calibration error %
Standard 1	0.0042	0.050	0.049	0.06	2
Standard 2	0.0089	0.100	0.107	7.14	7
Standard 3	0.0387	0.500	0.479	1.88	4.2
Standard 4	0.0774	1.000	0.962	0.25	3.8
Standard 5	0.1733	2.00	2.160	1.18	8
Standard 6	0.3849	5.00	4.802	0.59	3.96

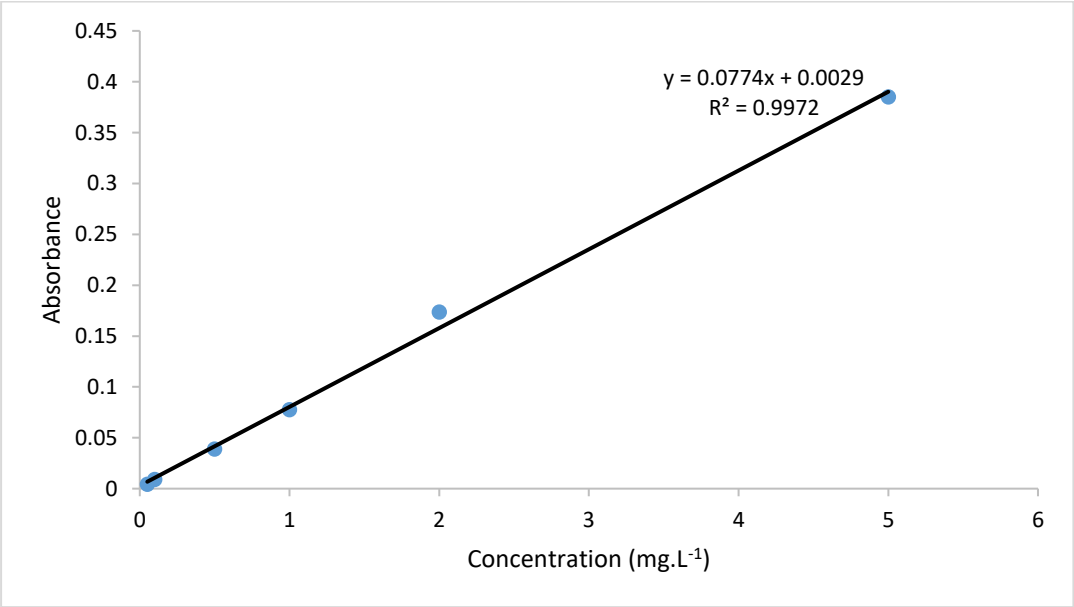

Figure 5.2 External calibration curve for gold on the AAS at a wavelength of 242.80 nm.

5.3.2 Cyanide leaching

The cyanide leaching was performed to partially leach out the gold to reduce it from a grade of 0.32 g.t^{-1} to at least 0.1 g.t^{-1} to cover tailing material in the lower ranges. The cyanide leaching was only performed at 24 h because it has been shown in the literature that it produces the highest recoveries (Altinkaya *et al.*, 2020). The only variable that was varied was the concentration of NaCN. The reaction of this procedure is shown in Equation 5.3.

$$4Au + 8NaCN + \frac{1}{2}O_2 + H_2O + OH^- \rightarrow 2Au(CN)_2^- + 4NaOH \qquad \textit{Equation 5.3}$$

As mentioned in Section 5.2.3, three concentrations of lixiviant were tested to ensure that at least 70% of the gold was extracted from the sample. As shown in Figure 5.3, the optimum concentration of NaCN that extracted most of the gold was 5 kg.t^{-1}, in which approximately 0.1 g.t^{-1} of the gold remained. This was the expectation as the recoveries of the gold during the leach are highly dependent on the time and concentration of the lixiviant before being affected by other factors such as dissolved oxygen, pH and mineralogy of the sample (Azizi and Ghaedrahmati, 2015; Fleming *et al.*, 2011). However, higher concentrations of lixiviant can deter recoveries, as it leads to the consumption of non-optimal cyanide if it is exceedingly in excess. Although the experiments were quite repeatable, as seen in the replicate for 1 kg.t^{-1}, the recovery of the gold was inconsistent. Another observation was that the repeatability of the fire assay method for head grade determination was flawed in earlier experiments.

According to Figure 5.3, the grade of the gold ranged from 0.23 to 0.33 g.t^{-1} in the feed sample, while the gold left in the residue after the process was quantified as 0.10-0.24 g.t^{-1}. Table 5.5 shows the percent of gold extracted and the mass balance. Most of the experiments at different concentrations of NaCN were able to extract high amounts of gold in the range of 36 to 104%. In this case, the optimum experiment would be the one in which the mass balances of the gold in the residue and the filtrate are closer to the head grade. However, only the experiment at 5 kg.t^{-1} CN was able to produce a satisfactory mass balance while having a high extraction rate of gold. In terms of 3 kg.t^{-1} CN, the mass balance is very satisfactory; however, it has a low extraction, and the grade in the residue is quite high compared to the head gold. Using cyanide leaching as a way to reduce the gold was beneficial as there are tailings emanating from the extraction of the major gold from ores using cyanide as a lixiviant.

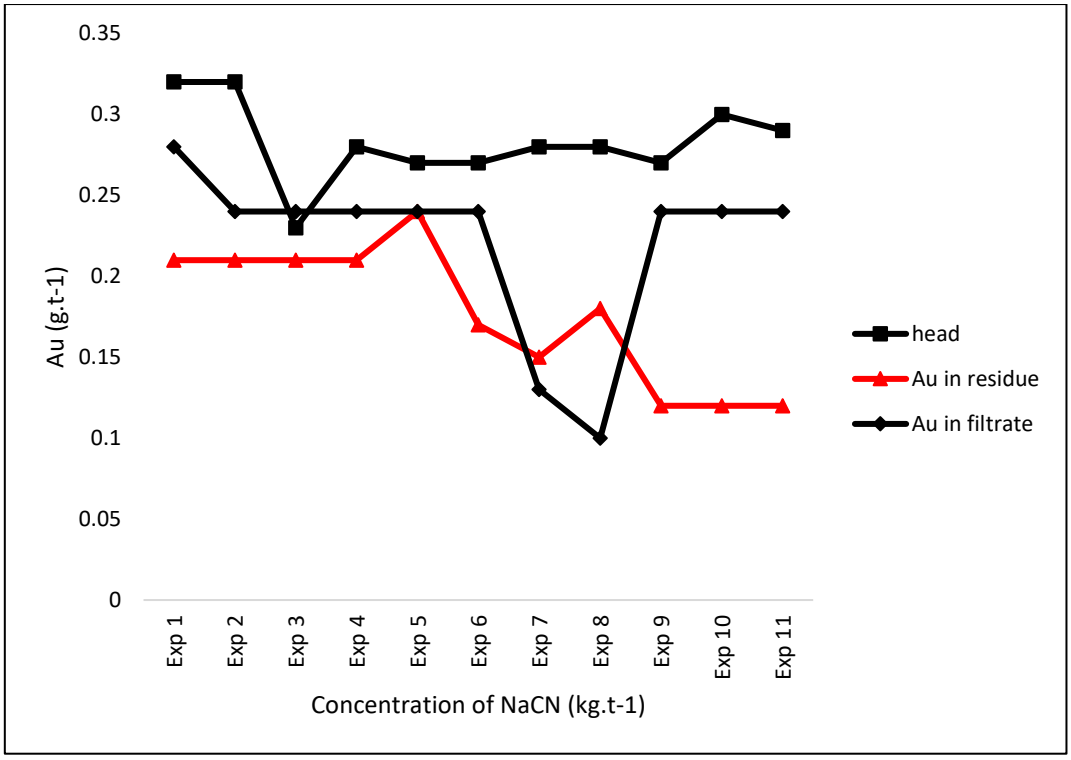

Figure 5.3 Recovery of gold in the residue and filtrate from cyanide leaching (n=3). Exp 1-4 (1 kg.t^{-1} CN), exp 5 (2 kg.t^{-1}), exp 6-8 (3 kg.t^{-1}) and exp 9-11 (kg.t^{-1}).

In this case, the fractions with remaining gold of 0.1 g.t^{-1} were used as the sample for the fire assay method development at a lower grade.

Table 5.5 Mass balance from the cyanide leaching process.

Experiment	Head (g.t^{-1})	Au in residue (g.t^{-1})	Au in filtrate (g.t^{-1})	%Au removed	Mass balance (g.t^{-1})
1	0.32	0.21	0.28	88	0.49
2	0.32	0.21	0.24	75	0.45
3	0.23	0.21	0.24	104	0.45
4	0.28	0.21	0.24	86	0.45
5	0.27	0.24	0.24	89	0.48
6	0.27	0.17	0.24	89	0.41
7	0.28	0.15	0.13	46	0.28
8	0.28	0.18	0.1	36	0.28
9	0.27	0.12	0.24	89	0.36
10	0.3	0.12	0.24	80	0.36
11	0.29	0.12	0.24	83	0.36

5.3.3 Effect of sample mass and flux

Since the ratio of gold to gangue material in mine tailings is reported to be 1:10 (Lottermoser, 2007), the mass must be at an optimum level. In fire assaying, the mass of the sample depends, among other factors, on the grade of the sample, which can be scanned using an XRF or visually analysed. With regard to the visual test, an ore darker in colour indicates medium to high grade, while that light in colour indicates a low-grade sample. In Figure 5.4, the tailings samples are shown, and it can be deduced from the colour they are low-grade. Based on these, the optimum mass is then chosen, with a guide on the mass selection shown in Table 5.6.

Figure 5.4 The tailings materials used for the study. Left (VCR matrix) and right (GSB matrix).

Table 5.6 Guide on sample mass depending on the grade.

Estimated grade ($g.t^{-1}$)	**Mass of sample (g)**
>1000	0.25-0.5
500-1000	0.5-1.5
200-500	1.5-3
100-200	3-6
50-100	6-10
30-50	10-12
25-30	12-15
15-25	15-25
10-15	25-30
5-10	30-40
<1-5	40-70

For a gravimetric finish, having the optimum mass of the sample is crucial because the produced prill must be large enough to be accurately weighed. Therefore, three masses of 50, 100 and 120 g were assessed against the different fluxes. The outcomes of these tests are displayed in Figure 5.5. In both of the matrices, it was observed that flux C (ratio of 8.3) had the lowest gold recoveries, with no recoveries for the VCR and approximately 0.04 $g.t^{-1}$ (40%) for GSB, while flux B (ratio of 10) yielded the highest recoveries among the three fluxes. In terms of the masses, 100 and 120 g seemed to give optimum recoveries; therefore, 100 g was selected for further chemical analysis. Another observation was that the GSB matrix recovered more than the VCR matrix, which is clearly seen in the recovery of gold for the lowest mass and flux C, in which no gold was recovered for the VCR. This is due to the differences in the mineralogy of the samples in which VCR has a higher pyrite and quartz content than GSB.

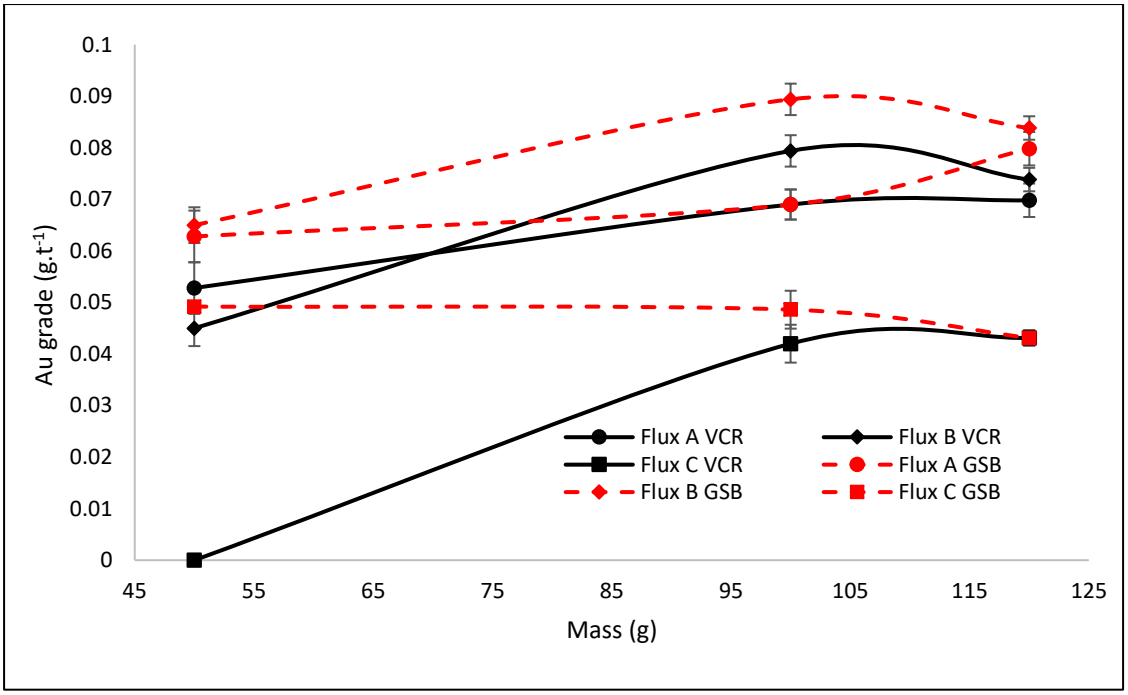

Figure 5.5 Effect of the mass on the recovery of gold from the tailings (n=3). Standard deviation is indicated by error bars.

5.3.4 Effect of co-collectors

As reported in the literature, the lead fire assay works well for most ores of various grades. The challenge would be in the case of tailings, especially when the quantification is by gravimetry. In this study, the collector was lead because of the various advantages it has over other metals, such as Sn, Bi, Cu and Fe. However, it was enhanced by the addition of co-collectors. The idea was that if the lead runs out or there was an inefficient reduction of the lead oxide into lead, the other metals would collect the remaining gold as there is a miscibility gap between them.

In this study, the co-collectors were applied to both the VCR and GSB matrix for the 0.1 $g.t^{-1}$ tailing sample. The concentrations of the co-collectors in the solutions were varied at 5, 10 and 20 $mg.L^{-1}$ using a sample mass of 100 g and flux B, as determined in Section 5.3.3. In Table 5.7 and Figures 5.6 and 5.7, the results from these experiments are shown. In both matrices, 10 $mg.L^{-1}$ solutions seemed to lead to higher recoveries than the other concentrations, with Sn yielding slightly higher recoveries.

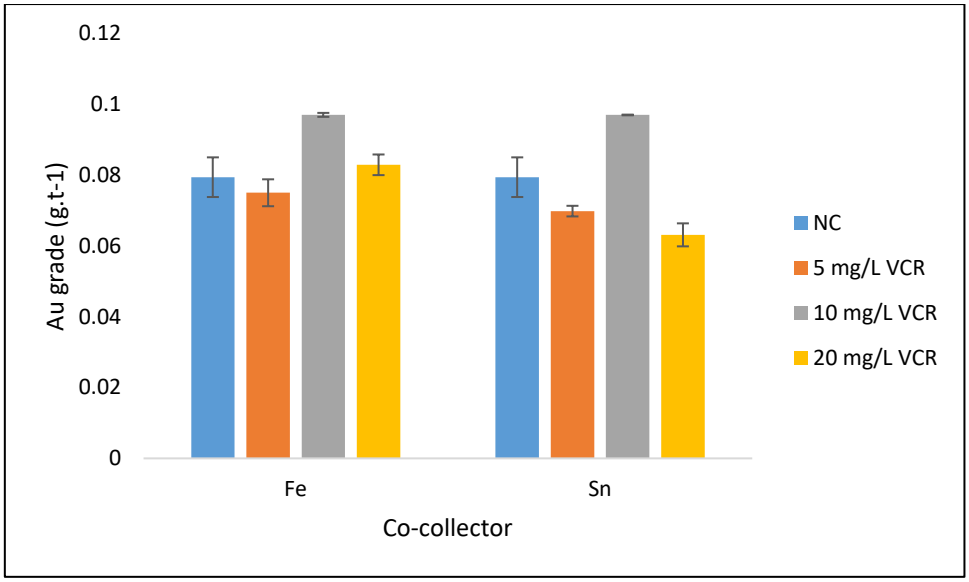

Figure 5.6 Recovery of gold in the VCR matrix after the addition of Sn and Fe during fusion (n=3). Standard deviation is indicated by the error bars.

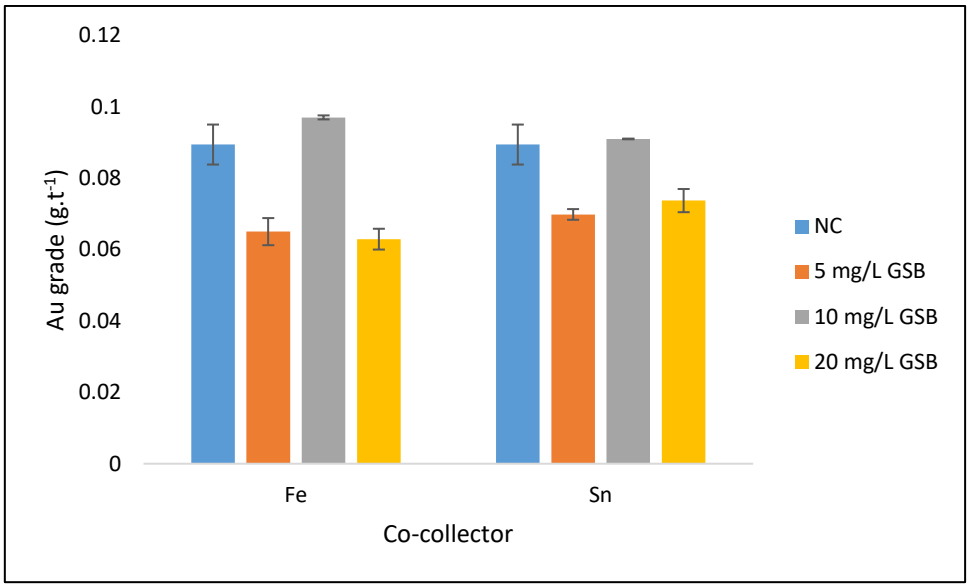

Figure 5.7 Recovery of gold in the GSB matrix after the addition of Sn and Fe during fusion (n=3). Standard deviation is indicated by the error bars.

Table 5.7 Recovery of Au from the tailings sample and the CRM, AMIS 610.

Matrix	Metal	CRM grade ($g.t^{-1}$)	Experimental grade ($g.t^{-1}$), CRM	Recovery (%)	Experimental grade ($g.t^{-1}$), Sample	Recovery (%)
GSB	Fe	0.068 ± 0.014			0.0870 ± 0.00067	87
	Sn				0.0908 ± 0.00045	91
	NC				0.0694 ± 0.00057	89
VCR	Fe		0.0715 ± 0.00032	104	0.0821 ± 0.00056	82
	Sn		0.07243 ± 0.00032	107	0.0967 ± 0.0001	97
	NC		0.05201 ± 0.00045	76	0.0794 ± 0.0056	79

NC: No co-collector added.

For gravimetric analysis, it is of utmost importance that the analyte of interest is solely alone at the end of the process to ensure that it is the only analyte being weighed. The alternative metals for gold collection can be a replacement for lead, but with the selectivity issues experienced, the difficulties in the removal of the collector after fusion and their low density (Ni et al., 2020), it can pose a big challenge in commercial laboratories. Between Fe and Sn, Sn seemed to enhance the collection more than Fe through all concentrations and the two matrices. This could be because Sn has a lower melting point (231.9 °C) than Fe (1538 °C), implying that it mixes with the lead and the sample in the liquid phase before the molten Fe. In the use of Fe and Cu as co-collectors by Masasire *et al.* (2022), it was reported that the recoveries were higher with Fe than with Cu, which could have been due to the presence of significant amounts of chromites, which affects Cu collecting of gold. In other studies, such as Ni. *et al*. (2021), Sb, Sb-Cu and Bi were reported to collect efficiently when used as the main collectors. Apart from the various fire assay methods for gold quantification, other methods have been developed and modified. Such methods include acid digestion (Chattopadhyay & Sahoo, 1992) and acid digestion with solvent extraction (Wang *et al.,* 2016), in which gold is quantified with the highest accuracy in medium-grade tailings but is not quantified in low-grade tailings. The method used in this study offers the benefits of the common fire assay but with increased recoveries and fewer matrix effects. The ability to quantify gold tailings at such low levels accurately is important to the mining industry, and it will benefit greatly.

5.3.5 Recovery of lead

Based on the mass of the flux weighed, which was 350 g and contained 21.50% PbO and the reduction of PbO to Pb in a 1:1 ratio, the amount of lead expected to be recovered after fusion was approximately 90.3 g, which converted to 23.91% (Equations 5.4 and 5.5). The recovery of lead is expected to have some discrepancies, as a small amount is oxidized into PbO.

$$PbO_{(S)} + C_{(S)} \rightarrow Pb_{(l)} + CO_{(g)} \qquad \textit{Equation 5.4}$$

$$Theoretical\ Pb\ recovery = \frac{g\ of\ Pb\ in\ flux}{g\ of\ flux} = \frac{83.7}{350} = 23.91\% \qquad \textit{Equation 5.5}$$

In Figure 5.8, the behavior of the lead recovery is plotted against the gold grade recovered and the theoretical lead. The main observation made was that the lead recovery for all the tests varied between 10.9% and 70%, meaning that some of the samples were recovering, while others were over recovering. For the samples where there was under- or over recovery, the gold recovered was compromised. For example, AMIS 610 B has a lead recovery of 21.49%, which

is a 90% recovery, and the gold recovery was 0.066 $g.t^{-1}$ (accurate value=0.068 $g.t^{-1}$), whereas in the case of AMIS 610 C, the lead recovery was 69.85%, which is 291% recovery, with the gold under recovered at 0.0237 $g.t^{-1}$. In terms of the control samples, which were the blanks, the lead had exceptional recoveries of 99%. This implies that there are reactions during sample fusion that affect these recoveries, such as the mineralogy. On the other hand, the third sample had a lead recovery of 68%, which did not affect the gold recovery, as was obtained at 0.28 $g.t^{-1}$, with the head grade being 0.32 $g.t^{-1}$. Due to the results being inconclusive, a second set of experiments was carried out on the samples with a head grade of 0.1 $g.t^{-1}$.

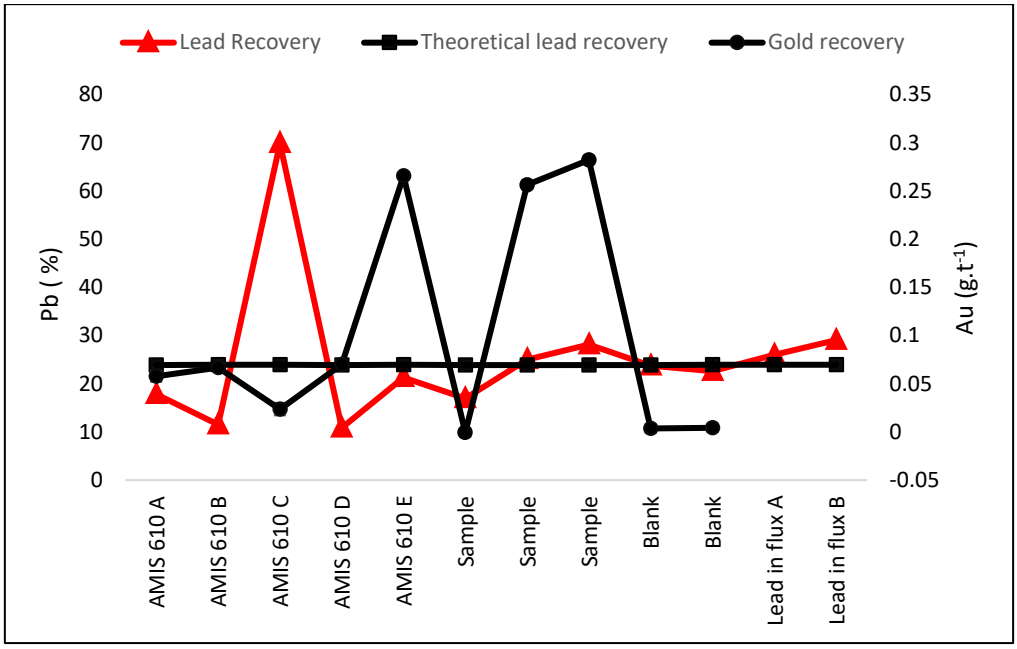

Figure 5.8 Comparison of lead recovery against gold recovery in CRMs and random samples after fusion (n=3).

A total of 12 samples were assessed for lead and gold recovery in this experiment. As shown in Figure 5.9, there was a positive relationship between the recovery of lead and gold. The gold recoveries ranged from 0.08 to 0.1 $g.t^{-1}$, and the lead recoveries ranged between 10.9 and 29.03%. This performance was quite satisfactory, and it showed that for the gold recoveries to be optimum, the lead must be recovered efficiently.

The main aim of this experiment was to assess whether the recovery of the lead after fusion can be an indication of whether the gold would be recovered or extracted efficiently. Having an idea of this behaviour would indicate the part of the fire assay process that has errors and halt the process before proceeding any further. The conclusion was that it is important to have optimum recovery of the lead. Furthermore, tailings are difficult to work with; therefore,

achieving optimum recovery when the sample is of a tailings nature indicates the ruggedness of the method and that the tailings can be quantified by fire assay.

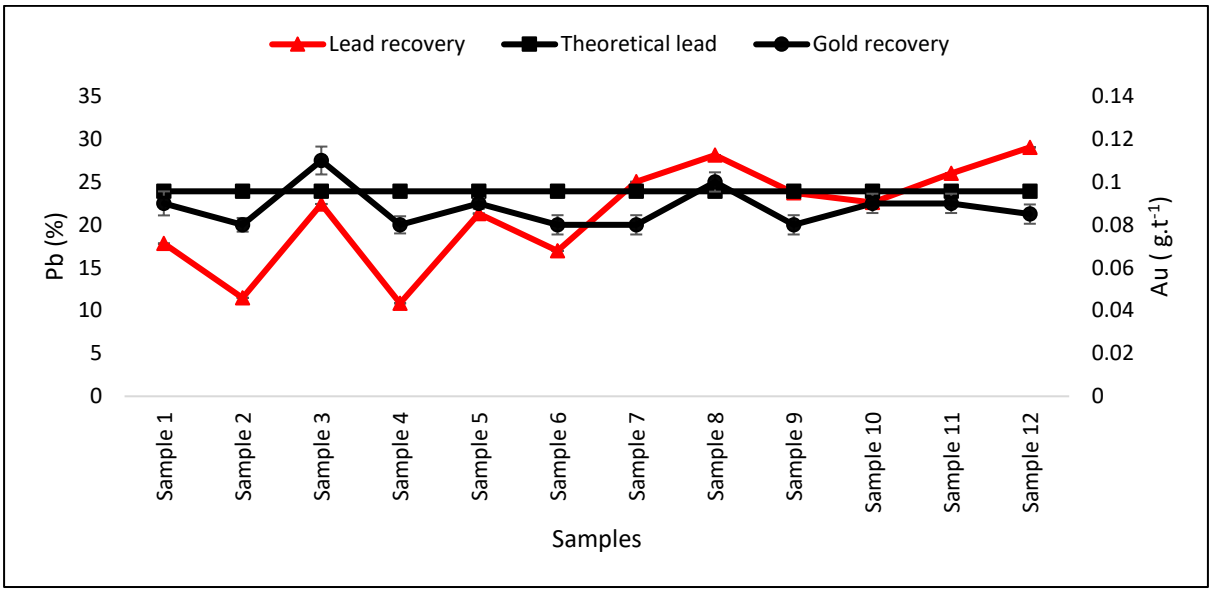

Figure 5.9 Comparison of lead recovery against gold in the tailings sample (n=3). Error bars indicate the standard deviation.

5.4 Statistical evaluations.

5.4.1 ANOVA

The ANOVA test was computed with Excel (Microsoft Office Professional Plus 2016) to determine if, based on the recoveries, it was necessary to vary the masses and the flux. This assumption will be satisfied by the rejection ($F_{stat}>F_{crit}$) of the null hypothesis.

$$H_0: \mu_1 = \mu_2 = \mu_3$$

$$H_1: \mu_1 \neq \mu_2 \neq \mu_3$$

where μ_1= Flux A, μ_2= Flux B and μ_3= Flux C for a 120 g sample mass, as shown in Tables 5.8 and 5.9. For a majority of the ANOVA tests, the alternative hypothesis is accepted, meaning the means of the three tests are different. Statistically, this means that the variation in the fluxes produces Au recoveries that are significantly different from each other, which is good. These statistical tests further support the conclusion that it was beneficial to change the flux in terms of the reducing agent and litharge ratio.

Table 5.8 ANOVA at 95% confidence interval, as obtained from Microsoft Excel.

Anova: Single Factor

SUMMARY

Groups	*Count*	*Sum*	*Average*	*Variance*
Flux A	4	0.27	0.069	2.87E-06
Flux B	4	0.29	0.074	6.34E-06
Flux C	4	0.17	0.043	2.93E-06

ANOVA

Source of Variation	*SS*	*df*	*MS*	*F*	*P value*	*F crit*
Between Groups	0.0021	2	0.0011	263.91	1.02E-08	4.26
Within Groups	3.64E-05	9	4.05E-06			
Total	0.0022	11				

df: Degrees of freedom, SS: Sum of squares, MS: Mean Square

Table 5.9 ANOVA with the decision rule.

Test	**SS**		**Fstat**	**Fcrit**	**Pvalue**	**Hypothesis**
	Between	**Within**				
50 g vs fluxes	0.00014	0.00014	6.92	5.59	0.034	H_1
100 g vs fluxes	0.00373	0.00013	178.59	3.89	1.17E-09	H_1
120 g vs fluxes	0.00279	0.00007	233.38	3.89	2.48E-10	H_1
Flux A vs masses	0.00092	0.00018	31.24	3.89	1.75E-05	H_1
Flux B vs masses	0.00405	0.00008	271.25	3.98	4.37E-10	H_1
Flux C vs masses	0.00000	0.00006	0.40	5.32	5.46E-01	H_0

5.4.2 Measurement Uncertainty

The operating model equation in the quantification of gold by gravimetric analysis is expressed as in Equation 5.1, meaning that the major sources of uncertainty are mainly from weighing the prill and weighing the samples. In this case, the uncertainty can be expressed as the standard deviation of repeated measurements of the prill and sample (Type A), or it can be obtained from the calibration certificate (Type B).

$$Au\ \left(\frac{g}{t}\right) = \frac{weighed\ prill\ (mg)}{Sample\ mass\ (g)} \times 1000 \qquad \text{Equation 5.1}$$

For the balance weighing the prill, the expanded uncertainty is reported as 0.0021 mg at a coverage factor of k=2, while the uncertainty weighing the mass of the sample is reported as 0.3 g at a coverage factor of k=2. These expanded uncertainties from the calibration certificates are a combination of eccentric error, accuracy, linearity and repeatability.

The standard and relative uncertainties were calculated using Equations 5.6 and 5.7:

$$u_{standard} = \frac{expanded\ uncertainty}{coverage\ factor} \qquad \textit{Equation 5.6}$$

$$u_{relative} = \frac{measured\ uncertainty}{measured\ quanity} \qquad \textit{Equation 5.7}$$

$$u_{s1} = \frac{0.0021}{2} = 0.00105 \qquad and\ u_{s2} = \frac{0.3}{2} = 0.15$$

Relative uncertainties: $u_s relative = \frac{0.15}{350} = 0.0042$

As stated in the GUM, the combination of uncertainties emanating from a model equation is calculated from Equation 5.8.

$$u_c(y) = \sqrt{(u_{s1})^2 + (u_{s2})^2} \qquad \textit{Equation 5.8}$$

Combination of standard uncertainties:

$$u_c(y) = \sqrt{(0.00105)^2 + (0.0042)^2}$$

$$u_c(y) = 0.00432\ g.t^{-1}$$

Therefore, the measurand with the expanded uncertainty (k=2), for gold quantified with Sn co-collector, is reported: 0.0908 ± 0.00432 g.t^{-1} for GSB and 0.0967 ± 0.00432 g.t^{-1} for VCR.

5.5 Conclusion

This study aimed to find or improve the method for quantifying gold in low-grade mine tailings. The gravimetric method is preferred in the mining industry over instrumental analysis because it reduces the errors that can be introduced into the analysis that would affect the measurand. This method was optimized for sample mass, the ratio of litharge to reducing agent and the addition of base metals before fusion as co-collectors. As assumed, a mass greater than 50 g was able to give better recoveries since the ratio of gold to gangue material is usually 1:10, while a flux ratio of 10 was the optimum. The method showed that to enhance or to obtain

better recoveries with a sample mass of 100 g and ratio of 10, 10 mg. L^{-1} Sn can be added, in which the recoveries improved from 70% to 97%. This is because Sn has typical physico-chemical properties, such as a density that is higher than that of the slag that is needed of a gold collector, which, together with lead, achieves a synergistic effect. The use of these metals as co-collectors needed that they be removed as oxides after collection so that they do not interfere in weighing, and this was achieved, as the CRMs that were used gave recoveries that were not indicative of their presence. This implies that gold can be recovered in higher amounts in low-grade samples. Furthermore, since these methods were optimized based on a residue from cyanide leaching, they can also be applied to tailings that are a result of cyanide leaching of the ore. The fewer factors affecting the measurand are further supported by the measurement uncertainties obtained, which were 0.0908 ± 0.00432 $g.t^{-1}$ for GSB and 0.0967 ± 0.00432 $g.t^{-1}$ for VCR, which are much lower than those offered by the instrumental analysis (uncertainty of ± 0.1 $g.t^{-1}$) (Chapter 4).

5.6 References

Altinkaya, P., Wang, Z., Korolev, I., Hamuyuni, J and Haapalainen, M. (2020). Leaching and recovery of gold from ore in cyanide-free glycine media. *Minerals Engineering*, *158*(August), 106610. https://doi.org/10.1016/j.mineng.2020.106610

Azizi, A and Ghaedrahmati, R. (2015). Optimizing and evaluating the operational factors affecting the cyanide leaching circuit of the Aghdareh gold processing plant using a CCD model. *Proceedings of the Royal Society A: Mathematical, Physical and Engineering Sciences*, *471*(2184). https://doi.org/10.1098/rspa.2015.0681

Baghalha, M. (2007). Leaching of an oxide gold ore with chloride/hypochlorite solutions. *International Journal of Mineral Processing*, *82*, 178–186. https://doi.org/10.1016/j.minpro.2006.09.001

Blyth, K. M., Phillips, D. N., & van Bronswijk, W. (2004). Analysis of gold ores by fire assay. *Journal of Chemical Education*, *81*(12), 1780–1782. https://doi.org/10.1021/ed081p1780

Bureau, S. C and Géologiques, D. R. (2008). A Remote-Sensing and GIS-Based Integrated Approach for Risk- Based Prioritization of Gold Tailings Facilities — Witwatersrand , South Africa. *Mine Closure*.

Caporali, S., Bellandi, S., Innocenti, M., Lopilato, O., Romualdi, L and Pezzatini, G. (2010). Determination of gold in alloys via potentiometric titration; An alternative to the fire assay. *Gold Bulletin*, *43*(2), 122–130. https://doi.org/10.1007/BF03214977

Chattopadhyay, P and Sahoo, B. N. (1992). Modified decomposition procedure for the determination of gold in geological samples by atomic absorption spectrometry. *The Analyst*, *117*(9), 1481–1484. https://doi.org/10.1039/an9921701481

DRDGOLD. (2016). *Sustainability*. https://www.drdgold.com/sustainability/tailings-management. Accessed: 16 September 2022

Fleming, C. A., Mezei, A., Bourricaudy, E., Canizares, M and Ashbury, M. (2011). Factors influencing the rate of gold cyanide leaching and adsorption on activated carbon, and their impact on the design of CIL and CIP circuits. *Minerals Engineering*, *24*(6), 484–494. https://doi.org/10.1016/j.mineng.2011.03.021

Ghosh, P., Mandal, H., Sirisha, B., Sen, U., Goswami, S and Kiran, N. V. R. (2019). A modified acid digestion method for analysis of gold in geological gamples: A comparative study. *Mapan - Journal of Metrology Society of India*, *34*(4), 551–558. https://doi.org/10.1007/s12647-019-00326-8

Haiss, W., Thanh, N. T. K., Aveyard, J and Fernig, D. G. (2007). Determination of size and concentration of gold nanoparticles from UV - Vis Spectra. *Analytical and Chemistry*, *79*(11), 4215–4221.

Kossoff, D., Dubbin, W. E., Alfredsson, M., Edwards, S. J., Macklin, M. G and Hudson-Edwards, K. A. (2014). Mine tailings dams: Characteristics, failure, environmental impacts, and remediation. *Applied Geochemistry*, *51*(January 2018), 229–245. https://doi.org/10.1016/j.apgeochem.2014.09.010

Lottermoser, B. (2007). *Mine waste: Characterization, treatment, environmental impact* (2nd ed.). Springer International Publishing: New York.

Masasire, A., Rwere, F., Dzomba, P and Mupa, M. (2022). A new preconcentration technique for the determination of PGMs and gold by fire assay and ICP–OES. *Journal of the Southern African Institute of Mining and Metallurgy*, *122*(1), 29–36. https://doi.org/10.17159/2411-9717/1638/2022

Ni, W., Mao, X., Yao, M., Guo, X and Sun, Q. (2022). Bismuth fire assay preconcentration and empirical coefficient LA - ICP - MS for the determination of ultra - trace Pt and Pd in geochemical samples. *Scientific Reports*, *12*(11555), 1–9. https://doi.org/10.1038/s41598-022-15881-5

Ni, W., Mao, X., Yao, M., Sun, Q., Guo, X., Zhang, H and Liu, L. (2021). Bismuth-remaining cupellation fire fssay preconcentration combined with inductively coupled plasma–mass spectrometry for the simultaneous determination of ultratrace Au , Pt , Pd , Ru , Rh , and Ir in geologic samples. *Internation Journal of Analytical Chemistry*, *2021*, 1–8.

Ni, W., Mao, X., Zhang, H., Liu, L., Guo, X and Sun, Q. (2021). Simultaneous determination of ultratrace Pt, Pd, Rh and Ir in geochemical samples by inductively coupled plasma–mass spectrometry following tin fire sssay preconcentration and microwave digestion. *Current Analytical Chemistry*, *17*(552–563), 552–563. https://doi.org/10.2174/1573411016999200715160650

Ni, W., Zhang, H., Mao, X., Liu, L., Guo, X and Xiao, F. (2020). Simultaneous determination of ultratrace Au , Pt , Pd , Ru , Rh , Os and Ir in geochemical samples by KED-ICP–MS combined with Sb-Cu fire assay and microwave digestion. *Microchemical Journal*, *158*(March), 105197. https://doi.org/10.1016/j.microc.2020.105197

Olobatoke, R. Y and Mathuthu, M. (2016). Heavy metal concentration in soil in the tailing dam vicinity of an old gold mine in Johannesburg , South Africa 1. *Canadian Journal of Soil Science*, *304*(March), 299–304. https://doi.org/10.1139/cjss-2015-0081

Pan African Resources. (2020). *Barberton Tailings Retreatment Plant*. https://www.panafricanresources.com/btrp/. Accessed: 16 September 2021

Rao, C. R. M and Reddi, G. S. (2000). Platinum group metals (PGM); occurrence, use and recent trends in their determination. *TrAC- Trends in Analytical Chemistry*, *19*(9), 565–586. https://doi.org/10.1016/S0165-9936(00)00031-5

Wang, Y., Baker, L. A and Brindle, I. D. (2016). Determination of gold and silver in geological samples by focused infrared digestion: A re-investigation of aqua regia digestion. *Talanta*, *148*, 419–426. https://doi.org/10.1016/j.talanta.2015.11.019

Ye, J., Liu, S., Tian, M., Li, W., Hu, B., Zhou, W and Jia, Q. (2014). Preparation and characterization of magnetic nanoparticles for the on-line determination of gold, palladium, and platinum in mine samples based on flow injection micro-column preconcentration coupled with graphite furnace atomic absorption spectrometry. *Talanta*, *118*, 231–237. https://doi.org/10.1016/j.talanta.2013.10.018

Yin, X., Yi, H., Wang, Q., Wang, Y., Sun, X., Lv, C., Guo, J and Yang, Y. (2017). Extraction and separation of multiple platinum group metals from hydrochloric acid solution with sole 1-hexyl-3-methylimidazole-2-thione using microextraction method. *Hydrometallurgy*, *174*(September), 167–174. https://doi.org/10.1016/j.hydromet.2017.10.009

6 LOW-GRADE GOLD EXTRACTION IN TAILINGS USING A CHLORINATION APPROACH

Kedibone Nicholine Mashale[1,2], Napo Godwill Ntsasa[1], Majimi James Sehata[1], James Tshilongo[1,2] and Luke Chimuka[2]

[1]*Analytical Chemistry Division, Mintek, 200 Malibongwe Drive, Praegville, 2194, South Africa.*

[2]*Molecular Sciences Institute, School of Chemistry, University of the Witwatersrand, Braamfontein, 2000, South Africa.*

[*]*Corresponding author: kedibonema@mintek.co.za; Tel: 011 709 4050.*

ABSTRACT

A method for the extraction of low-grade gold from mine tailings using chlorination was developed. The method was based on the oxidation of the gold particles using commercial sodium hypochlorite (NaOCl) to chlorinate the gold and extract it into solution. The parameters that were studied were the leaching time (2, 4 and 6 hrs), the concentration of the oxidant (1, 1.5 and 2 M) and pH (4 and 12) for the Ventersdorp contact reef (VCR) and Greenstone belt (GSB) matrix. The extraction was carried out in an ultrasonic bath at 200 kW to facilitate mass transfer between the two phases. Scanning electron microscopy (SEM), X-ray diffraction, and Brunauer, Emmett, and Teller (BET) analysis were employed to characterize the mineral samples and reaction residues. The results indicated that there was a slight increase in the quartz content (from 78 to 85% for VCR and 65 to 80% GSB), which was due to the breakdown of minerals such as chlorite, which was higher in the residues than in the head sample. Furthermore, the process enhanced the crystallinity of the sample, which was seen by the appearance of two mineral phases that were not detected in the head sample, kaolinite and nitratine. This was an early indication of an oxidation process that has occurred. In terms of the recovery of gold, the optimum leaching conditions were found to be 1 M NaOCl, pH 4 and 2 h leaching time. Under these conditions, the extraction ranged between 60 and 90%, with AMIS 646 (CRM) recovering the most gold. Furthermore, the analysis of the surface area of the residues against the sample showed that there was an increase from 3.3 and 2.3 $m^2.g^{-1}$ to 5.3 $m^2.g^{-1}$.

Keywords: Chlorination, low-grade tailings, gold, sodium hypochlorite.

6.1 Introduction

There are various ways to extract or quantify gold from different ores of different grades. In most of the methods, the mineralogy of the sample plays an enormous role. Such methods include fire assays, which are good for separating gold from gangue material, thereby decreasing spectral interference during instrumental analysis and having the capability of having a gravimetric finish. Leaching with various lixiviants, such as cyanide (CN^-) and thiosulfate ($S_2O_2^{3-}$), is also an alternative (Zhang *et al.*, 2022); however, cyanide is dangerous and requires high leaching. The third method would be acid digestion, which has the advantage of fast times depending on the acids used (Liu *et al.*, 2019). Other methods incorporate methods such as gravity separation to concentrate gold before any chemical analysis using chemicals such as tellurium and selenium (Forrest *et al.*, 2001).

Among all these methods, chlorination is based on the chlorination of metal oxides into metal chlorides (Equations 6.1 and 6.2) (Baghalha, 2007), which are more stable than oxides. Two types of chlorination are currently being used: dry chlorination, which uses chlorine gas as the source of chloride ions, and wet chlorination, which supplies chloride ions from solvents such as sodium hypochlorite (NaOCl), hydrochloric acid (HCl) and calcium hypochlorite ($Ca(OCl)_2$). The advantage of chlorination is that it allows for the use of large sample masses of up to 250 g, already mitigating the effects of homogeneity on the chemical analysis (Ojeda *et al.*, 2009). Wet chlorination is similar to cyanide leaching but has more advantages. With wet chlorination, the extraction rate is quite high, with values of 13 $mg.cm^{-2}$ h being reported, while that of cyanide is reported as 2.5 $mg.cm^{-2}$ h. This is also evident in the duration of the leaching between the two; 2 h versus 24 h. However, it does also have its shortcomings, which include that it is tricky for low-grade gold and in some cases, some of the base metals can leach into solution, thereby affecting analysis.

$$2Au + 3Cl_2 + 2Cl^- \rightarrow 2[AuCl_4]^- \qquad \textit{Equation 6.1}$$

$$2Au + 3HClO + 5Cl^- + 3H^+ \rightarrow 2[AuCl_4]^- + H_2O \qquad \textit{Equation 6.2}$$

NaOCl is gaining momentum as a lixiviant to use during wet chlorination due to its strong oxidation capabilities, in which case the hypochlorous ion is the active component (Baghalha, 2007). The other advantage is that it is the major component of bleach, meaning that commercial bleach can be used to carry out wet chlorination. As with other methods, the extraction rate of gold using hypochlorous ions is affected by the pH of the solution, the concentration of the oxidizing agent and the duration of leaching. In Baghalha (2007), they used $Ca(OCl)_2$ vs NaOCl for a gold sample of 1-2 $g.t^{-1,}$ and the most recovered was 58%, after

48 h for $Ca(OCl)_2$, while with NaOCl, the leaching time was 24 h under acidic conditions. It was then reported that the best recoveries are obtained when the hypochlorous ions are greater than 10 g. L^{-1} and under acidic conditions, which is when the ions are mostly dominant. However, in Fu *et al.* (2017), where NaOCl was used, good recoveries of at least 60% were obtained under alkaline conditions. Other studies have used dry chlorination as an alternative, in which good recoveries were obtained (Ojeda *et al.,* 2009). However, it does pose a safety challenge because it uses chlorine gas and requires complicated equipment.

The greatest challenge with quantifying gold from mine tailings is the sample size and the grade, which limits the maximum recovery of the gold. However, due to the nature of the tailings, in that they have already been processed, the mineralogy of the sample is not necessarily the same as the original ore. This means that some chemical analyses might be easier than others, especially those that are greatly affected by the mineralogy of the samples. For example, in wet chlorination, large amounts of pyrite can affect the capability of the oxidant to react with the gold; instead, the oxidant will react with the pyrite and form boundary layers, inhibiting the gold from diffusing from the solid into the solution. Therefore, the expectation is that the chlorination process should work to a certain extent. Therefore, this study aimed to recover low-grade gold (0.32 $g.t^{-1}$) from mine tailings by chlorination with commercial hypochlorite at various pH values and oxidant concentrations.

6.2 Materials and methods

6.2.1 Materials

The chemicals and reagents utilized in this study were of analytical quality and were used as received. While hydrochloric acid (HCl, 37%) was acquired from Sigma Aldrich (Missouri, United States of America), sodium chloride (NaCl, platinum line) was purchased from Associated Chemical Enterprises Pty Ltd. (Johannesburg, South Africa). Glassworld (Robertville, South Africa) provided the filter papers (Grade 1-185 mm) and commercial sodium hypochlorite (15% m/v, NaClO). The Milli-Q system from Sigma Aldrich (Missouri, United States of America) was used to make all solutions. Two 25 kg samples of mine tailings were collected from the Green Stone Belt (GSB) in Barberton and the Ventersdorp Contact Reef (VCR) using the grab sampling technique. The CRMs (AMIS 610 and AMIS 646) were selected based on the matrix and gold grade. For complete characterization data, elemental composition and fire assay method for head grade determination, refer to Chapter 4.

6.2.2 Characterization

The material was analysed by a backloading preparation process after being pulverized in a swing mill to -50 µm. The diffractogram was produced using a Malvern Panalytical Aeris diffractometer (Malvern Pan Analytical Ltd, Worcestershire, United Kingdom) equipped with a PIXcel detector, fixed slits, and Fe-filtered Co-K radiation. The diffractometer has a scanning range of 5-80° 2 and a step scan of 0.022° 2 with a measurement time of 48 s. PAN-ICSD and the X'Pert Highscore plus software were used to identify the phases. Using the Rietveld method, the relative phase quantities (wt%) were calculated, with the method detection limit being specified as 0.5-3 wt%.

BET analysis was performed using the Tristar II 3020 analyser using nitrogen as the adsorbate. The samples were degassed at 60 °C overnight before running the adsorption-desorption experiments. The isotherms were then constructed from the relative pressure and quantity adsorbed.

6.2.3 Chlorination

For the chlorination process, various parameters were varied, as shown in Tables 6.1 and 6.2. A 100 g sample was weighed and added to a 1000 mL beaker. The appropriate amount of NaOCl was added to obtain concentrations of 1, 1.5 and 2 M in a total volume of 600 mL. The experiments were carried out in both alkaline (pH of 12) and acidic (pH of 4) environments. NaOCl (15%) has a pH of 12, so for the alkaline environment, the pH was not adjusted. For the acidic environment, the pH was adjusted using 36% HCl. A certain amount of NaOH was also added to the slurry to maintain alkalinity. For the acidic experiments, 10 g of NaCl was added to the slurry to increase the amount of available chloride ions. The mixtures were then put in an ultrasonicator set at 200 kW in a set up that included an overheard stirrer to continuously mix the mixture to avoid the settling of the particulate matter. The experiments were carried out for 2 h and then filtered under vacuum to obtain the residue and the filtrate, which were analysed by fire assay and AAS as in Chapter 5, respectively. The residues were also analysed by SEM–EDS (Tescan, Brno, Czech Republic) and XRD to assess if there were differences between the before and after.

Table 6.1 Experimental parameters for the chlorination processes.

Experiment	S:L	pH	HCl (mL)	[NaOH] M	NaCl (g)	[NaOCl] M	Time (hrs)
1	0.2	12	-	1.5	-	2	2
2	0.2	12	-	1.5	-	1.5	2
3	0.2	12	-	1.5	-	1	2
4	0.2	4	100	-	10	2	2
5	0.2	4	100	-	10	1.5	2
6	0.2	4	100	-	10	1	2

Table 6.2 Concentrations of the main ions in chlorination.

Experiment	Solid: liquid Ratio	Oxidant	$[Cl^-]$ $(g.L^{-1})$	$[OCl^-]$ $(g.L^{-1})$	[HCl] $(g.L^{-1})$
1	0.2	NaOCl	40	103	60
2	0.2	NaOCl	40	77	60
3	0.2	NaOCl	40	51.5	60
4	0.2	NaOCl	40	103	60
5	0.2	NaOCl	40	77	60
6	0.2	NaOCl	40	51.5	60

6.2.4 Time-integrated chlorination

To determine the rate at which the gold becomes chlorinated and moves into the solution phase, 3 time intervals were investigated. The method was followed as above, but the amount of sample and reagents were scaled up to a final volume of 1800 mL. A 600 mL aliquot of the slurry was removed from the bulk reactor every 2 h at 2, 4 and 6 h.

6.3 Results and discussion

6.3.1 Sample composition.

The two matrices used, VCR and GSB, are characterized by a high quartz amount (67-79), a minimal amount of iron (1.78-3.4%) and a minimal amount of sulfur (1-1.5%). The surface areas of the feed samples as determined by BET analysis were 2.7 and 3.3 $m^2.g^{-1}$ for GSB and VCR, respectively. This is characteristic of a microporous mineral ore. The grade of the tailings was determined by fire assay, which was approximately 0.32 $g.t^{-1}$. This information is shown in Table 6.3.

Table 6.3 Chemical compositions and content of minerals.

Matrix	SiO_2	Fe	Al	Mg	Mn	As	S	Au	pH	Surface area	SG
GSB	67.5	1.78	2.02	0.60	-	1.5	1-1.5	0.32	7-9	2.7	2.65
VCR	78.9	3.4	3.4	0.97	0.042	0.0880	1-1.5	0.32	7-9	3.3	2.74

Base metals and quartz reported in %, Au in $g.t^{-1}$ and surface area in $m^2.g^{-1}$.

6.3.2 Change in the mineralogy

In terms of the mineralogy obtained by XRD (Figures 6.1 and 6.2), there were minimal differences between the head sample and the residues from the chlorination process. The distinctive difference was the appearance of two minerals, kaolinite ($Al_2Si_2O_5(OH)^{4-}$) and nitratine ($NaNO_3$), which had averages of 3.24 and 2.5 wt%, respectively. Kaolinite is a secondary mineral usually formed from oxidized samples where it is altered from aluminum silicates. Nitratine is usually associated with other minerals, such as gypsum, calcite and halite, and its presence would explain why the gypsum that was in the head sample was not detected in the chlorinated residues. In both sample materials, the amount of chlorite decreased from 7.6 to 0.5-2.6% in the various experiments, which can be explained by the fact that under oxidative conditions, chlorite can be destroyed, leading to the formation of muscovite or quartz. This explains the increase in the quartz amount in the chlorinated residues. This was an early indication of the oxidation process that occurred and that it altered the crystalline structure of the sample material (Sjöström e*t al.,* 2019).

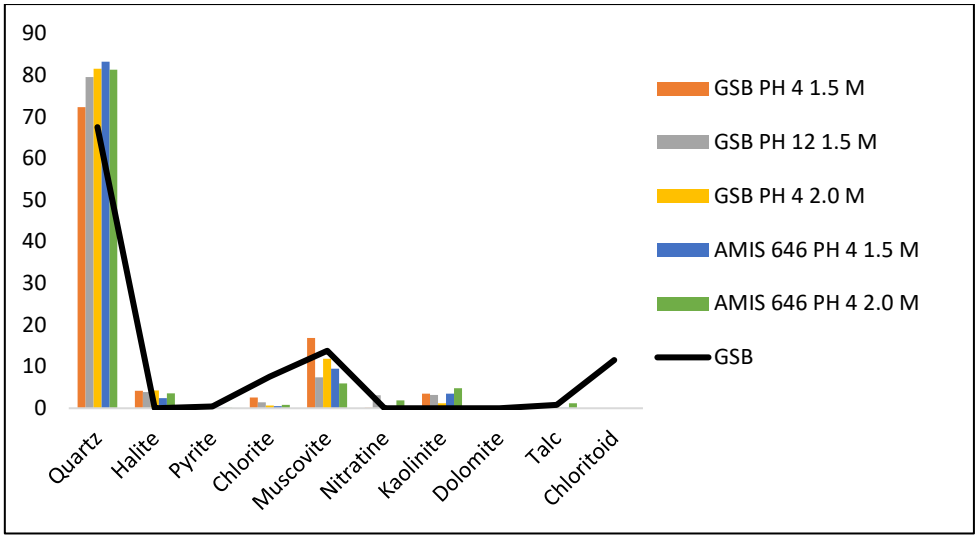

Figure 6.1 Comparison of the mineralogical composition of the head sample and the chlorinated residues for GSB.

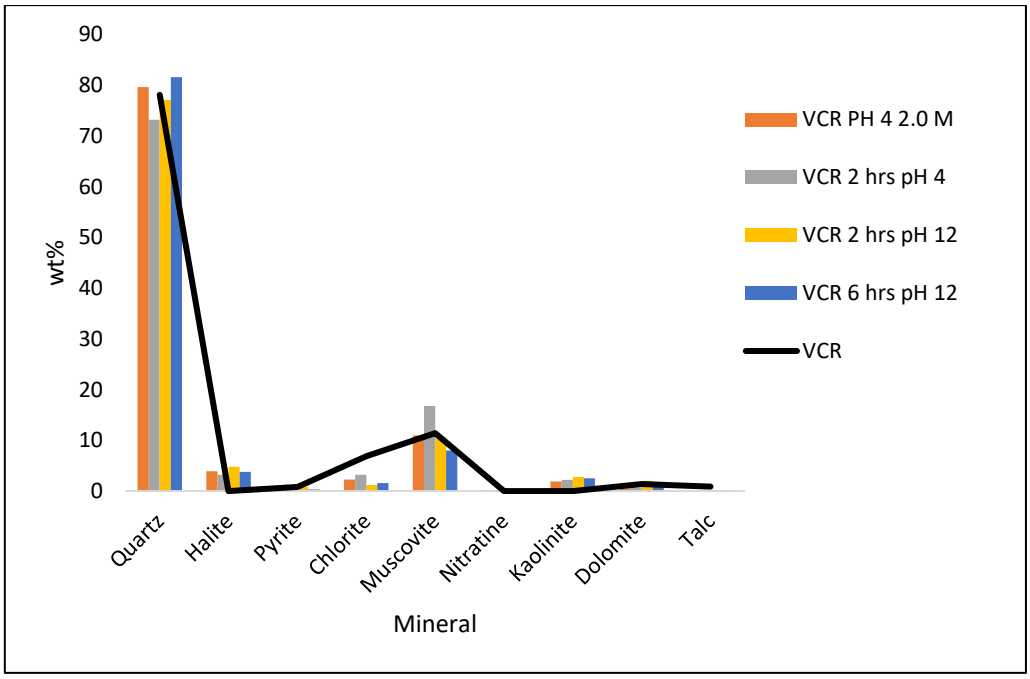

Figure 6.2 Comparison of the mineralogical composition of the head sample and the chlorinated residues for VCR.

6.3.3 Effect of time on recovery

In terms of chlorination time, there were no significant differences in the amount of gold extracted into the solution. In Figures 4.3 and 6.4, the amount of gold extracted increased from 0% to 41.25% in 2 h and to 42.5% in 4 h. Although at 6 h it was at 46%, it was a slow rate of mass transfer, which could have been due to the boundary layer that forms on the surface of the material from the silicates and the iron oxides and the concentration of the hypochloruos

ions depleting. Based on that, the optimum time for extraction was 2 h, as it had the highest mass transfer rate of the gold. Having a long extraction time allows for reaction 6.3 to occur, in which the gold will have difficulty extracting into the gold.

$$2FeS_2 + 15OCl^- + 7H_2O \rightarrow 2Fe(OH)_3 + 4SO_4^{-2} \qquad \textit{Equation 6.3}$$

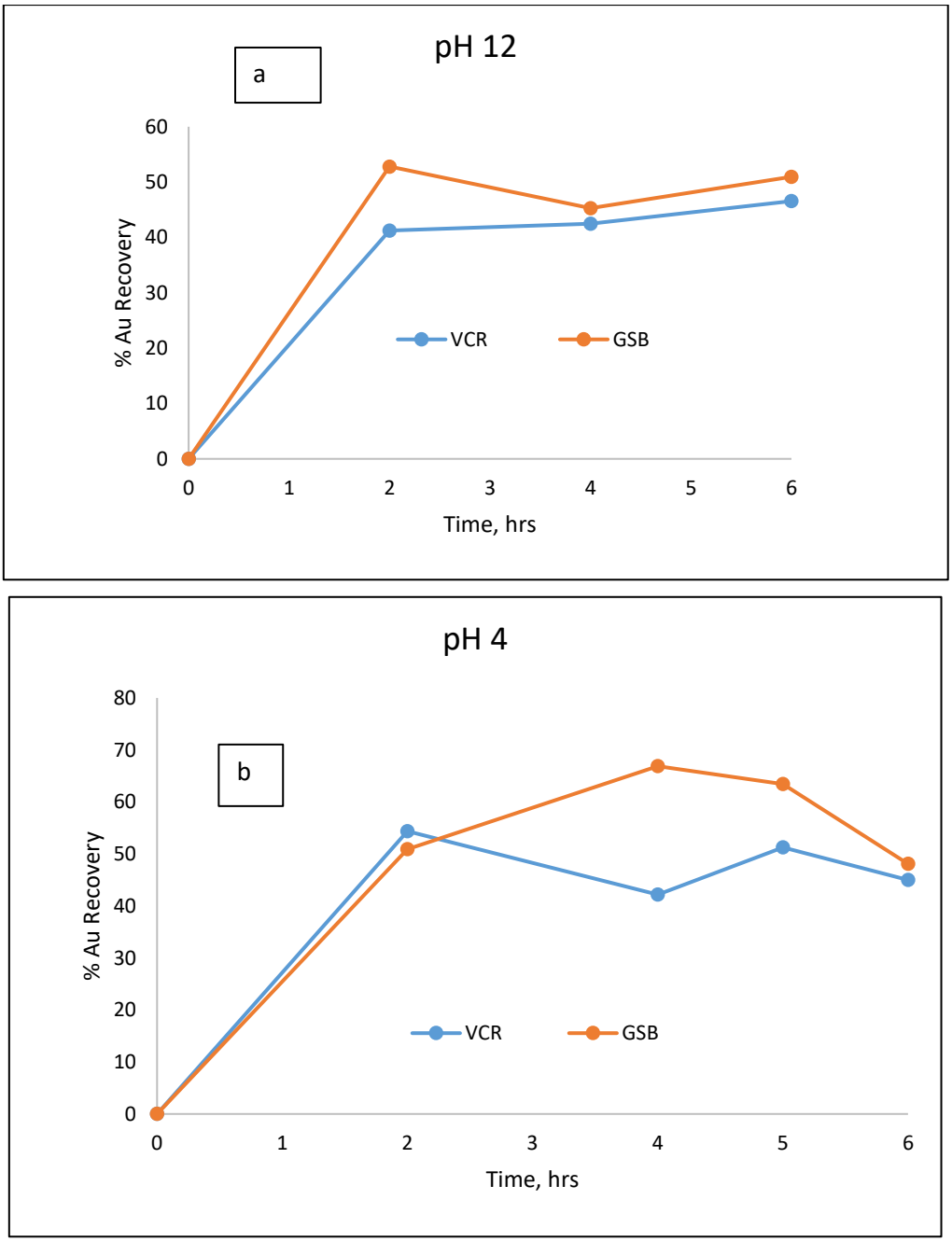

Figure 6.3 Relationship between extraction time and gold recovery at pH 12 (a) and pH 4 (b). Standard deviation is indicated by error bars.

6.3.4 *Effect of pH on recovery*

The extraction efficiency of the gold by NaOCl relies on the pH of the solution, as it depends on the presence and amount of the HClO and ClO^-, of which the latter is a stronger oxidizing agent than the former. This implies that, at acidic pH, the extraction of the gold will be driven by HClO, which will be dominant and the same for the ClO^- under basic conditions. In these experiments, which were at pH 4 and 12 for 1, 1.5 and 2 M NaOCl, the results are shown in Figures 6.4a and 6.4b. The optimum concentration of the oxidant was 1.0 M at both pH values.

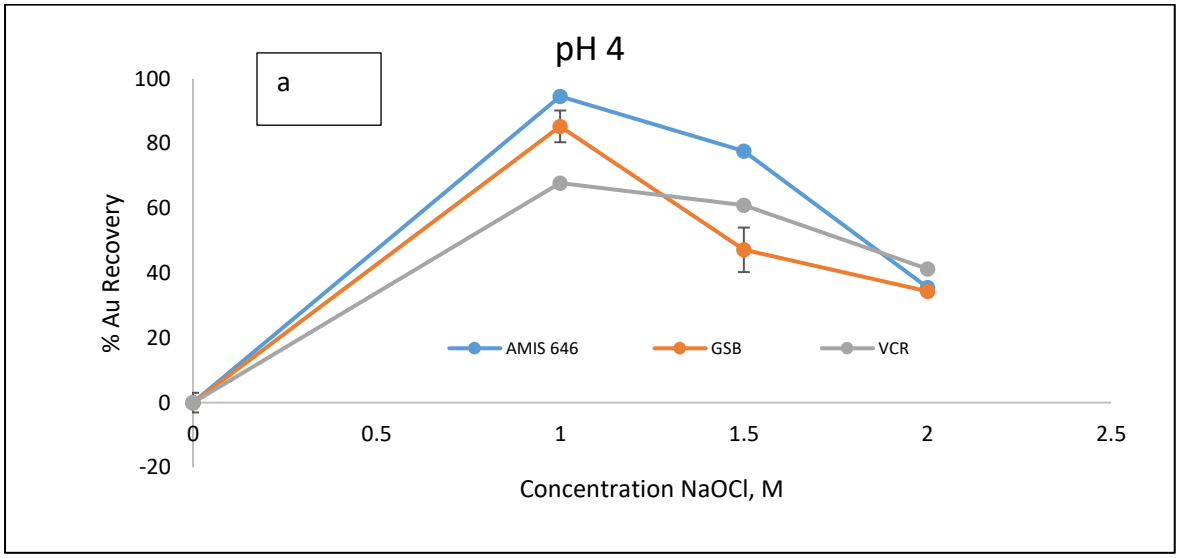

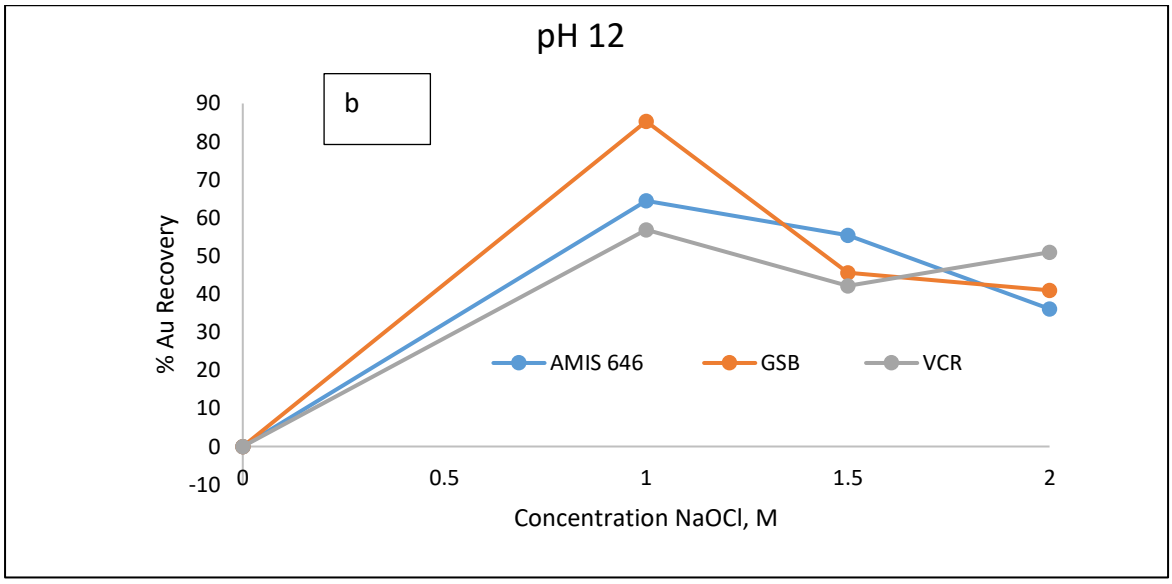

Figure 6.4 Relationship between the concentration of the oxidant and gold recovery at pH 12 (a) and pH (4). Standard deviation is indicated by error bars.

In the acidic environment, the extraction recoveries were in the order of AMIS 646>VCR>GSB and GSB>AMIS 646>VCR for the basic conditions. The highest amount of gold extracted was

94% at 1 M and pH 4, which was impressive, as it implies that there were fewer challenges involved with the mineralogy or any other factor that affects the chlorination process. Furthermore, these recoveries obtained are quite good for the samples, as they were low grade, compared to the grade of the samples used in Baghalha (2007) and Fu *et al.* (2017). Another factor that could have had a positive effect on the recoveries was the use of ultrasound during chlorination, which always kept the molecules in the solution agitated, leading to the bursting of the molecules to release the particles, thereby increasing the surface, allowing for more reactions to occur.

6.3.5 Surface area and morphology variation

The residues from chlorination were analysed by BET for surface area to assess if there were changes due to the ultrasound and oxidation processes. The observation made was that the original surface area was 3.3 $m^2.g^{-1}$, which is typical of mine tailings (Panchal *et al.*, 2018). In Figure 6.5, the BET plot is shown between the head sample and two residues obtained at different pH values. The isotherms obtained showed that the residues were of a microporous type (Okrugin *et al*., 2014). The surface area increased from 3.3 to 5.3 $m^2.g^{-1}$ in the GSB at pH 4 and 1 M, which had an extraction of 85%, while for the same sample under basic conditions, the surface area dropped to 2.1 $m^2.g^{-1}$, and the extraction was 55%. This drop in the extracted gold is due to the boundary layer, which is mostly formed under basic conditions. However, because the pyrite amount in the same layer is low, 0.8%, the layer does not have an intense effect. This implies that there is a correlation between the extraction and the change in the surface area of the material.

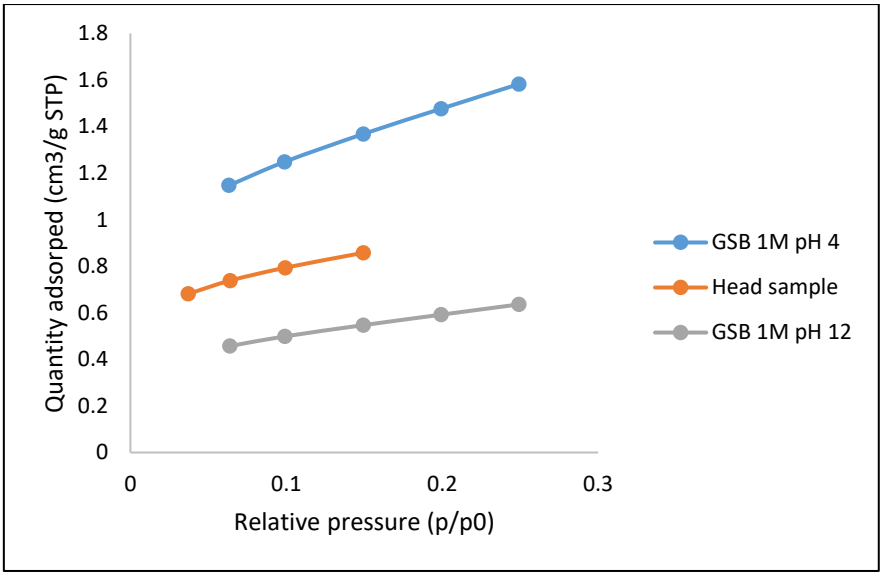

Figure 6.5 Surface area plot comparing the head sample and the chlorinated sample at different concentrations.

The residues from the chlorination and the original sample were also analysed by SEM–EDS to assess the morphology and if there were changes thereof. In Figures 6.6a and 6.6b, the SEM images of the original VCR and GSB are shown, which show high quartz (Si), which collaborates with the XRD mineralogy analysis.

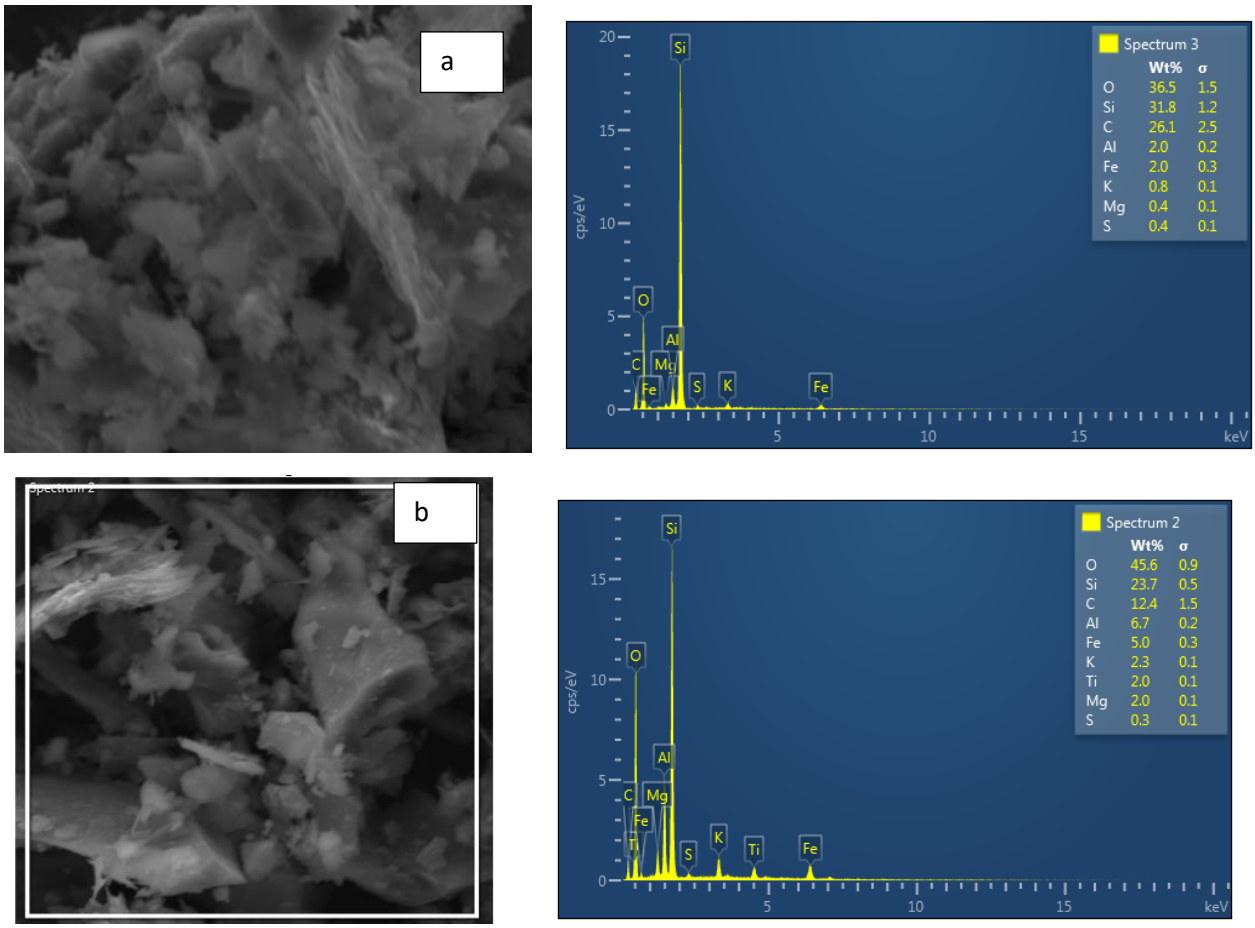

Figure 6.6 SEM images of the samples before chlorination. VCR (a) and GSB (b).

In Figure 6.7a to 6.7b, SEM images of various residues are shown, and it can be seen that the surface morphology has been altered. The main difference in these SEM images is the quantity of iron, which decreased from 2 to 5% (GSB and VCR) to below 2%. As stated in Section 6.3.3, pyrite (FeS_2) is known to readily react with the oxidant, which explains the change in the iron content. In terms of morphology, the residues of the process have a more shattered structure with a large amount of quartz on the surface than the original sample, as seen when comparing Figure 6.7.

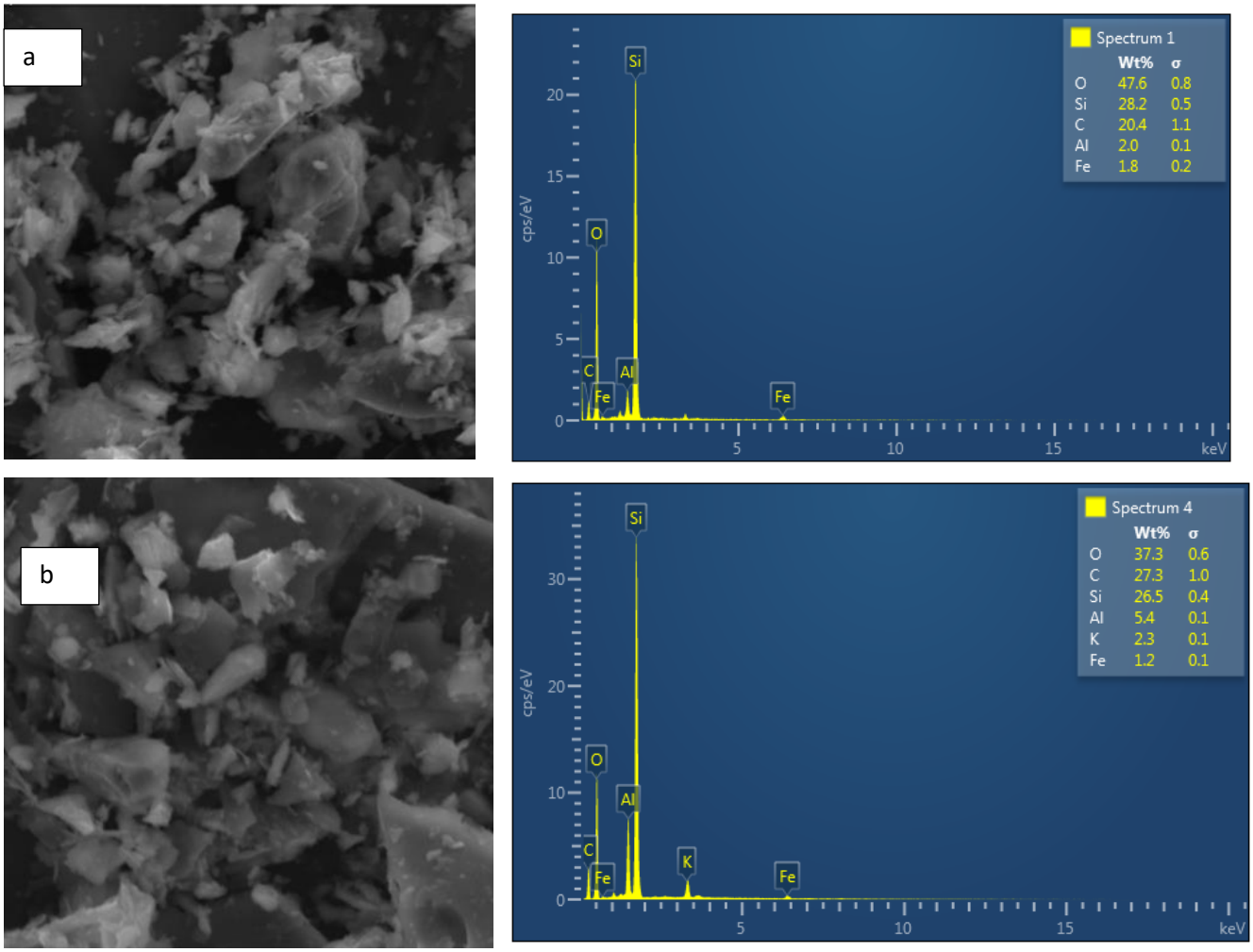

Figure 6.7 SEM images of samples after chlorination. VCR pH 4 1.5 M (a) and GSB pH 12 1.5 M (b).

6.4 Conclusion

In this paper, gold was extracted and quantified from low-grade tailings using NaOCl in the presence of HCl. The varied parameters were the concentration of NaOCl, pH of the solutions and leaching time, while conditions such as the solid-to-liquid ratio were kept constant at 0.5. The optimum conditions were NaOCl of 1.5 M, pH of 4 (acidic) and extraction time of 2 h. At higher extraction times, there was an increase in the recovery of gold; however, the rate was slower than that between 0 and 2 h. This is reported to be due to the formation of a boundary layer that forms with increasing extraction time. Under these optimum conditions, CRM AMIS 646 achieved a recovery of 96%, while under basic conditions, only 65% was obtained. The tailings samples also had satisfactory recoveries. The XRD and SEM characterization of the residues showed that minerals such as gypsum and calcite were decomposed, leading to an increase in the quartz amount, while two minerals that were not in the head sample, kaolinite and nitratine, were detected. Furthermore, the analysis of the surface area of the residues

against the sample showed that there was an increase from 3.3 and 2.3 $m^2.g^{-1}$ to 5.3 $m^2.g^{-1}$, which indicated that the structural properties of the sample were altered by the chlorination process.

This method was performed to counter issues that may arise due to small sample masses, as it used large masses (above 100 g) and a commercial solvent such as NaOCl (bleach). However, given that based on the mineralogy of the sample, an acidic environment might be needed and the process of adjusting the pH from basic to acidic, chlorine gas is evolved, which can be toxic. Therefore, the recommendation drawn from this method is to use alternative methods that have fewer effects.

6.5 References

Baghalha, M. (2007) 'Leaching of an oxide gold ore with chloride / hypochlorite solutions', *international journal of mineral processing*, 82, 178–186. https://doi.org/ 10.1016/j.minpro.2006.09.001.

Forrest, K., Yan, D and Dunne, R. (2001) 'Optimization of gold recovery by selective gold flotation for copper-gold-pyrite ores', *Minerals Engineering*, 14(2), 227–241. https://doi.org/10.1016/S0892-6875(00)00178-3.

Fu, L., Zhang, L., Wang, S., Cui, W and Peng, J. (2017) 'Ultrasonics Sonochemistry Synergistic extraction of gold from the refractory gold ore via ultrasound and chlorination-oxidation'. Elsevier., 37,471–477. https://doi.org10.1016/j.ultsonch.2017.02.008.

Liu, Y. H., Wan, B and Xue, D. S. (2019) 'Sample digestion and combined preconcentration methods for the determination of ultralow gold levels in rocks', *Molecules*, 24(9). https://doi.org10.3390/molecules24091778.

Ojeda, M. W., Perino, E and Ruiz, M. C. (2009) 'Gold extraction by chlorination using a pyrometallurgical process', *Minerals Engineering*, 22(4), 409–411. https://doi.org.10.1016/j.mineng.2008.09.002.

Okrugin, V., Andreeva, E., Etschmann, B., Pring, A., Li, K., Zhao, J., Griffiths, G., Lumpkin, G., Triani, G and Brugger, J. (2014). Microporous gold: Comparison of textures from Nature and experiments. *American Mineralogist*, *99*(5-6), 1171-1174. https://doi.org/10.2138/am.2014.4792

Panchal, S., Deb, D and Sreenivas, T. (2018) 'Mill tailings based composites as paste backfill in mines of U-bearing dolomitic limestone ore', *Journal of Rock Mechanics and Geotechnical Engineering*. Elsevier Ltd, 10(2), 310–322. https://doi.org 10.1016/j.jrmge.2017.08.004.

Sjöström, J. K., Bindler, R., Granberg, T and Kylander, M. E. (2019) 'Procedure for Organic Matter Removal from Peat Samples for XRD Mineral Analysis', *Wetlands*. Wetlands, 39(3), 473–481. https://doi.org10.1007/s13157-018-1093-7.

Zhang, Y., Cui, M., Wang, J., Liu, X and Lyu, X. (2022) ‘A review of gold extraction using alternatives to cyanide : Focus on current status and future prospects of the novel eco-friendly synthetic gold lixiviants’, *Minerals Engineering*, 176, 107336. https://doi.org 10.1016/j.mineng.2021.107336.

7 CONCLUSION AND RECOMMENDATIONS

7.1 Conclusion

The development and optimization of methods for the quantification of gold in mine tailings can be deemed successful and can be used in laboratories that process such samples. The results obtained were satisfactory for each method, and they confirmed that fire assay by gravimetry would be the best method, although it does have its own shortcomings. This depends on the nature of the laboratory; for a fast moving lab, the fire assay and acid digestion method would work, while chlorination has severe drawbacks.

Quantification of the gold using a minimal amount of sample mass was achieved using acid digestion that employed reverse aqua regia ($3HNO_3$:1HCl) in the absence of hydrofluoric acid, which is typically used to decompose quartz. It was found that it is important to carry out a gold depot analysis on the bulk sample prior to the chemical analysis to determine the association of the gold with the minerals in the sample. This then assisted in choosing the right combination of acids to use. The concern with this method was that it uses a small sample mass of 1 g, which might affect the homogeneity of the sample. However, after carrying out a homogeneity test, it was discovered that the method did not suffer from factors arising from homogeneity, with a homogeneity indicator of 8.9% and standard uncertainty due to homogeneity of ± 0.031 $g.t^{-1}$. Furthermore, the homogeneity indicator is typical of gold samples, as the grains can be inhomogeneously distributed compared to that of base metals. This method produced LODs of 0.14-0.33 $\mu g.kg^{-1}$ and recoveries of over 80% for the digests with reverse aqua regia, which are satisfactory given the method parameters that were used. The measurement uncertainties that were quantified for this method were ± 0.09-0.1 $g.t^{-1,}$ which were comparable to that with an ICP–OES finish (± 0.09 $g.t^{-1}$). This implied that this acid digestion method could be used in place of fire assays and would lead to similar measurement uncertainties.

To assess whether the problems (homogeneity) that arise from acid digestion can be mitigated, a fire assay method with a gravimetric finish was employed. The fire assay method typically works for medium- to high-grade gold, but it is a challenge when the sample is of low grade and is also a gravimetric finish. To enhance this and to obtain better recoveries, the process was optimized for mass, ratio of the litharge to reducing agent (PbO:C) and the addition of base metals (Sn and Fe) as co-collectors. It was found that at a sample mass of 100 g, a ratio of 10 and the addition of base metals, significant improvements are made in the gold recoveries, with a head grade of 0.1 $g.t^{-1}$ giving a recovered grade of 0.0904 $g.t^{-1,}$ which translates to 90%,

compared to the 70% obtained when the conditions used are those of high grade samples. Furthermore, the measurement uncertainties reported from this method were ±0.00432 $g.t^{-1}$. This is sensible as the only major contributors of measurement uncertainty would be the weighing balances for the sample and for the prill.

In an attempt to use wet chlorination using commercial NaOCl to quantify the gold to allow for a large sample mass, it was found that in acidic conditions, NaOCl concentrations of 1 M gave the highest recoveries for both the VCR and GSB matrix. Physical characterization of the residues with XRD, SEM and BET analysis also indicated the change in the mineralogical composition, morphology and surface area. Although this method worked and produced satisfactory recoveries, the drawbacks are as follows: when NaOCl is reacted with HCl, it produces a toxic chlorine gas that is very harmful when inhaled, it requires a large scale-up of chemicals and consumables, and it is unfriendly for commercial laboratories. However, its great advantage is that it allows for the use of large sample masses, which would mitigate homogeneity problems.

The main aim of the study was to find a method to quantify gold from tailings that is expected to be low in grade using methods that are environmentally friendly, cost efficient and result in low measurement uncertainties. These three methods produced satisfactory recoveries and can compete against each other; however, the acid digestion and the fire assay with the addition of Sn and Cu were proven to be much better methods.

7.2 Future prospects

- To improve the characterization of the tailings materials with relation to the original ore body, more especially on the characterization of the gold. The current challenge that exists is that the techniques that can be used have detection limits of at least 2 $mg.kg^{-1}$, which for tailings is high, as they are usually below 1 $mg.kg^{-1}$. This would eliminate the need to use processes such as gold depot, which are long and laborious.
- To apply the methods to tailings materials containing platinum group metals (PGMs) and thereafter optimize the PGM matrix.
- Use of a fluorescent material such as a glucose carbon nanosheet to precipitate the gold and PGMs out of the solution after the chlorination and acid digestion process. This will be beneficial, as there will be no need for specialized equipment, which is often needed for solutions containing sodium hypochlorite, hydrofluoric acid, etc.

8 APPENDIX: FIRST PAGE OF PUBLICATIONS

RESEARCH ARTICLE Kedibone Mashale, Bambesiwe May, James Sehata, James Tshilongo and Luke Chimuka 42
S. Afr. J. Chem., 2023, 77, 42–47
https://journals.co.za/content/journal/chem/

Statistical evaluation of the uncertainties in the characterization of South African mine tailings

Kedibone Mashale[1, 2,*], Bambesiwe May[1], James Sehata[1], James Tshilongo[1, 2] and Luke Chimuka[2]

[1]*Analytical Chemistry Division, Mintek, Praegville, South Africa*
[2]*Molecular Sciences Institute, School of Chemistry, University of the Witwatersrand, Braamfontein, South Africa*

ABSTRACT

In this study, a South African mine tailing sample was characterized for base metals using X-Ray fluorescence, alkaline fusion, and acid digestion to subsequently evaluate the uncertainties involved. This was based on the importance of characterization data in subsequent methods and obtaining confidence in such methods. It was determined that instrument repeatability and reproducibility contributed most to the overall uncertainty. At a coverage factor of 2 (k=2), the measurement result for iron through alkaline fusion, XRF, and acid digestion was found to be 3.476 ± 0.026%, 3.835 ± 0.023%, and 3.741 ± 0.020%, respectively, and that of arsenic were 88 ± 11 mg kg^{-1} and 85.5 ± 8.3 mg kg^{-1} for fusion and acid digestion, respectively. Based on the calculated expanded uncertainties which are at an average of 0.8% of the measurement results, the three methods can be associated with high statistical confidence and therefore eases decision-making regarding subsequent analytical methods.

KEYWORDS

characterization; measurement uncertainty; measurement reliability; measurement confidence; mine tailings

Received 12 September 2022, revised 24 April 2023, accepted 28 April 2023

INTRODUCTION

Characterization of geological material is part of subsequent method development and selection. This is based on the knowledge that these materials often contain a variety of minerals and elements which can interfere with analytical procedures. The abundance of the minerals (and elements) is dependent on the matrix, which is further determined by the location and processes it has undergone.[1] For example, geological samples from the Witwatersrand Basin are expected to be high in silica whilst samples from the Merensky reef are expected to be high in chromium.[2,3] These materials are usually characterized by both qualitative (e.g., mineralogy with X-Ray Diffraction, XRD) and quantitative techniques X-Ray Fluorescence (XRF) for elemental and oxide composition, and ICP-OES/MS which is often coupled with alkaline fusion or acid digestion. For the base metal characterization, acid digestion and alkaline fusion were chosen as they are suitable for the determination of oxides such as CaO, SiO_2, Al_2O_3, Fe_2O_3, MgO,[4] whilst it is also understood that loss of elements such as As, Os, Sb, and Se can occur during the open vessel digestion, making it difficult to compare the methods.[5] Due to the processed nature of mine tailings, the concentration of base metals can be expected to be in the lower percentages for elements such as calcium, iron, and magnesium, and higher amounts are expected for

the evaluation of measurement uncertainty. Quantification of measurement uncertainty in chemical analysis is fast becoming standard procedure as it can highlight the steps that contributed to high errors and uncertainties. In analytical chemistry, it is rather important to evaluate the confidence that can be placed on obtained data, which also represents the quality of the data.[12] Therefore it is beneficial for the analytical data to be presented with its uncertainty value. In the ISO/IEC 17025:2017, it is stated that for method validation, uncertainty evaluations must be completed,[13] however, this can also be applied to the day-to-day analysis. This includes identifying the sources of uncertainty and formulating the model equation, followed by the combination of the individual uncertainties into the overall uncertainty using the law of propagation.[14] In previous studies, the uncertainty of arsenic was evaluated and it was discovered that sample weighing contributed more to the uncertainty.[15] Whilst in the uncertainty evaluation of rare earth elements in geological reference materials, the most contribution emanated from analytical instruments[16], indicating that such evaluations are rarely predictable. Furthermore, the importance of evaluating the measurement uncertainty was illustrated during a method validation process, thus adding more relevance to the analytical results.[17] It is known that most analytical testing laboratories operate using the calibration

Journal of Water Process Engineering 49 (2022) 102944

Contents lists available at ScienceDirect

Journal of Water Process Engineering

journal homepage: www.elsevier.com/locate/jwpe

Detection and separation of silver ions from industrial wastewaters using fluorescent D-glucose carbon nanosheets and quaternary silver indium zinc sulphide quantum dots

Bambesiwe M. May [a,b], Olayemi J. Fakayode [a], Kedibone N. Mashale [b], Mokae F. Bambo [c], Ajay K. Mishra [d,e,f,*], Edward N. Nxumalo [a,**]

[a] Institute for Nanotechnology and Water Sustainability (iNanoWS), College of Science, Engineering and Technology, University of South Africa, Florida Campus, 28 Pioneer Avenue, Roodepoort, 1709 Johannesburg, South Africa
[b] Analytical Chemistry Division, Mintek, 200 Malibongwe Drive, Randburg, Johannesburg, South Africa
[c] DSI/Mintek Nanotechnology Innovation Centre, Advanced Materials Division, Mintek, 200 Malibongwe Drive, Randburg, Johannesburg, South Africa
[d] College of pharmaceutical and chemical engineering, Hebei University of Science and Technology, Shijiazhuang 050018, China
[e] Academy of Nanotechnology and Wastewater Innovations, Johannesburg, South Africa
[f] Department of Chemistry, School of Applied Sciences, KIIT Deemed University, Odisha, India

ARTICLE INFO

Keywords:
Ag^+ ions
Carbon nanosheets
Quaternary quantum dots
Industrial wastewater
Heavy metals

ABSTRACT

Carbon nanomaterials are essential for functions such as electronic connectivity, wastewater purification, energy and environmental sustainability applications. In this report, fluorescent carbon nanosheet was obtained from D-glucose (F-GCNS) via a low-temperature in-situ pyrolysis. The as-synthesized F-GCNS were characterized using conventional spectroscopic and microscopic techniques. Furthermore, the nanosheets were used to detect and separate silver ions (Ag+) from aqueous solutions with a detection limit (LOD) of 1.74 ppm and about 98.42 ± 0.69 % removal for concentrations ranging between 0 and 20 ppm and 100 and 200 ppm respectively. Comparably, at all concentrations, the nanosheets exhibited an LOD better than that of the quaternary silver indium zinc sulphide quantum dots (Glu-AISZ) (LOD = 7.96, R2 0.6524 for 0–20 ppm and 28.01, R2 = 0.95418 for 30–100 ppm respectively). The F-GCNS showed attractiveness for simultaneous detection and removal of heavy metal pollutants from industrial wastewater.

1. Introduction

The growing applications of heavy metal ions such as silver (Ag) ions have raised concerns about their potential impacts on the environment [1,2]. Ag ions are mainly released into the environment from several products such as clothing, printable electronics, personal care products, health care products, medical devices and drinking water filters [3,4]. Elevated levels of silver are toxic to fish and other aquatic organisms [5,6]. Furthermore, the emerging silver-based nanotechnology applications have driven more research to engage in laborious use of Ag ions [7–10], resulting in generation of huge silver wastes. To achieve the objective of environmental sustainability, removal of heavy metal ions such as Ag ion from industrial wastewaters has become a necessity. However, while separation is one resolution, the material to use for the removal and how the ions are being removed are other vital questions to be addressed. Materials used for the removal of environmental pollutants are required to be biocompatible to achieve current sustainability goal.

D-glucose, an important reducing carbohydrate exists widely in fruits, honey, kombucha tea and wine. It is easily hydrolysed in the presence of an acid, base, chemical oxidant or enzymes to various hydrolysates such as carboxylic acids and lower chain hydrocarbons [11–13]. The carboxylates are strongly chelating agents of heavy metals [11,14]. It is perceived that glucose may be the real intermediate raw materials required for the future biofuel production. Glucose is biocompatible as it is produced from degradation of foods for energy production.

Carbon materials are essentially valuable tools for many

* Correspondence to: A.K. Mishra, Academy of Nanotechnology and Wastewater Innovations, Johannesburg, South Africa.
** Corresponding author.
E-mail addresses: ajaykmishraedu@gmail.com (A.K. Mishra), nxumaen@unisa.ac.za (E.N. Nxumalo).

https://doi.org/10.1016/j.jwpe.2022.102944